DISPLAY ONLY

ISSN 1366-7300

ENVIRONMENTAL CHANGE RESEARCH CENTRE

University College London

RESEARCH REPORT

No. 4

Lake sediment analyses

N.G. Cameron, N.L. Rose, P.G. Appleby, R.W. Battarbee, S.T. Patrick, R.J. Flower & S. Juggins

A Report to AL:PE 1 Contract

1993

Environmental Change Research Centre
University College London
26 Bedford Way
London
WC1H 0AP

ALPE 1: PALAEOLIMNOLOGY

Cameron, N.G[1]., N.L. Rose[1], P.G. Appleby[2], Ø.A. Schnell[3], R.W. Battarbee[1], S.T. Patrick[1], & R.J. Flower[1]

[1]Environmental Change Research Centre,
University College London,
26, Bedford Way,
London WC1H OAP
UK

[2]Department of Applied Maths & Theoretical Physics,
University of Liverpool,
Liverpool L69 3BX
UK

[3]Institute of Zoology,
University of Bergen,
N-5007 Bergen,
Norway

ACKNOWLEDGEMENTS

This work forms part of the ALPE 1 project (Alpine Lakes: Palaeolimnology and Ecology) and was funded by an EC grant under the STEP programme.

We wish to thank our colleagues in the ALPE project for their help in this work, both in the planning stages and during the fieldwork. In particular we thank those who made us welcome in their countries and guided us to the lakes: Lief Lein in Norway, Daniello Tait in the Tyrol, Gerard Blake in the French Alps, Rossario Mosello & Andrea Lami in Ossola Valley, Italian Alps. Also Jean-Charles Massabeau for his advice on and directions to the Pyrenean lakes.

In addition we thank our colleagues at ECRC who have kindly given up their own time and helped with the sometimes strenuous hikes with a boat, engine and sediment coring & extruding equipment to these alpine lakes. In particular thanks to Don Monteith, Jane Reid & Cath Fletcher

CONTENTS

LIST OF FIGURES AND TABLES

FIGURES

TABLES

1 INTRODUCTION

Following the very successful use of palaeolimnological techniques in studies of acid lakes in North-west Europe in the 1980s the analysis of lake sediment cores from the main sites is one of the central aspects of the ALPE project.

The aim of the lake sediment studies was to use carbonaceous particle analysis to assess the degree of atmospheric contamination at each site, and diatom analysis to assess the extent to which acidification had occurred. By selecting similar types of lakes in each region (remote, high altitude, above tree-lines and with very low concentrations of base cations) it was hoped that any catchment influences on water quality would be eliminated, the chance of identifying acidified lakes would be maximised and, most importantly, useful comparisons could be made between regions with differing pollution climates.

These criteria were necessary for all aspects of the ALPE programme, but for the palaeolimnological work it was also important to find sites with good sediment records, especially since the available financial resources limited analysis to only one lake site in each region.

During field work a number of sites were visited and sampled in each region and the final choice of site, in most cases, was made only after preliminary data from all sites were available. In all regions except one, sites were chosen that filled all criteria. The exception was Milchsee (Lago di Latte) in the Italian Tyrol, a remote site, above the tree-line and with a good sediment record but with a relatively high base cation concentration.

Data from all sites are presented in this report. We describe the field and laboratory methods used and present for each site core stratigraphy, dating, carbonaceous particle analysis, diatom analysis and pH reconstruction. In addition chironomid analyses of duplicate cores taken at 5 of the 6 sites (Øvre Neådalsvatn, Stavsvatn, Paione Superiore, Milchsee and Étang d'Aubé) are presented.

2 METHODS

2.1 FIELD METHODS

2.1.1 Lake sediment coring

Sediment cores c. 20 - 40 cm long were taken at all primary sites. The bathymetry, if not known, was first estimated using an echo sounder. Test corings were made to examine the surface sediment composition across the lake. In most cases the deepest point of the lake was found to be the optimum position for coring. A modified Kajak gravity corer (Glew 1989) was used. All primary cores were extruded on site using apparatus (Glew 1988) that allowed fine slicing of the uppermost levels, (0-4 cm sliced at 0.25 cm intervals).

2.2 LABORATORY METHODS

2.2.1 Wet density, dry weight and loss on ignition determinations

Wet densities were measured by filling a 2 cm^3 weighed brass vial with a subsample of homogenised sediment. Dry weights were determined by placing 1-2 g of wet sediment in a weighed crucible and drying overnight to constant weight at 105°C. Loss on ignition was measured after placing the crucible in a muffle furnace at 550°C for 2 hours. Crucibles were cooled in a desiccator before reweighing.

2.2.2 Dating

Sediment samples from the master core taken from each lake were analysed for ^{210}Pb, ^{226}Ra and ^{241}Am by gamma spectrometry using a well-type coaxial low background intrinsic germanium detector fitted with a NaI(Tl) escape suppression shield (Appleby *et. al.* 1986).

2.2.3 Carbonaceous particles

The method for carbonaceous particle analysis followed that of Rose (1990) except that nitric acid was used to remove the organic fraction rather than basic peroxide.

Diagrams were produced using TILIA and QUATTRO.

2.2.4 Diatom preparation, identification and counting

Preparation and counting of diatoms from sediment cores followed standard procedures (Battarbee 1986). Cleaned diatoms were identified and counted under oil immersion at a magnification of x 1000 or x 1200 under phase contrast illumination. Diatom cell concentrations were determined using the microsphere method of Battarbee & Kneen (1982), for the core samples 500 - 600 valves were counted per sample. Identification of diatoms was aided by the use of a comprehensive collection of floras and taxonomic papers lodged at the ECRC, London.

2.2.5 Data analyses

Site information and diatom counts have been entered on the database at the Environmental Change Research Centre (ECRC), UCL. Data were manipulated using a combination of programmes and packages on both a VAX mainframe computer and on IBM compatible PC. pH reconstructions were carried out using the SWAP calibration set (Stevenson *et al.* 1991) and the weighted averaging programme WACALIB (Line & Birks 1990). Data were transformed and manipulated using programs (TRAN, RB2TIL) written by S. Juggins.

2.2.6 Chironomid head capsule analysis

Chironomid head capsules were picked directly from fresh sediment and mounted in Hoyer's Solution on microscope slides for

identification. In most studies, however, the sediments are treated prior to sorting following the recommendations given by Warwick (1980), Walker & Paterson (1983, 1985), Hofmann (1986, 1988), and Walker (1987). These procedures include the use of chemicals (deflocculation in 5-10 % KOH) and sieving (using a 100 µm or finer sieve). This reduces the amount of sediment needed for chironomid analysis and saves time. Working with fresh sediments is tedious, but vastly improves the taxonomic precision. Subfossil chironomid head capsules are extremely fragile, and most of the taxonomically important structures, such as mandibles, labrum with premandibles, and maxillae are easily disarticulated. These are then lost during sieving, leaving only the head capsule itself, which is usually of limited importance in determining the remains to species or species-group level. The larval stage of chironomids is generally difficult to determine, but because of the careful treatment of the subfossils in this study it would actually have been difficult to get much better species resolution even if the specimens had been sampled as living animals.

One additional advantage in using untreated sediments is that, after the animals remains have been picked out, the sediments are not destroyed and can be used for other purposes.

In the samples analysed all head capsules were picked out and identified. Because sorting and determination of chironomid head capsules is very time-consuming, it was decided first to look at the bottom, middle, and top samples of the cores to see if there had been changes in the chironomid communities. Further samples were analysed if significant trends were found. The fauna of Øvre Neådalsvatn, Lago di Latte, and Etang d'Aubé are regarded as more or less unchanged, i.e. no impacts caused by human activity, while in lakes Paione Superiore and Stavsvatn the chironomid communities showed marked alterations. However, so far additional samples have been analyzed only from Paione Superiore.

2.2.7 Pollen analysis

Material from the primary cores has been sent to Dr. A.C. Stevenson, Department of Geography, University of Newcastle, UK, for pollen analysis. This work, which is not part of the original project design, is in progress and will be reported on in publication.

3 RESULTS

3.1 AUBE

Two sediment cores were taken from the deepest point of Etang d'Aube (July 1991) in 46 m of water. The core AUBE1 was 26 cm long and AUBE2 was 33 cm long.

3.1.2 Lithology and core correlation

Both cores were visibly undisturbed, consisting of a homogenous dark brown mud, however, with a low, but varying concentration of small mineral particles (<1 mm diameter). Exceptionally, a large stone, of about 1 cm diameter, was removed from the 4.5 cm level of AUBE2 during extrusion. Profiles of dry weight and LOI are plotted for both AUBE1 and AUBE2 (Figure 3.1.1) and wet density measurements for AUBE1 are also shown.

AUBE1 has a fairly high inorganic content (PDW 6 - 33%) and low to medium organic content (LOI 11 - 30%). From the base of the core at 26 cm to a depth of approximately 6.5 cm there are steady, but small overall increases in PDW (13 - 15 %) and WD (1.06 - 1.13 g cm^3) values with a concomitant decline in LOI (29 - 20%). A low LOI value (18%) and peak PDW (21%) occurs at 11.5 cm. At 4.25 cm there are maxima in WD (1.29 g cm^3) and PDW (33%) and LOI declines to a minimum of 11%. The distinct peak of inorganic content at this depth and corresponding decline in organic content is the result of the inwash of catchment derived minerals. PDW and DW decline sharply from this maximum to low values of 6% and 1.09 g cm^3 respectively at the surface. LOI increases steeply and reaches 23% at the surface.

AUBE2 has a similar inorganic (7 - 19%) and organic content (15 - 33%) to AUBE1, but the magnitude of the inorganic inwash is not as great. From the base of the core at 33 cm to a depth of approximately 4.75 cm there is an small overall increase in DW and at the same time a small overall decrease in LOI. This gradual change is interrupted at a depth of 18.5 cm where there is a peak in DW (18%) with a corresponding minimum LOI (17%). A pronounced minimum LOI (15%) and maximum DW (19%) is recorded at 2.75 cm, LOI then increases sharply to 22% at the surface whilst DW declines to 7%.

Both AUBE1 and AUBE2 record similar trends in DW and LOI parameters with gradual overall declines in organic content and at 4.25 cm and 2.75 cm respectively a pronounced maximum in inorganic content. The large peak in DW (and other smaller peaks) relate to the inwash of catchment derived minerals and a corresponding dilution of organic material within the core, shown by the troughs in LOI.

3.1.2 Radiometric measurements and dating

The results of ^{210}Pb and ^{226}Ra analyses are given in Table 3.1.1, and shown graphically in Figure 3.1.2. The ^{137}Cs and ^{241}Am results are given in Table 3.1.2 and Figure 3.1.3. The radiometric profiles for this core were quite unusual. Following a sharp decline in unsupported ^{210}Pb and ^{137}Cs concentrations in the top 4cm of the core from quite high surficial values, activities of both these radionuclides had small but significant secondary peaks at depths 6.75 cm and 20.5 - 22.5 cm in the core. A possible explanation of the observed results is preferential absorption onto layers of different mineralogy following downwards diffusion of the radionuclides in the pore waters. Such

mobility is commonly observed in ^{137}Cs, but less so in ^{210}Pb which is usually strongly bonded onto the sediment particles. Conditions likely to increase ^{210}Pb mobility are low organic content and low clay content. In the case of the more recent feature, the radionuclide peaks (at 6.75 cm) lie just below a well defined layer of dense sediment which spans the 3 - 6 cm section of the core. Sediments within this section are observed to have a low LOI value and may originate in an inwash of dense, highly inorganic material. The profiles at this level would then be responding to two different processes, mobility within the porewaters and dilution by the inwash event. At the older feature, there are however only minor changes in LOI and sediment density.

Simplistic calculations of the age depth relation using the CRS and CIC ^{210}Pb dating models (Appleby and Oldfield 1978) date the basal level at 25.5 cm to as recently as ca. 1870 - 1910. Since both models suggest very low accumulation rates in recent years, it would however appear that the calculations are being highly perturbed by the apparent unsupported ^{210}Pb at the deeper levels in the core. Calculations based on the very recent accumulation rates put the 1900 level at not more than 8 cm. Assuming that sedimentation rates (excluding any inwash events) have not changed dramatically during the past 100 years, the CIC model probably gives the best guide to the date of the 6.75 cm ^{210}Pb peak, which just predates the recent inwash event. The date that we obtain is 1930. From 6.75 cm down to about 10.5 cm the principle mechanism controlling the ^{210}Pb profile would appear to be radioactive decay. For this section of the core, a best estimate of the mean sedimentation rate based on the slope of the ^{210}Pb profile is 0.0093 g cm-2 y-1, from which the date of the 10.5 cm level is calculated to be about 1856. Using this as a dated reference level, the constrained CRS model (Oldfield and Appleby 1984) can be used to construct a chronology for the entire sequence post-dating 1856. The results of these calculations are given in Fig. 3.1.4 and Table 3.1.3. They date the recent inwash event to the period 1930 - 1941, and suggest a slow accumulation rate during the past 50 years of ca. 0.0083 g cm^{-2} y^{-1}. The 1963 level is put at about 2 cm . Since the very highest ^{137}Cs values occur in the top 1 cm of the core, and within this section there are also traces of ^{241}Am, it is possible that even this ^{210}Pb chronology overestimates the true sedimentation rate.

3.1.3 Carbonaceous particles

The CP record for the core AUBE 1 (Figure 3.1.5) starts between 5.0 and 6.0cm. This is at a point where the ^{210}Pb chronology is unable to give definite dates due to an inwash event and so the start of the record can only be dated to 'the mid-late 1930's'. The CP concentration increases slowly up to about 1cm depth (1980 ± 2) where there is a rapid increase in concentration up to the surface (1991). There is no surface decline. The surface concentration and flux for AUBE 1 are 15418 gDM^{-1} and 128 cm^{-2} yr^{-1} respectively.

10 mountain lakes from the Vosges region of France have been analysed for carbonaceous particles (Kreiser *et al.*, 1992). These sites are generally at a lower altitude than Etang d'Aube and have afforested catchments. All but one site shows a surface decline in CP concentration the peak being assigned the date c.1980. Surface concentrations varied between 3300 and 144000 gDM^{-1}. It was suggested that these lakes were influenced, at least in part, by fossil-fuel combustion in Germany and so the profiles are not directly comparable to those of Etang d'Aube.

3.1.4 Diatom analysis and pH reconstruction

Diatom cell concentrations for AUBE1 are presented in Figure 3.1.6, cell concentrations below 6 cm range from 2 - 2.5 $x10^8$ cells g^{-1} dry wt. Cell concentrations are diluted to 0.7 $x10^8$ where the inwash event occurs and recover slightly towards the surface. A summary diagram showing taxa occurring at abundances of greater than 2% is presented (Figure 3.1.7). A total of 180 diatom taxa were identified, of these 20 taxa occurred at abundances of more than 2% in any sample. The diatom profile is stable with no significant floristic change throughout the core. The flora is dominated by non-planktonic forms typical of oligotrophic, acid mountain lakes (Flower and Jones 1989). In particular *Achnanthes scotica* (11 - 18%) and *Cymbella perpusilla* (7 - 12%) are common, along with other *Achnanthes* and *Aulacoseira* taxa such as *Achnanthes minutissima* (4 - 7%), *Achnanthes helvetica* (3 - 7%), *Aulacoseira distans* var. *nivalis* (1 - 7%) and *Aulacoseira lirata* var. *alpigena* (3 - 8%). A very small decline in the circumneutral species *Achnanthes minutissima* from approximately 7% to 4% occurs in the top 3 cm of the core, which might support the idea that there has been a small pH decline as a result of acidification (see below). The presence at low, but increased, abundances of the aerophilous species *Navicula perpusilla* (maximum 3% at 3.125 cm) around 3 - 4 cm may relate to accelerated catchment erosion.

The reconstructed pH curve is consistent with the stable diatom flora varying between 5.32 and 5.20. A slight decline of pH of approximately 0.1 pH units is detected at the top of the core, however the magnitude of this change is within the error of the reconstruction method. The measured pH of Lake Aube is 6.13, clearly the reconstructed pH of the surface sediment, 5.20, is significantly different from this figure.

3.1.5 Chironomid head capsule analysis

The chironomid taxa found in the core from Étang d'Aubé are shown in Table Chir. X-5. As in Lago di Latte the chironomid community seems to have been stable for a long period, and includes acid-sensitive taxa like *Micropsectra radialis*, *Tanytarsus lugens*-group (sp. B), and *Zavrelimyia* cf. *barbatipes*. However, for unknown reasons the top 0.25 cm of the core contained 9 specimens of only 1 species, compared to 38-61 specimens and 5-6 taxa for the other three samples within the top centimetre (Chir. Fig. 8). Also, *Micropsectra radialis*, which is the dominant chironomid in the core samples, was not found in the bottom samples of the

extant fauna taken in 1991. Problems were encountered when taking these samples (E. Willassen, pers. comm.), and they are not regarded as representative of the profundal chironomid community. The species found both in the core and bottom samples are common in the Pyrenees (Laville & Vinçon 1986).

3.1.6 Site summary: Etang d'Aube

Etang d'Aube is a corrie lake lying well above the tree line, and with minimal anthropogenic disturbance in the catchment. The granitic geology and resulting low lakewater Ca concentration (Ca 36 $\mu eq\ l^{-1}$) would suggest that this lake is susceptible to acid deposition, a sensitive site fulfilling all ALPE project criteria. The carbonaceous particle record of the core AUBE1 indicates that the lake has been subject to significant atmospheric deposition beginning approximately 50 years ago and rising sharply from about 1980 to a maximum at the present time. The sediment diatom record however, indicates that there has been only a small decline in pH, of the order of 0.1 pH units. The mean measured 1991 pH (6.31), stable, acid-sensitive chironomid communities and presence of brown trout and char in the lake support the idea that acidification has not been so severe as in other lakes in North-west Europe lying in sensitive areas but with higher levels of acid deposition.

3.2 ØVRE NEÅDALSVATN

Three short sediment cores were taken from Øvre Neådalsvatn on 19 and 20 August 1991. The cores were taken from the same area of the lake, at its deepest point, in 16 - 17 m of water.

3.2.1 Lithology and core correlation

The cores consisted of homogeneous dark brown sediment with sub-millimetre, mica-like mineral particles, there were no visible changes in stratigraphy. Lithostratigraphic profiles are plotted for two cores (Figure 3.2.1) OVNE1 (WD, DW, LOI) and OVNE2 (DW, LOI).

OVNE1 has a fairly high inorganic content and low organic content. DW declines gradually from 17% at 24.5 cm to 10% at the top of the core whilst LOI increases from 17% at 24.5 cm to a maximum of 23% at 3.4 cm, declining to 19% at the surface. In the same part of the sequence WD is fairly consistent varying between 1.10 g cm^3 - 1.15 g cm^3. However at the base of the core a significant inwash of catchment derived minerals is indicated by the peak DW (39%) and WD (1.22 g cm^3) at 27.5 cm and depressed LOI (8%) at the same level.

OVNE2 has a similar lithostratigraphic profile to OVNE1. Towards the base of the core at 27.5 cm there is a maximum in DW (41%) and minimum LOI (9%) suggesting an inwash of inorganic catchment material around this level. DW then declines more or less gradually from 22% at 25.5 cm to 14% at 2.25 cm, reaching a minimum of 5% at the surface. However, a sharp peak in DW (21%)

occurs at 8.5 cm without any large change in LOI. LOI increases steadily from 17% at 25.5 cm to 19% at 7.25 cm. There is a peak LOI (25%) at 6.25 cm, declining to 19% at 2.25 cm and increasing again to a maximum of 31% at the surface.

3.2.2 Radiometric measurements and dating

The ^{210}Pb and ^{226}Ra results are given in Table 3.2.1, and shown graphically in Figure 3.2.2. The ^{137}Cs, ^{134}Cs and ^{241}Am results are given in Table 3.2.2 and Figures 3.2.3 & 3.2.4.

^{210}Pb chronologies have been calculated using both the CRS and CIC ^{210}Pb dating models (Appleby and Oldfield 1978) and the results are shown in Figure 3.2.5. The two models are in good agreement, both indicating a constant sedimentation rate of 0.0094 ± 0.0009 g cm-2 y-1 during the past 140 years. The ^{210}Pb chronology determined by these calculations is given in Table 3.2.3.

The high ^{134}Cs activity in the surficial sediments (Figure 3.2.3b) indicates that ^{137}Cs activity at this level (Figure 3.2.3a) is dominated by fallout from the 1986 Chernobyl accident. ^{134}Cs derives from Chernobyl fallout alone, and has been corrected for decay since 5th May 1986. The ^{134}Cs can be used to partition the ^{137}Cs into its Chernobyl and weapons test components, and the weapons test ^{137}Cs determined by this process is plotted in Figure 3.2.4a. The apparently high values of weapons ^{137}Cs in the top 1 cm of the core are almost certainly spurious, and arise from uncertainties in the partition. Deeper in the core there is however a reasonably well defined peak at about 2 cm which would appear to denote the 1963 level. This is reasonably consistent with the ^{210}Pb chronology, which puts the 1963 level at 2.2 cm. The ^{241}Am record, also indicative of the 1963 level (Appleby *et al.* 1991), has a peak value within the 1.5 - 1.75 cm sample, dated 1969 -72 by the ^{210}Pb. In this core precise measurements of ^{241}Am activity were difficult to obtain because of the relatively high ^{238}U activity, and the relatively small discrepancy is probably insufficient to warrant any adjustment of the ^{210}Pb dates.

3.2.3 Carbonaceous particles

The CP record for the core OVNE 1 starts between 3.75 and 4.5cm depth (1932 ± 4 and 1943 ± 3) (Figure 3.2.6). The concentrations and fluxes are low and increase only slowly until 1.0 - 1.25cm (1976 - 1979 ± 2) when both profiles increase more rapidly. There is no surface decline although there is a slight levelling off in the surface (0.0 - 0.25cm) sample. Both surface concentrations and flux levels are very low. The surface concentration of 1319 gDM^{-1} is comparable to sites in the north of Scotland, although the surface flux (12 cm^{-2} yr^{-1}) is lower than any so far calculated in the U.K.

Carbonaceous particle analyses have been undertaken on other (low altitude) sites in mid-Norway. Rōyrtjōrna analysed by Wik & Natkanski (1990) showed a peak concentration of 1600 (gDM^{-1}). This was dated (by varve counting) at 1969 after which there was

a decline in concentration to the surface. Rose (1991) analysed 3 sediment cores from lakes in this region although these have not been dated. These sites included Rôyrtjörna and also Langtjorna and an unnamed lake "Granite A". The Rôyrtjörna profile was very similar to that of Wik & Natkanski (i.e. peak concentration of 1600 gDM^{-1} and a surface decline). The other sites, Langtjorna and "Granite A", show no surface decline and give surface concentrations of 1034 and 1251 gDM^{-1} respectively.

3.2.4 Diatom analysis and pH reconstruction

A ^{210}Pb dated profile of diatoms occurring at abundances of more than 2% is presented alongside the reconstructed pH (Eigure 3.2.8). Species diversity was high and a total of 184 diatom taxa were identified from OVNE1, of these 26 species occurred at abundances of 2% or more. Diatom cell concentrations were variable (Figure 3.2.7), in the range $1.2 \times 10^8 - 4.0 \times 10^8$ cells g^{-1} DW, however there were no trends down the core. The variation in diatom abundances is accounted for by some high counting errors resulting from a low ratio of microspheres to diatom valves counted.

Examination of diatom abundances over the whole 30 cm profile reveals that the diatom assemblages remain stable throughout. The most common species and their range of abundances were: *Achnanthes marginulata* (8 - 15%), *Achnanthes helvetica* (5 - 10%), *Cymbella perpusilla* (2 - 8%), *Achnanthes scotica* (3 - 10%) and *Frustulia rhomboides* var. *saxonica* (3 - 9%). Although there are consistent changes of small magnitude in the diatom percentage curves, for example the decline from 3% to 1% of *Achnanthes kreigeri* in the top 3 cm, no sustained or significant trends in species abundance are perceptible. Reconstructed pH, in the range 5.10 - 5.26, is consistent with the stable diatom assemblages showing no significant variation. However, the mean measured pH for Øvre Neådalsvatn for 1991 was 6.37. Clearly there is a large difference between this measured pH and the inferred surface sediment pH of 5.13.

3.2.5 Chironomid head capsule analysis

Four sediment samples were analysed from this site, the species found in each assemblage are listed in Table Chir. X-1. Thirty taxa were identified from the deepest sample (at 28-29 cm) while 20 taxa were found in the sample from the middle of the core (11-12 cm). The two samples from the top centimetre (0.75-1.0 and 0.0-0.25) contained 15 and 17 taxa, respectively (Chir. Fig. 1). These figures are quite high for a deep water fauna at more than 700 m a.s.l., especially the 28-29 and 11-12 cm samples. However, in the 28-29 cm sample a large number of the genera are not typical of deep water. Most species of the genera *Chaetocladius*, *Corynoneura*, *Diamesa*, *Eukiefferiella*, *Georthocladius*, and *Thienemanniella* are members of the lotic chironomid community in mountainous areas in Europe, and will dominate the invertebrate fauna of the inlet river to Øvre Neådalsvatn. These genera make up 25 % of the total number of specimens in the deepest sediment sample and are most likely transported into the lake indicating

a much higher discharge in the inlet river at the time of deposition. This is confirmed by the presence of a high percentage of sand in the sediments of the bottom core sample. The presence of *Heterotrissocladius subpilosus* and *Pseudodiamesa* cf. *arctica* in the bottom of the core is interesting. These species are very good indicators of ultraoligotrophic conditions and are not present in the lake today. The chironomid communities both in the samples analysed from the top centimetre and in recent surface sediment samples indicate more moderate oligotrophic conditions. In particular this is shown by the development of *Heterotrissocladius brundini*. This species is an indicator of less severe conditions and has a relatively low abundance (10 %) in the bottom of the core, but becomes the dominant species in the 11-12 cm sample (42 %). In the 2 samples analysed from the top centimetre of the core this species dominates, comprising 47 % of the specimens. Also, bottom samples of the live fauna taken in 1991 showed *H. brundini* dominating comprising about 65 % of the chironomid larvae found. The composition of the chironomid communities both in the core and in the lake today is typical of the lake type (Brundin 1949, 1956), and shows no indication of acidification (Chir. Fig. 2).

3.2.6 Site summary: Øvre Neådalsvatn

Øvre Neådalsvatn is a large lake, with an area of 50 ha, lying above the tree line remote from human activity. The underlying geology is of gneiss and the lakewater has a low Ca concentration (Ca 20 $\mu eq\ l^{-1}$). Øvre Neådalsvatn fulfils ALPE project criteria and is susceptible to acid deposition. The carbonaceous particle record of the core OVNE1 indicates that the lake has been subject to a low level of atmospheric deposition beginning approximately 50 - 60 years ago and rising more rapidly from about 1979 to a maximum at the present time. Concurrent with this evidence for a low level of deposition, the sediment diatom assemblages show little change through time and reconstructed pH varies only by approximately 0.1 pH unit with no trend towards the core surface. The results of chironomid head capsule analysis and the presence of a reproducing brown trout population support the assertion that Øvre Neådalsvatn can be considered a relatively clean site.

3.3 STAVSVATN

Three sediment cores were taken on 21.8.91 from the deepest point of Stavsvatn. The cores were taken from the same area in 17 - 18 m of water to the north side of the island at the north end of the lake.

3.3.1 Lithology and core correlation

The cores consisted of dark brown mud with a visible darkening of the sediment towards the core surface. WD, DW and LOI profiles are plotted for STVN1 and STVN2; DW and LOI are plotted for STVN3 (Figure 3.3.1).

STVN1 is 29 cm long and has a high organic content (LOI 38 - 46%) and shows an overall increase in LOI from 40% at the base to 46% at the surface. DW declines gradually from 9% at the base to 2% at the surface and WD varies between 1.03 g cm^{-3} - 1.09 g cm^{-3} showing a slight overall increase from the base to the top of the core.

STVN2 is 32 cm long and has a high organic content throughout (LOI 39 - 48%) with an overall increase in LOI from 40 - 43% at the base to a maximum of 48% at the surface. There is very little variation in DW (6 - 8%) except for a slight, but pronounced decline at the surface (4%). The WD profile also shows very little variation, values vary only slightly (1.04 - 1.06 g, cm^{-3}).

SVTN3 is 34 cm long and has a high organic content throughout. LOI shows an overall gradual increase from 41% at the base of the core to 46% at 0.75 cm. There is a sharp increase in LOI, to 60%, in the surface level. Except at the surface, where there is a decline to 2%, there is little variation in DW which fluctuates from 6 - 8%.

All three cores from Stavsvatn reflect the undisturbed nature of the lake catchment, with no large changes in the lithological parameters measured. The relatively high organic content of the sediments (compared with other ALPE sites) is probably a reflection both of higher lake productivity and perhaps of the supply of catchment derived organic material to the lake from the surrounding blanket peat.

3.3.2 Radiometric measurements and dating

The results of ^{210}Pb and ^{226}Ra results are given in Table 3.3.1, and shown graphically in Figure 3.3.2. The ^{137}Cs, ^{134}Cs and ^{241}Am results are given in Table 3.3.2 and Figures 3.3.3 & 3.3.4.

^{210}Pb chronologies have been calculated using both the CRS and CIC ^{210}Pb dating models (Appleby & Oldfield 1978) and the results are shown in Figure 3.3.5. Down to a depth of about 6 cm (dated to about 1900) the two models are in good agreement, both indicating a very low but constant sedimentation rate of 0.0039 ± 0.0005 g cm-2 y-1. Below this level there is a significant divergence, the CRS model indicating a period of accelerated sedimentation in the late 19th century. This difference may however be an artefact of the calculations, arising from particular difficulties in determining supported ^{210}Pb (or ^{226}Ra) activity in this core. ^{226}Ra is determined from the ^{222}Rn decay product ^{214}Pb. The sediments in this core have a very low density, and in these circumstances a high degree of radon mobility has often been observed (Appleby unpublished observations). An analysis of the results of the radiometric measurements suggests that radon escape from the samples has been significant in spite of the measures taken to seal the sample holders. Although corrections for this effect have been made, there is some uncertainty as to the precise levels of unsupported ^{210}Pb at depths close to equilibrium. Since this affects CRS model calculations near equilibrium much more significantly than those of the CIC model, the latter is probably

a better guide to the chronology of the pre-1900 levels in the core. The CIC model indicates no variations in the accumulation rate since at least the mid 19th century, and this forms the basis of the ^{210}Pb chronology of the core given in Table 3.3.3.

^{134}Cs is derived from Chernobyl fallout alone, and has been corrected for decay since 5th May 1986. The high ^{134}Cs activity in the surficial sediments (Figure 3.3.3b) indicates that a significant proportion of the total ^{137}Cs activity at this level (Figure 3.3.3a) derives from fallout from the 1986 Chernobyl accident. The ^{134}Cs can be used to partition the ^{137}Cs into its Chernobyl and weapons test components, and the weapons test ^{137}Cs determined by this process is plotted in Figure 3.3.4a. Neglecting the spurious value at a depth of 1 cm that almost certainly arises from uncertainties in the partition, there is a reasonably well defined weapons ^{137}Cs peak at about 2.25 cm which would appear to denote the 1963 level. As shown in Figure 3.3.5 this is in excellent agreement with the ^{210}Pb chronology. ^{241}Am, also indicative of the 1963 level (Appleby *et al.* 1991), was detected in the 1.25 - 1.5 cm sample but not in the 2 cm sample. It should however be noted that ^{241}Am activities are generally very low, and in this core were particularly difficult to measure due to the adjacent 63 keV ^{234}Th gamma peak arising from the very high ^{238}U activity levels.

3.3.3 Carbonaceous particles

The CP record for the core STVN 1 (Figure 3.3.6) starts between 6.0 and 7.5cm depth (1875 ± 15 and 1901 ± 10). The concentrations and fluxes throughout the core are low although higher than those from Øvre Neådalsvatn. Both profiles increase slowly, up to about 2cm (1966 ± 2) where the increase becomes more rapid. This trend continues up to 0.5 - 0.75cm (1984 - 1986 ± 2) where there is a peak in both concentration and flux followed by a decrease to the surface.

Wik & Natkanski (1990) show a carbonaceous particle profile from Verevatn also in southern Norway. Here the marked concentration increase dates to about 1930 and the concentration maximum of 59000 gDM^{-1} occurs in 1970. The concentration is very much higher than that of Stavsvatn and Wik (1989) found it to be twice as high as that of Åbuvatnet a lake 8km from Verevatn. The maximum concentration in Åbuvatnet was found to date to the late 1960's.

3.3.4 Diatom analysis and pH reconstruction

A summary percentage diatom diagram, showing diatom taxa occurring at abundances of greater than 2% in the core SVTN1 is presented (Figure 3.3.8). Species are ordered on the diagram left to right by their weighted average abundances. A total of 130 taxa were recorded in the core and 23 taxa occurred at more than 2%.

From the base of the core at 27.5 cm up to a depth of 8.5 cm the diatom assemblages are dominated by the planktonic diatom *Cyclotella kuetzingiana* which occurs at percentages ranging from

57 - 43 %. Other, non-planktonic, diatoms occurring in the same part of the core include *Frustulia rhomboides* var. *saxonica* (maximum abundance 9%), *Achnanthes marginulata* (maximum abundance 8%), *Brachysira brebissonii* (maximum abundance 7%) and *Achnanthes scotica* (maximum abundance 5%). From 8.5 cm to a depth of 4.25 cm *Cyclotella kuetzingiana* declines to 4% whilst *Achnanthes marginulata* increases to 17% along with small increases in other diatoms such as *Achnanthes scotica* and *Frustulia rhomboides* var. *saxonica*. From 4.5 cm to the top of the core *Cyclotella kuetzingiana* declines further reaching a minimum abundance of 2% at the surface. *Achnanthes marginulata* increases to a maximum of 20% at 0.6 cm and there are increases in the percentages of several acidphilous and acidobiontic diatoms in the uppermost 3 cm of the core, for example *Eunotia* spp. and *Aulacoseira* spp.

The diatom cell concentration in SVTN1 generally reflects the relative abundance of planktonic (*Cyclotella kuetzingiana*) and non-planktonic species. Between the base of the core and 8.5 cm the cell concentration varies from 8 x 10^8 cells g^{-1} DW to 4 x 10^8 cells g^{-1} DW declining to 1 x 10^8 cells g^{-1} DW to 2 x 10^8 cell g^{-1} DW between 6.5 cm and the top of the core (Figure 3.3.7). A peak cell concentration of approximately 4 x 10^8 cells g^{-1} DW occurs at 2.25 cm.

The reconstructed pH is stable from the base of the core at 27.5 cm to 8.5 cm, varying from a maximum of 6.0 to a minimum of 5.8. From 8.5 cm to 4.25 cm pH declines from 5.9 to 5.1 and between 4.25 cm and the top of the core pH declines to 5.0. In the upper part of the core there is clearly a significant pH decline of approximately 1 pH unit following the stable pH recorded in the bottom part of the core. The measured pH of Stavsvatn (5.99) from 1991 is significantly different from the reconstructed pH of the surface sediment, 0 - 0.25 cm (5.00).

3.3.5 Chironomid head capsule analysis

Table Chir. X-2 shows the chironomid taxa found in the core from Stavsvatn (STVN2). Five sediment samples were analysed. There was a pronounced decrease in the number of taxa towards the top of the core, with 25 species in the deepest sample and only 9 in the top 1.5 cm (Chir. Fig. 3). All taxa found in the bottom of the core are typical of the sublittoral/profundal chironomid communities in alpine areas of Scandinavia (Brundin 1949, 1956), and there are no input of typically littoral and rheophilic taxa. In the middle section of the core (11-12 cm) the chironomid community was reduced to 15 taxa, but was still similar to the bottom sample. The decline in chironomid diversity, and the particular species eliminated, strongly suggests acidification of the lake. Species sensitive to acidification like *Heterotrissocladius grimshawi*, *Micropsectra groenlandica/-insignilobus*, *Stictochironomus rosenshoeldi*, and *Tanytarsus lugens*-group were all represented in the 32-33 and 11-12 cm samples but missing in the top 1.5 cm (Table Chir. X-6, Chir. Fig. 4). Except for the presence of *Micropsectra radialis* the species/taxa in the top sediments are all tolerant to acidification and are common members of the profundal community

in the severely acidified Lake Lille Hovvatn (Schnell, in prep.). Only two chironomid taxa, *Procladius* spp. and *Sergentia coracina*, were found in the bottom samples of the recent fauna taken in 1991. These chironomid taxa are perhaps the most acid tolerant. It is surprising to find such a species-poor chironomid fauna in the lake when the measured pH-values are as high as 5.9-6.0 for the years 1991-92. However, based on the chironomid fauna the lake is clearly acidified.

3.3.6 Site summary: Stavsvatn

Stavsvatn is a large lake with an of area 40 ha, lying just above the tree line and with little human disturbance in the catchment. The underlying geology is of granite and the lakewater has a low Ca concentration (Ca 42 $\mu eq\ l^{-1}$). Stavsvatn fulfils ALPE project criteria and is susceptible to acid deposition. Before 1860 the lake has a stable pH and supports a population of the planktonic diatom *Cyclotella kuetzingiana*. The carbonaceous particle record of the core STVN1 indicates that the lake has been subject to a low level of atmospheric deposition since the end of the 19th century, rising more rapidly from about 1966 and declining slightly at the present time. The onset of atmospheric deposition, indicated by the initiation of the carbonaceous particle record in the late 1800 s, is accompanied by a significant pH decline of 0.8 pH units in the period to 1930. pH continues to decline from 1930 until the present resulting in a decline of about 1 pH unit. Chironomid analysis supports the diatom evidence for a significant acidification.

3.4 PAIONE SUPERIORE

Two sediment cores were taken from Paione Superiore (14.10.91) in 13.7 m of water, close to the deepest point of the lake. PSUP1 was 21 cm long and PSUP2 was 19 cm long. Cores were also taken from the deepest point of a lower lake in the same valley, Paione Inferiore (15.10.91), in 14 m of water, but these cores have not been analysed.

3.4.1 Lithology and core correlation

Both cores from Paione Superiore consisted of dark brown mud with some mineral particles (mostly < 1 mm diameter) and irregular bands of lighter coloured mud. Towards the surface of both cores the sequence graded towards a blacker sediment. The results of wet density, percentage dry weight and percentage loss on ignition analyses of PSUP1 and percentage dry weight and percentage loss on ignition analyses of PSUP2 are presented in Figure 3.4.1.

Overall the core PSUP1 has a high mineral content, reflected by high percentage dry weight values (25 - 60%), and a low organic content, reflected by low percentage loss on ignition values (4 - 15%). From the base of PSUP1, at 20.5 cm, to 12.5 cm wet density, percentage dry weight and percentage loss on ignition profiles are relatively stable at 1.22 - 1.31 gcm^{-3}, 30 - 37% and

11 - 15% respectively. Maximum wet density (1.60 gcm^{-3}) and percentage dry weight (60%) values are attained at 11.5 cm depth with a corresponding minimum in percentage loss on ignition (4%). Wet density and percentage dry weight decline to minimum values at 7.25 cm (1.22 gcm^{-3} and 26%) whilst percentage loss on ignition increases to 13%. A second maximum in wet density occurs at 3.9 cm (1.43 gcm^{-3}) and percentage dry weight increases to 36 - 40% between 3.75 - 6.25 cm. Percentage loss on ignition reaches a maximum of 15% at 6.75 cm and declines to 7% at 3.75 cm. Wet density and percentage dry weight show overall declines towards the surface reaching minima of 1.19 gcm^{-3} and 26% respectively, however there is a peak in percentage dry weight (33%) at 2.25 cm. Percentage loss on ignition increases to a maximum of 13% at the sediment surface.

The core PSUP2 shows similar trends in percentage dry weight and percentage loss on ignition to those seen in PSUP1 with a series of sharp peaks and troughs seen particularly in the dry weight profile. A high mineral content is indicated by PDW values of 19 - 54% and a low organic content is shown by LOI values of 4 - 18%. From the base of the core at 18.5 cm to 12.5 cm PDW varies from 30 - 39% and LOI varies from 12 - 14%. Corresponding maxima and minima occur at 11.5 cm in PDW (54%) and LOI (4%) respectively. PDW declines to 36% at 8.5 cm and LOI increases to 12% at the same level. PDW increases to 48% at 7.75 cm, decreasing to 28% at 7.25 cm and with sharp peak values of 38% and 39% at 5.75 cm and 4.25 cm respectively. LOI values consistently show an inverse relationship with the maxima and minima seen in PDW, however the magnitude of the variation in LOI is less than that of PDW values. PDW shows an overall decline from 4.25 cm to the surface where there is a minimum value of 19%. Corresponding with the decline in PDW, LOI values increase to 13% at the sediment surface.

The high mineral content of the sediments and spiky WD and PDW profiles of the cores from Paione Superiore, indicate that a considerable proportion of sediment material is derived from the lake catchment. Further, events of accelerated catchment erosion are recorded in the lake sediment by peaks in the WD and PDW profiles and reduced LOI values, for example at 11.5 cm depth in both PSUP1 and PSUP2. These events of increased catchment erosion may be directly related to local climatic variation, such as increased precipitation, or alternatively they may reflect episodic collapse of surrounding slopes and inwash of material.

3.4.2 Radiometric measurements and dating

The results of ^{210}Pb and ^{226}Ra analyses are given in Table 3.4.1, and shown graphically in Figure 3.4.2. The ^{137}Cs, ^{134}Cs and ^{241}Am results are given in Table 3.4.2 and Figures 3.4.3 and 3.4.4.

^{210}Pb chronologies have been calculated using both the CRS and CIC ^{210}Pb dating models (Appleby and Oldfield 1978) and the results are shown in Figure 3.4.5. Down to a depth of 2.25 cm (dated to 1961 by the CRS model) the two models are in relatively good agreement, both indicating a more or less constant sedimentation

rate of 0.027 ± 0.002 g cm-2 y-1. For the section of the core from 2.5 cm down to 4.25 cm (dated 1917 by the CRS model) the calculations suggest a significantly lower sedimentation rate of 0.016 ± 0.002 g cm-2 y-1. The transition to higher sedimentation rates about 1960 appears to be very abrupt, and as a consequence CIC model dates beneath this level are significantly younger than those given by the CRS model. The sharp decline in unsupported ^{210}Pb activity between 2.5 cm and 2.25 cm is indicative of a dilution of the atmospheric flux, in accordance with the CRS model. There is a similar feature at a depth of 4.75 cm, though this appears to represent a relatively brief episode of accelerated sedimentation dated to about 1910. Dilution events violate the assumptions of the CIC model, and the ^{210}Pb dates given in Table 3.4.3 have accordingly been based primarily on the CRS model. Significant differences between the two occur however only in sediments prior to 1960. Accumulation rates prior to 1900 are difficult to assess, but appear to be typical of those for the period 1920 - 1960.

The ^{137}Cs record (Figure 3.4.3a) is dominated by very heavy fallout from the 1986 Chernobyl accident. The Chernobyl origin of the bulk of the ^{137}Cs is confirmed by the parallel ^{134}Cs record (Figure 3.4.3b), ^{134}Cs derives from Chernobyl fallout alone and has been corrected for decay since 5th May 1986. Chernobyl derived ^{137}Cs activities in the near-surface sediments are two orders of magnitude higher than those from weapons test fallout. The ^{137}Cs inventory of the core was calculated to be 145.6 ρCi cm-2 (53900 Bm m-2). Because of the large disparity in values, it was not possible to use the ^{134}Cs record to achieve an accurate partition of the ^{137}Cs into its Chernobyl and weapons test components. As a consequence, the depth recording the 1963 weapons fallout peak could not be determined. A small peak in ^{241}Am activity (Figure 3.4.4), also a fallout product from nuclear weapons testing (Appleby *et al.* 1991), was observed in the 1.25 - 1.5 cm sample. The ^{210}Pb chronology suggests that the 1963 level should occur at a depth of about 2 cm. However, since ^{241}Am was detected in just a single sample, and the 1.5 - 2 cm sample was not measured, the ^{241}Am record is not sufficiently definite to shed any doubts on the reliability of the ^{210}Pb chronology.

3.4.3 Carbonaceous particle analysis

The carbonaceous particle (CP) record in the core PSUP 1 (Figure 3.4.6) starts between 5.0 and 5.5cm depth which corresponds to the ^{210}Pb dates of 1899 ± 7 to 1906 ± 5. From about 2.0 - 2.25cm (1961-1965 ± 2) to the surface (1991) there is a rapid and steady increase in CP concentration and flux with a small levelling off at about 1cm depth (1979 ± 2). There is no surface decline in concentration or flux. The surface flux of 4094 cm^{-2} yr^{-1} is similar to the highest fluxes observed in the U.K. (i.e. Tunnel End Reservoir, North Pennines - 5755 cm^{-2} yr^{-1} and Loch Grannoch, Galloway - 2800 cm^{-2} yr^{-1}). The surface concentration is also very high, again, as high as peak concentrations in polluted areas of U.K. e.g. Round Loch of Glenhead, Galloway, Scotland or in the French Vosges mountains e.g. Lac de Gerardmer (Kreiser *et al.*, 1992).

Guilizzoni *et al.* (1992) produced carbonaceous particle profiles for two sediment cores taken from Italian alpine lakes, Paione Superiore and Lake Leit, in 1989. The profiles they described for Paione Superiore showed similar trends to that shown in Figure 3.4.6 although the increase in concentration was less dramatic and the surface concentration was much lower, approximately 8000 gDM^{-1}. The Lake Leit core again showed similar trends (short profile, surface maximum) but in this core the maximum concentration was even lower, approximately 2000 gDM^{-1}.

3.4.4 Diatom analysis and pH reconstruction

A summary diatom percentage diagram is plotted (Figure 3.4.8) which shows the profiles of the 18 diatom taxa which occurred at abundances of more than 2% in any sample. A total of 84 taxa from the SWAP dataset were identified in the 12 levels counted.

Diatom cell concentrations for the core are presented in Figure 3.4.7. From the base of the core to a depth of approximately 1.5 cm cell concentration remains stable at around 0.6×10^8 - 1.0×10^8 cells g^{-1} DW. However, at 8.5 cm the cell concentration falls to a minimum (0.4×10^8 cells g^{-1} DW), coinciding with a peak in the abundance of *Pinnularia biceps* (see below) and with high, but falling PDW. Diatom analysis was not performed at the level of maximum PDW and minimum LOI, but the dilution of diatom cells close to this level would support the hypothesis that there is accelerated catchment erosion in this part of the sequence. From a depth of about 1 cm to the top of the core diatom cell concentration increases sharply reaching a maximum of over 4×10^8 cells g^{-1} DW.

At the base of the core (20.5 cm and 16.5 cm) the diatom assemblages are dominated by *Pinnularia microstauron* (maximum 40%), *Achnanthes helvetica* var. *minor* (maximum 17%) and *Achnanthes marginulata* (maximum 14%). At 12.5 cm there is an increase in *Achnanthes scotica* (16%) and also *Pinnularia biceps* (11%) and *Achnanthes helvetica* (10%). *Pinnularia microstauron* continues to be well represented (21%), as it is throughout the core, whilst the percentages of other taxa abundant at the base of the core, *Achnanthes marginulata* (8%) and *Achnanthes helvetica* var. *minor* (6%) are slightly depressed. At 8.5 cm *Pinnularia biceps* increases to a maximum of 20% and *Achnanthes marginulata* reaches a maximum of 19%. *Pinnularia biceps* and *Achnanthes marginulata* decline and from just below 4 cm there are increases in *Aulacoseira lirata* var. *alpigena* and *Cymbella hebridica*. These 2 diatoms reach maximum abundances between 1 - 2 cm (14% and 11% respectively). There are minor peaks in *Neidium affine* var. *longiceps* (7%) at 4.25 cm, and *Neidium affine* (4%) and *Neidium affine* var. *amphirhynchus* (3%) at around 3 cm. In the top 2 cm of the core *Achnanthes helvetica* var. *minor* increases to a maximum of 25% along with *Achnanthes helvetica* (maximum 11%) and *Achnanthes marginulata* (maximum 14%). In the surface 1 cm there are small but significant increases in *Eunotia exigua* (maximum 8%) and *Aulacoseira distans* var. *nivalis* (maximum 4%).

The reconstructed pH is presented with the summary diatom diagram (Figure 3.4.8). The reconstructed pH shows negligible variation throughout the core and is in the range 5.1 to 5.2 throughout. The measured lakewater pH for Paione Superiore for the period 1991 - 1992 was 5.32. (Ca 1.3 mg l-1)

Despite the fluctuations in the floristic composition of the diatom assemblages the reconstructed pH reflects little of their variation. This is probably the result of a combination of 2 factors. Firstly the modern diatom/lakewater pH data-set used in the WA reconstructions lacked some taxa common in the PSUP1 core. pH optima were therefore unavailable for these diatoms and they were omitted from the reconstruction for example the taxon *Achnanthes helvetica* var. *minor*. The second factor may have been the source habitats of diatoms reaching the lake sediment. The accelerated inwash of inorganic sediment from the catchment in the middle part of the core may have altered lake water chemistry and itself may have introduced terrestrial diatoms to the lake (*Pinnularia biceps*) immediately before the period when atmospheric contamination reached a maximum. Another aspect of this problem is that *Pinnularia microstauron* was most probably growing *in situ* on sediments, it is therefore abundant in the core. This species has also been found in the epipelon of Spanish mountain lakes (Flower *pers. comm.*) Thus any change in the floristic composition of the diatoms as a result of increased atmospheric deposition eg. the small but significant increases in acidobiontic diatoms such as *Aulacoseira distans* var. *nivalis* and *Eunotia exigua* at the top of the core are swamped by species better represented in the core.

3.4.7 Chironomid head capsule analysis

Table Chir. X-3 shows the chironomids found in the 11 core samples analyzed from the lake. The sample from the bottom of the core contained 12 taxa, however, at least 3 of these (*Bryophaenocladius* sp., *Limnophyes* sp., and *Pseudosmittia* sp., and probably also *Chaetocladius* sp.) are partly or completely terrestrial. These species are therefore likely to have been introduced from the lake catchment. Disregarding these species the other samples analysed contained between 4 and 7 taxa (Chir. Fig. 5), typical of sublittoral chironomid communities at these altitudes in the Alps (Bretschko 1975, Pechlander & Zaderer 1985). The two most important species were *Micropsectra radialis* and *Tanytarsus lugens*-group (sp. B), which together constituted between 79 and 92 % of the total number of specimens in the samples. It is not possible to state with certainty to which species within the *Tanytarsus lugens* species group the specimens belongs, however, the most likely taxon is *Tanytarsus lugens* Kieffer. Together with *Heterotrissocladius marcidus* and *Procladius* spp. these 4 taxa made up between 93 and 99 % of the chironomids. The relationship between the populations of *Micropsectra radialis* and *Tanytarsus* sp. B is shown in Chir. Fig. 6. The population of *Tanytarsus* sp. B started to increase in the beginning of this century, and the species gradually displaced *Micropsectra radialis* as the dominant chironomid in the deepest parts of the lake. Today (1992) only a small population of

Micropsectra radialis were found. Ecologically *Micropsectra radialis* and *Tanytarsus lugens* are regarded as good indicators of ultraoligotrophy and moderate oligotrophy, respectively (Brundin 1956, Sæther 1979). The development of these two chironomids unambiguously shows that Lago Paione Superiore is slightly eutrophicated and has changed to a more moderately oligotrophic lake during the last few decades. It is not likely that acidification is the reason for the observed changes, since both species are regarded as acid sensitive, *Tanytarsus lugens* even more so than *Micropsectra radialis* (Table Chir. X-6).

A new species belonging to the genus *Corynocera* Zetterstedt was found in the 0.5-0.25 cm sediment sample. Only the hypopygium (the genital segment at the tip of the adult male abdomen) remained, but this is very distinctive and clearly different from the two other species so far described in the genus. A taxonomic description of the new species is planned.

3.4.6 Site summary: Paione Superiore

Paione Superiore is a small lake, lying above the tree line and with little human disturbance in the catchment. The underlying geology is of gneiss and the lakewater has a low Ca concentration (Ca 65 $\mu eq\ l^{-1}$) with a mean 1991-1992 pH of 5.32. Paione Superiore fulfils ALPE project criteria and is susceptible to acid deposition. The onset of atmospheric deposition occurs around 1900, however reconstructed pH remains stable to the present. In contrast, in response to the rapid increase in atmospheric deposition from the early 1960s, there are significant changes in the diatom assemblages during the last 30 years, with a shift to more acid tolerant species. The concentration of carbonaceous particles is similar to that found in the most polluted upland lakes in the UK. Earlier shifts in the composition of diatom assemblages appear to be related to events of accelerated catchment inwash. Analysis of chironomid head capsules suggests that the recent changes in the fauna are the result of a slight eutrophication.

3.5 MILCHSEE (LAGO DI LATTE)

Two cores were taken from Milchsee (11.10.91) in 14.2 m water depth, the deepest part of the lake basin.

3.5.1 Lithology and core correlation

MILC1 was 25 cm long and MILC2 was 14 cm long; both cores were banded throughout by sediment of changing composition. The sediment varying from light brown, grey or blackish muds with mica-like inclusions to the lower layers of mud which had many small (<1 mm) stones and at the base predominantly sandy layers. The lithostratigraphic profiles of these cores are accordingly variable. The results of lithostratigraphic analyses of MILC1 (WD, DW and LOI) and MILC2 (DW and LOI) are plotted in Figure 3.5.1.

MILC1 shows an overall decrease in DW measurements from 46% at 23.5 cm to 10 % at the core top. The organic content of MILC1 is low with a slight trend towards increasing LOIs from the base of the core to the surface, from about 9 - 13%. WD declines from about 1.30 gcm^{-3} at the base of the core to 1.11 gcm^{-3} at the surface. However, superimposed on the overall lithostratigraphic trends are larger variations in the parameters measured, seen most clearly in the WD and DW profiles. In particular there are pronounced maxima in WD and DW at 12.5 cm (1.64 gcm^{-3}, 61%), 6.75 cm (1.36 gcm^{-3}, 40%) and 4.25 cm (1.26 gcm^{-3}, 31%), with corresponding minima in LOI values (2%, 5% and 7%) at the same levels.

MILC2 also has a low organic content and shows an overall trend towards decreasing DW and increasing LOI values. LOI reaches a maximum of 13% at the top of the core, increasing from a maximum value of about 10% at the base of the core. DW declines to around 18 - 20% at the top of the core. Three distinct peaks are seen in DW at 13.5 cm (46%), 8.5 cm (44%) and 5.5 cm (42%) with corresponding minima in WD (5%, 6%, and 7%).

The high mineral and low organic content of the sediment cores from Milchsee reflect the catchment of the lake, which is dominated by bare rock surfaces with negligible development of soils or peat. The sharply defined peaks in DW and WD with corresponding minima in LOI record events of accelerated catchment erosion.

3.5.2 Radiometric measurements and dating

The results of ^{210}Pb and ^{226}Ra analyses are given in Table 3.5.1, and shown graphically in Figure 3.5.2. The ^{137}Cs, ^{134}Cs and ^{241}Am results are given in Table 3.5.2 and Figures 3.5.3 and 3.5.4.

^{210}Pb chronologies have been calculated using both the CRS and CIC ^{210}Pb dating models (Appleby and Oldfield 1978) and the results are shown in Figure 3.5.5. Except for the top 2 cm of the core, there are significant differences between the two sets of dates. The CRS model suggests that although there have been quite large fluctuations in the sedimentation rate over the past 100 years, there has been a significant net decline in accumulation during the past 50 years. The episodes of high sedimentation rate, dated about 1954, 1926 and 1880, appear to coincide with zones of inorganic sediments in the core with high dry bulk densities, and may represent intermittent inwash events. A consequence of the decline in sedimentation rates is that CIC model dates are necessarily younger than those given by the CRS model.

The high ^{134}Cs activity in the surficial sediments (Figure 3.5.3b) indicates that a significant proportion of the ^{137}Cs activity at this level (Figure 3.5.3a) derives from the fallout from the 1986 Chernobyl accident. The ^{134}Cs derives from Chernobyl fallout alone, and has been corrected for decay since 5th May 1986. The ^{134}Cs can be used to partition the total ^{137}Cs into its Chernobyl and weapons test components, and the weapons test ^{137}Cs determined in this way is plotted in Figure 3.5.4a. The Chernobyl ^{137}Cs has

a maximum value in the 0.75 - 1.0 cm sample, and this would appear to denote the 1986 level in the core. The weapons ^{137}Cs has a maximum in the 1.5 - 1.75 cm sample which would appear to denote the 1963 level. The ^{241}Am profile (Fig. 3.5.3), also an indicator of the 1963 level (Appleby *et. al.* 1991), has a peak value in the 2.0 - 2.25 cm sample. The Chernobyl ^{137}Cs date (Figure 3.5.5) is in good agreement with the ^{210}Pb dates. The weapons fallout date however, although in good agreement with the CIC model, shows a significant discrepancy from the CRS model dates, which put the 1963 level at just below 3 cm. The two artificial radionuclide dates taken together suggest a hiatus in the sediment record during the period 1963 - 1986, the mean sedimentation rate for this interval being only about a third of that for other time intervals.

Since the non-monotonic features of the ^{210}Pb profile are evidence of the dilution of the atmospheric ^{210}Pb flux, in contradiction to the basic assumptions of the CIC model, the CRS model would appear to be more appropriate in spite of the conflict with the 1963 fallout date. Using the techniques indicated in Oldfield & Appleby (1984), a composite CRS model chronology can be constructed using the weapons test date as a reference level. The raw CRS model ^{210}Pb dates for this core are given in Table 3.5.3. The adjusted values are given in Table 3.5.4. In the absence of any conclusive evidence for a sediment hiatus, the two sets of values should give a reasonable guide to the range of possible dates for the core.

3.5.3 Carbonaceous particles

For the MILC 1 core the CP record begins between 6.0 and 7.5cm depth (1926 ± 3 and 1911 ± 5) (Figure 3.5.6). NB. For the reasons stated above, the dates used here are adjusted CRS model dates (Table 3.5.4). A rapid increase in concentration starts between 2.5 and 3.0cm depth (1953 - 1958 ± 2) although this is less marked in flux terms. Towards the surface of the core there are a number of fluctuations in both concentration and flux profiles and these may be due to inwash events evident from the lithostratigraphy of this core (Figure 3.5.1). A surface decline occurs in both profiles but the peaks occur at slightly different times. The peak in concentration occurs at 0.75 - 1.0cm (1980 - 1983 ± 2) and the peak in flux occurs at 0.25 - 0.50cm (1986 - 1989 ± 2). Both surface concentration and flux are lower than for Paione Superiore by an order of magnitude

3.5.4 Diatom analysis and pH reconstruction

A total of 114 diatom taxa were recorded in the core MILC1, of these 24 species occurred at abundances of greater than 2%. A summary percentage diatom diagram showing the reconstructed pH is presented in Figure 3.5.8. Diatom cell concentrations for MILC1 are presented in Figure 3.5.7 concentrations vary from about 2 $x10^8$ cells g^{-1} dry weight, to a maximum of about 12 $x10^8$ cells g^{-1} dry weight. Higher cell concentrations generally coincide with peak percentage abundances of the diatom *Synedra acus*.

The base of the core from 16.5 - 24.5 cm is dominated by *Achnanthes minutissima* (maximum 29%) and other non-planktonic species such as *Achnanthes lacus-vulcani* (maximum 10%) and *Fragilaria brevistriata* (maximum 11%). Between 16.5 cm and 12.5 cm there is a sharp increase in *Synedra acus* from percentages of less than 1% to a maximum of 73%. The peak in *Synedra acus* correlates with the increase in DW and decrease in LOI seen in the lithostratigraphic profile. This species decreases to 20% at 8.5 cm but continues to dominate the assemblage, along with *Achnanthes lacus-vulcani* (11%), *Navicula digitulus* (maximum 6%) and other *Achnanthes* spp. *Synedra acus* increases again reaching 54% at 6.25 cm and 62% at 4.25 cm. It seems likely that these high abundances nearly relate to 2 peaks in DW seen in the lithostratigraphic profile at 6.75 cm and 4.25 cm. *Synedra acus* declines to 12% at 1.125 cm whilst *Achnanthes minutissima* increases to 18% at 2.125 cm, *Achnanthes lacus-vulcani* increases to 19% at 1.125 cm and *Fragilaria breviatriata* reaches a maximum of 8% at 0.625 cm. *Synedra acus* increases to 28% in the surface sample and there are also low percentage peaks in species such as *Navicula pupula*, *Fragilaria construens* var. *venter* and *Stauroneis anceps* fo. *gracilis*.

From the base of the core to 16.5 cm reconstructed pH declines from 6.4 to a minimum of 5.7, increasing to a maximum of 6.8 at 12.5 cm. The pH declines to 6.2 at 8.5 cm, increasing to 6.8 at 4.25 cm and then declining to 6.4 at the surface. The fluctuations in reconstructed pH following the rise in *Synedra acus* are driven to a large extent by this species, whose abundance appears to be related to events of accelerated catchment erosion. The measured pH of Milchsee was in the range 6.66 - 6.80.

3.5.7 Chironomid head capsule analysis

Table Chir. X-4 shows the chironomids found in the core from Lago di Latte, while Chir. Fig. 7 illustrates the number of specimens and number of taxa found. Four samples from the core were analysed. The lake has a very species-poor chironomid community which apparently has been stable during the last century. This is also confirmed by the present chironomid fauna which is similar to the one found in the core. At the 13-14 cm level only 3 specimens were found; at the same time the wet density and dry weight profiles shows pronounced maxima, indicating inwash events from the catchment of the lake (Figure 3.5.1). The chironomid species composition is typical of lakes in the area (Bretschko 1975, Pechlander & Zaderer 1985) and is regarded as unaffected by human activity.

3.5.6 Site summary: Milchsee

Milchsee (Lago di Latte) is a small corrie lake, lying above the tree line and with minimal human disturbance in the catchment. The underlying geology is of gneiss and the lakewater has a rather higher Ca concentration (Ca 93 $\mu eq\ l^{-1}$) than other ALPE sites investigated in the sediment studies. The 1991 pH ranged between 6.66 - 6.80. Milchsee fulfils some ALPE project criteria

in that it is a remote and undisturbed site, however lakewater chemistry suggests that the site is well buffered and would be unlikely to respond to acid deposition. The same reasoning applies to Langsee (Lago Lungo) the larger lake, close to Milchsee, studied in the ALPE project. In addition the recent damming of the Langsee outflow made this lake unsuitable for sediment investigations, Milchsee was therefore selected as the less disturbed site. The onset of atmospheric deposition at Milchsee occurs around 1920 and there is a rapid increase in carbonaceous particle concentrations from the mid-1950s. There are however no perceptible changes in the diatom flora in response to acid deposition. The primary factor affecting diatom assemblages appear to be events of accelerated catchment inwash and of particular interest is the appearance in abundance of *Synedra acus* in the mid-19 th century.

3.6 LOCHNAGAR

Two cores were taken from Lochnagar during June 1991 from the deepest point of the lake, in 24 m of water

3.6.1 Lithology

WD and DW profiles (Figure 3.6.1) for NAG6 indicate little change in sediment composition other than a slight overall decline in DW, from a maximum of 14% at the base of the core to 10% immediately below the surface, falling to 7% in the surface level. A maximum DW of 15% occurs at 13.5 cm falling to a minimum of 8% at 10.5 cm. WD values are fairly stable with a maximum of 1.10 g cm^3 at the base of the core and a minimum of 1.05 g cm^3 at 5.75 cm and a slight increase to 1.09 g cm^3 at the surface.

3.6.2 Radiometric measurements and dating

The ^{210}Pb and ^{226}Ra results are given in Table 3.6.1, and shown graphically in Figures 3.6.2 & 3.6.3. The ^{137}Cs and ^{241}Am results are given in Table 3.6.2 and Figures 3.6.4 & 3.6.5. In Figures 3.6.2 - 3.6.5, results for the present core, NAG6, are compared with those from and earlier 1986 core, NAG3 (for details of the earlier core see Jones *et.al.* 1993)

^{210}Pb chronologies have been calculated using both the CRS and CIC ^{210}Pb dating models (Appleby and Oldfield 1978) and the results are given in Figure 3.6.6. The determination of dates near the base of the core is a little problematical in view of the relatively high ^{226}Ra concentrations in the sediments of this lake. The bottom three samples appear to be just above the ^{210}Pb equilibrium level, but the unsupported activities have a large uncertainty which significantly affects the CRS model calculations. In order to minimise this effect, CRS model dates have been calculated using the 11.5 cm level as a dated reference point (Oldfield & Appleby 1984). The date of this level has been determined by an iterative procedure which makes use of the fact that sedimentation rates appear to have been fairly constant

between the 5.75 cm and 11.5 cm levels, the mean value during the period spanned by this interval being about 0.0095 g cm^{-2} yr^{-1}. The CRS model chronology, summarised in Table 3.6.3, dates the 5.75 cm level to 1958, and suggests that sedimentation rates since that time have increased substantially, the mean post-1960 value being 0.018 g cm^{-2} yr^{-1}. A similar acceleration in sedimentation rates dating from the same time was observed in the 1986 core. Because there is virtually no change in ^{210}Pb activity between the 5.75 cm and 1.25 cm levels, CIC model dates for this part of the core are not very meaningful. The maximum ^{137}Cs activity in the core occurs in the topmost samples and is presumably due to fallout from the Chernobyl accident. Since ^{134}Cs activities were below the limits of detection, it was not however possible to partition the ^{137}Cs activity into its Chernobyl and weapons fallout components. ^{241}Am, which derives solely from weapons test fallout (Appleby *et al.* 1991), was detected between the 3.75 cm and 5.75 cm levels in the core (Figure 3.6.5). Because of the high ^{238}U concentrations, the low activities of this radionuclide are difficult to measure accurately. Nonetheless it would seem reasonable from the distribution to place the 1963 level recording the weapons test fallout maximum at 4.75 ± 1.25 cm. As shown in Figure 3.6.6, this date is in excellent agreement with the CRS model ^{210}Pb chronology, and confirms the recent increase in sedimentation.

3.6.3 Carbonaceous particles

The CP record for the core NAG 6 starts in the mid-19th century before the start of the ^{210}Pb chronology (Figure 3.6.7). CP concentration and flux increase slowly up to 4.5 - 5.0cm (1964 - 1967 ± 2) where both profiles rapidly increase to a peak at 2.5 - 3.0cm (1976 - 1979 ± 2). From this point to the surface there is a general decline in both profiles except for the surface sample where concentration increases once more.

Many Scottish lake sediment cores have been analysed for carbonaceous particles. In general, the start of the particle record falls between 1840 and 1870, the rapid increase in concentration between 1940 and 1960 and the peak in particle concentration between 1974 and 1980 (Rose, 1991). The NAG 6 core agrees well with these dates except for the rapid increase where it is later than usual.

3.6.4 Diatom analysis and pH reconstruction

A summary diatom diagram showing diatoms occurring at abundances of greater than 2% is presented (Figure 3.6.8), taxa are ordered left to right according to their weighted average abundance.

At the base of the core diatom assemblages are dominated by *Achnanthes scotica* (maximum 13%), *Achnanthes minutissima* (maximum 8%) and *Fragilaria virescens* var. *exigua* (10%). *Eunotia incisa* increases to a maximum abundance of 19% at 10.5 cm and *Achnanthes marginulata* increases from 6% at 14.5 cm to 48% at 5.25 cm. Species dominant at the base of the core decline and *Achnanthes marginulata* becomes dominant remaining at abundances of 40 - 49%

to the top of the core. Percentages of *Aulacoseira distans* var. *nivalis* increase in the top 5 cm of the core, reaching a maximum of 15% at 0 - 0.25 cm. There are also increases in the percentages of other *Aulacoseira* spp. along with *Achnanthes helvetica* var. *minor* (maximum 7%) and *Achnanthes altaica* var. *minor* (maximum 3%).

Reconstructed pH falls from 5.5 at the base of the core (16.5 - 14.5 cm) to 5.0 at 6.75 cm, declining to a minimum of 4.9 at 0.625 cm. Between 1986 and 1991 annual mean pH varied between 5.0 and 5.4 with a value of 5.3 in the year 1990 - 1991. The reconstructed pH of the surface sediment (5.0) from NAG6 is therefore somewhat lower than the measured values but within the range of the reconstruction method.

3.6.5 Site summary: Lochnagar

Lochnagar is a corrie lake lying above the tree line, having a small catchment with minimal anthropogenic disturbance. The granitic geology and resulting low lakewater Ca concentration (Ca 30 $\mu eq\ l^{-1}$) indicate that this lake is susceptible to acid deposition, a sensitive site fulfilling all ALPE project criteria. The carbonaceous particle record of the core NAG6 indicates that the lake has been subject to significant atmospheric deposition beginning in the mid-19th century and rising rapidly from the mid-1960s to a maximum in the late-1970s and declining from then until to the present time. Reconstructed pH declines by 0.5 units between the mid-19 th century and 1950 declining to a minimum of 4.9 just below the surface. There is an increase in reconstructed pH of about 0.1 unit at the surface perhaps corresponding with the overall decrease in atmospheric deposition since the late-1970s.

4 DISCUSSION

4.1 DISCUSSION: CARBONACEOUS PARTICLE RECORD

The timing and main features of the carbonaceous particle profiles from ALPE1 sites are summarised in Table 4.1.1. The carbonaceous particle profiles presented here for Milchsee and Etang d'Aube represent the first reported profiles for lakes in the Italian Tyrol and French Pyrenees respectively. Consequently, it is difficult to ascertain how well the profiles represent the depositional record in these areas. In ALPE 2 other sediment cores from nearby areas (i.e. Austria and Spanish Pyrenees) will be analysed and hopefully will be able to confirm the results.

In the meantime, it is possible to compare the carbonaceous particle profiles with United Nations' energy statistics data (United Nations 1952, 1976, 1979, 1981, 1986, 1990, 1992) to ascertain whether the carbonaceous particle profile reflects the fossil-fuel combustion record of the country. Atmospheric pollutants are, of course, trans-boundary and it may be that at sites close to national boundaries the particle record reflects the combustion history of a neighbouring country (especially

where the 'receptor' country burns little fossil-fuel e.g. Norway) or at least has components from more than one country as has been seen in the French Vosges mountains (Kreiser *et al.*, 1992).

The two Italian sites show examples of this. As outlined above, the carbonaceous particle profile for Paione Superiore in the Italian Alps shows the start of the particle record at the turn of the century and a rapid increase in concentration from the early 1960's. There is no surface decline but there is a slight levelling off dated to 1979 ± 2 years. This is shown in Figure 3.4.6. Figure 4.1.1 shows the United Nations statistics for electricity production by type (i.e. thermal, hydroelectric, nuclear and geothermal) in Italy between 1929 and 1990. The thermal production of electricity is produced by the combustion of fossil-fuels and so it is this record which is of interest. The figure shows that there was a low amount of fossil-fuel combustion taking place until the early 1960's when there was a more rapid increase in production until the present day. There is one period when thermal production of electricity does not increase and that is in the late 1970's/ early 1980's. In short, the carbonaceous particle profile for Paione Superiore is very similar to the record of fossil-fuel combustion for Italy (see Figure 4.1.2). One conclusion that can be drawn from this is that the majority of carbonaceous particles (and by inference other products of fossil-fuel combustion e.g. SOx, PAH) deposited on Paione Superiore originate from Italy itself.

Paione Superiore is only about 70 km from Milan. Industry and electricity production in this area are most likely to be the sources of these particles. This site is close to the Swiss border (and 130km south-east of Bern) but it is unlikely that many of the particles are derived from Switzerland as very little energy is produced by fossil-fuel combustion (2.2% ≡ 1158 million kW hours in 1989). The majority of electricity is produced from hydroelectric (55.4%) and nuclear (42.4%) production (United Nations, 1991).

The carbonaceous particle profile for Milchsee in the Italian Tyrol (Figure 3.5.6), however, does not follow the same pattern as that of Paione Superiore, or therefore, Italian fossil-fuel combustion history. The particle profile starts later than Paione, in the early part of this century and there is a slower but more steady increase in concentration until the 1950's when there is a more rapid increase to a peak concentration in the mid-1970's. After the mid-1980's there is a general decrease in particle concentration to the sediment surface, although the particle flux generally tends to increase. This region of Italy is very close to the Austrian border and it can be seen from Figure 4.1.3 that the particle flux profile for Milchsee is more similar to the thermal electricity production graph for Austria. This suggests that the majority of deposition at this site is derived from Austrian sources, although there is still likely to be an Italian input.

Wind direction data from two nearby weather stations, Brenner Pass (just to the north-west of the site) and Mayrhofen (25km further north-west) suggest that the main wind directions in this region are from due north (337.5° - 022.5°) and due south (157.5° - 202.5°). In autumn and winter the direction is fairly evenly shared between these two but in spring and summer the dominant direction is from the north (Steinhauser, 1982). Innsbruck is 60 - 70 km north-north-west of the site and Munich is approximately 150 km distant in the same direction. To the south, Bolzano is 30 - 40 km, Trento is about 80 km and Verona is 140 - 150 km away. It seems likely, therefore, that the particles are derived from both Austria and Italy with Austria contributing the larger share. It is quite possible that some will have travelled from Germany.

The two Norwegian sites, Øvre Neådalsvatn in mid-Norway and Stavsvatn in southern Norway show much lower carbonaceous particle concentrations (by 1-2 orders of magnitude) than the Italian sites. The surface concentration (and maximum) for Øvre Neådalsvatn (1319 gDM^{-1}) is less than half of that for Stavsvatn (3591 gDM^{-1}) and less than a third of the maximum concentration (4108 gDM^{-1}), although the surface fluxes of the two lakes are fairly similar (12 and 14 cm^{-2} yr^{-1} respectively).

Energy statistics for Norway show that almost all electricity production is produced from hydroelectric means and very little by the combustion of fossil-fuels (less than 0.5% in 1990, United Nations, 1991) (Figure 4.1.4). Because of this and because lakes in southern Norway show higher levels of acidification than those further north, it has been suggested that the majority of fossil-fuel derived pollutants (e.g. acid deposition, carbonaceous particles) are transported from other countries. The Co-operative Programme for Monitoring and Evaluation of the Long-range Transmission of Air Pollutants in Europe (EMEP) has clarified the amounts and origins of deposited sulphur and nitrogen in Norway and concluded that the vast majority originates from outside Norwegian boundaries (Alcamo *et al.*, 1990). The carbonaceous particle record for Stavsvatn begins in the second half of the 19th century whereas that of Øvre Neådalsvatn begins in 1920 - 1940. This difference may be due to local sources in southern Norway as long-range transport of particles is more likely to effect both lakes at more or less the same time.

The particle profiles for both lakes increase to the surface although that of Stavsvatn shows a slight decline in the surface sample. Swedish energy statistics show that although considerably more fossil-fuel was burned to produce electricity in Sweden than in Norway, a peak in combustion occurred in the 1970's and there has been a decline since that time. It is unlikely then, that Sweden is the main source of carbonaceous particles.

Long term wind direction data exist for stations close to both of the Norwegian sites (Johannesson & Håland, 1969). Dalen i Telemark (59°27'N 8°00'E) is near Stavsvatn (59°38'N 8°07'E) and Gjermundnes (62°37'N 7°10'E) near Øvre Neådalsvatn (62°46'N 9°00'E). The dominant wind direction all year for Dalen i

Telemark is north of west (285°-315°) and to a lesser extent west (255°-285°). Winds from the south-east (105°-165°) are more frequent between March and August but never dominate the westerlies. At Gjermundnes the prevailing wind direction is west of south (195°-225°) between September and April (especially in December and January) and north of west (285°-315°) between May and August. These data suggest that carbonaceous particles in the Norwegian lakes could be derived from the United Kingdom and also possibly from Central Europe.

The carbonaceous particle profile for Etang d'Aube in the French Pyrenees is similar in shape to that of Paione Superiore although the concentrations and fluxes are an order of magnitude lower. Both cores have low accumulation rates but in the Aube core the particle profile appears longer due to an inwash event between 3.5 - 6.0 cm. The Aube particle profile resembles neither the French nor the Spanish record of thermal production of electricity both of which have declined since the 1970's due to an increase in nuclear power. This lack of correlation may be due to the low sediment accumulation rate for this site giving low temporal resolution. This, of course, may also be the reason for the Paione Superiore profile being the shape it is, in which case the correlation with Italian fossil-fuel combustion is merely coincidental.

The Lochnagar carbonaceous particle flux profile differs from other Scottish profiles in not closely resembling the fossil-fuel combustion record for the United Kingdom (Figure 4.1.5). From the start of the particle record to the 1950's and again from the mid-1970's to the mid-1980's the records compare well but in the interim period whilst fossil-fuel combustion increases, particle flux remains steady until in the 1970's when it increases dramatically to peak at about the same time as fossil-fuel combustion. This rapid increase is late compared with other Scottish cores (1940's - 1960's) which usually follow the fossil-fuel combustion record. Both the start of the particle record and the peak in concentration/flux occur at the same time as other Scottish cores (Rose, 1991). In the mid-1980's the particle flux decreases rapidly whilst the fossil-fuel combustion record remains fairly level. This could be due to a delayed sediment response to the implementation of particle arrestors on United Kingdom power stations in the 1970's. Similar delays in the sediment record of carbonaceous particles to deposition events have been suggested previously (Rose, 1991).

Carbonaceous particle analysis was also undertaken on a sediment core taken from Lochnagar in 1986 (Patrick *et al.*, 1989). In this instance, the start of the particle record occurred at the usual time although the rapid increase in particle concentration and the concentration peak occurred earlier than usual for Scotland (1930's and late 1960's respectively). This could be an artefact of the large sampling interval (analyses were only performed at every 1cm).

4.2 DISCUSSION: DATING, DIATOM ANALYSES & pH RECONSTRUCTION

The context of recent palaeoecological reconstruction rests on the quality of the chronology available in the investigation. At all six of the lakes investigated in the ALPE lake sediment programme it has been possible to produce useful chronologies using ^{210}Pb dating models and by comparison with the record of radioisotope fallout from nuclear weapons testing or the Chernobyl nuclear accident. Although problems with constructing a chronology might have been anticipated at such high altitude lakes, where lake sediments often have low organic content, slow accumulation rates and on occasions, for example in areas of granitic bedrock, high background ^{226}Ra making the determination of unsupported ^{210}Pb difficult (eg. Jones *et al.* in press) only in the case of Aube was the construction of a chronology particularly problematic. Here there appears to be unusual downward mobility of ^{210}Pb within the sediment profile and preferential absorption onto layers of different mineralogy. Nevertheless it has been possible to construct a chronology for Aube and the anomalous conditions found at this site are in themselves of interest. It is intended that radiometric analyses will be performed on the core AUBE2 at a later date for comparison with the conditions found in the primary core AUBE1.

An independent test of the accuracy of radiometric dating is to use the carbonaceous particle record as a proxy-dating method. The initiation and changes in the concentrations of carbonaceous particles in sediment cores from areas with known deposition histories can be used to derive a skeleton chronology which can be compared with the radiometric methods. This is illustrated above in the discussion of the carbonaceous particle profiles from Norway, Scotland, Italy and Austria and their comparison with appropriate fossil fuel combustion statistics and meteorological data. In each case where histories of likely sources are available they correspond quite well with the respective carbonaceous particle profiles and support the radiometric chronology.

Age/depth curves have been constructed for the six primary ALPE cores (Figure 4.2.1). With the exception of Aube (see above) the rates of accumulation are stable through time, ranging from Paione Superiore where less than 6 cm of sediment has accumulated during the last 100 years, to Lochnagar where over 12 cm of sediment has accumulated in the same period. In the other cores approximately 6 - 10 cm of sediment has accumulated during the same period. If the significant inwash event is ignored, Aube has a similar sediment accumulation rate to Paione Superiore. It should be noted that these accumulation rates refer only to the primary cores from each site taken in one area of the lake. Though the distribution of sediments in each lake was briefly surveyed before selecting a primary coring area, it is possible that areas of slightly faster accumulation exist which would give better resolution of environmental changes. Variation in sediment accumulation rates between closely spaced cores is demonstrated by the different accumulation rates of other cores taken from the same lakes. For example the slower accumulation rate of a core

taken from the Lochnagar in 1986 (Jones *et al.* in press) and the faster accumulation rate of a core taken from Paione Superiore (Guilizzoni *et al.* 1992). In each case the cores were taken from close to the deepest point of the lake, the same location as the ALPE cores. This effect can also be seen in the lithostratigraphic correlations of cores analysed for chironomids (Report of University of Bergen, Zoological Museum) used to produce a chronology from the primary cores. Distinct features of the lithostratigraphic profiles from Milchsee and Aube indicated consistently faster and slower accumulation rates in the respective backup cores despite their close proximity.

The ALPE study programme was specifically designed so that catchment disturbance was reduced to a minimum so that the major forces of change for the lakes would be regional rather than local. Since some lakes are situated within reach of densely populated areas minor human disturbance, resulting from recreational activities such as mountain walking, is inevitable. Non-intensive animal grazing would also be expected in the catchments of some lakes for example at the Alpine lakes. However, despite their sensitivity, at none of the sites is there any evidence for local human disturbance such as eutrophication. Only at sites eliminated from the sediment studies, for example Lac Rond in the French Alps, Etang d'Hillette in the French Pyrenees and Langsee in the Tyrol was there severe catchment disturbance or lake manipulation which made the sites unsuitable.

In some cases; Lochnagar, Stavsvatn, Ovre Neadalsvatn the lithostratigraphic profiles of sediment cores are relatively stable throughout or at least in the dated section of the core, suggesting that there has been minimal catchment disturbance. In contrast the lithostratigraphic profiles from Aube, Paione Superiore and Milchsee are spiky, reflecting the important contribution of minerals washed in from the catchment to lake sediment supply. However, at none of the latter sites was there any evidence for anthropogenic disturbance in the small lake catchments and it is assumed that these catastrophic episodes are 'natural' processes. Diatom analysis of the sediment cores supports the idea of catchment inwash. Aerophilous diatoms, able to survive in damp terrestrial environments were recorded in the cores from Aube and Paione Superiore, their peak abundances corresponding with inwash events. At Milchsee it appears that the appearance and abundance of *Synedra acus*, most probably a planktonic species, is directly related to inorganic inwash events. In this case changes in lakewater quality related to accelerated inwash events is the most likely link between species abundances and catchment erosion.

Dr. A.C. Stevenson (Dept. of Geography, University of Newcastle) has kindly undertaken pollen analysis on some of the ALPE cores. This work will provide further information on catchment stability and the behaviour of local and regional vegetation.

Unlike a large number of vascular plants, the majority of alpine diatom species are cosmopolitan across Europe and beyond (see for example Flower *et al.* in preparation). The composition of diatom

floras in alpine lakes is determined principally by water chemistry and local conditions in the lakes (see ALPE1 report on epilithic diatoms). Given the general similarity in alpine conditions it is not therefore surprising that a great many species are common to the six ALPE study sites. It is particularly interesting to find what appear to be high altitude forms recurrent in such lakes, for example *Achnanthes helvetica* var. *alpina* recently named from one lake, Lochan Uaine in the Cairngorm Mountains of Scotland (Flower & Jones 1989), was found in cores from Aube and Paione Superiore and has also been found by Schmidt & Psenner (1992) in Tyrolean lakes.

However, despite the general similarities in diatom floras from the ALPE sites the abundances of species are clearly different between sites. Before the onset of acid deposition we do not find a uniform diatom flora in the lakes. Sediment core diatom assemblages record the response of living diatom communities primarily to changes in water chemistry, but other factors, for example the introduction of terrestrial species (see above) and the influence of lake size on habitat diversity (compare the species richness of assemblages from the small lake Paione Superiore with those from the large Øvre Neådalsvatn), can be important. At two lakes, Milchsee and Stavsvatn sediment core diatom assemblages are considerably different from those found in the other ALPE study lakes. Stavsvatn in the past supported a population of the planktonic diatom *Cyclotella kuetzingiana*. The site is surrounded by blanket peat and is not far above the present tree line with development of some young coniferous trees in the catchment. The site is clearly a sensitive one but it is perhaps not the ideal analogue for higher altitude sites which have longer periods of ice cover and poorer development of peat or soil in the catchment. In contrast to Stavsvatn, Milchsee is a true alpine lake, a small corrie site with bare rock covering the majority of the catchment, however the site is not sensitive to acidification as a result of the high buffering capacity provided by the underlying rocks. This is reflected in the very different diatom assemblages recorded in the core from this site which, though containing elements of the floras found at other ALPE sites, are dominated by species characteristic of waters with higher base cation concentrations.

Although there is considerable variation amongst diatom assemblages from the other ALPE lakes, Øvre Neådalsvatn, Lochnagar, Aube and Paione Superiore, some elements link the floras and may be considered typical of alpine lakes lying on rocks of low buffering capacity. Planktonic diatoms are absent from the sediment core diatom assemblages from these lakes and the flora is therefore composed of non-planktonic species. The reasons for the absence of planktonic species from such lakes is unclear. It is presumably related to the long period of ice cover and perhaps low nutrient status of lakewater, although the second condition occurs in lower altitude oligotrophic lakes such as Stavsvatn and does not arrest plankton development. The non-planktonic flora of these lakes is dominated by a characteristic suite of Achnanthes and Aulacoseira taxa and other species such as Cymbella perpusilla (see for example Flower *et al.* in prep).

These diatoms are transported from their lifetime habitats attached to rock and plant surfaces in the photic zone, and in the case of lakes like Paione Superiore where photosynthetically active radiation penetrates to the profundal zone, the sediment assemblages will include epipelic species such as *Pinnularia microstauron* deposited *in situ*

The evidence for acidification derived from sediment core diatom assemblages and reconstructed pH is summarised in Table 4.2.1. In summary two of the study sites Stavsvatn and Lochnagar have been found to have acidified significantly, by about 1 pH unit and 0.6 pH units respectively. This is consistent with their acid sensitive nature and situation in areas of significant sulphur deposition. Stavsvatn, lying in southern Norway is subject to deposition of around 1.0 g m-2 a-1 S (Eliassen *et al.* 1988) an amount comparable with that impacting on acidified lakes in the Galloway region of South-west Scotland. Lochnagar lies in a slightly cleaner area with moderate deposition levels (Jones *et al.* in press), but clearly cannot be regarded as pristine.

Øvre Neådalsvatn, despite being subject to a detectable level of atmospheric contamination, recorded in the carbonaceous particle profile, remains relatively unaffected by the impact of acid deposition. This is consistent with the situation of this lake in mid-Norway in an area of low sulphur deposition (Eliassen *et al.* 1988).

Etang d'Aube, is subject to a moderate level of sulphur deposition, the flux of carbonaceous particles at this site is rather less than that recorded at Lochnagar for example. A slight acidification is detectable, however the sediment record is interrupted by a large inwash event during the period of interest.

Paione Superiore has been subject to a rapidly increasing level of atmospheric deposition in the last 3 decades . A clear response is recorded in the diatom assemblages during this period however, for reasons discussed below and in the site discussion this response is not shown in the pH reconstruction.

Milchsee lies in an area of moderate sulphur deposition, however because of the high base cation content of the lakewater this site is not sensitive to lake acidification.

The pH reconstructions performed in this first stage of the ALPE project have been based on the SWAP calibration set (Stevenson *et al.* 1991). Surface sediments from the six lakes investigated in the ALPE sediment programme were not part of this calibration set. This has led to two general problems in pH inference. Most of the ALPE lakes are unlike those lakes investigated in the SWAP programme which were generally at lower altitudes and below the tree line in more biologically productive environments (Battarbee *et al.* 1990). It might therefore be anticipated that some diatom taxa would be missing from the calibration set used in the pH reconstructions and secondly, given the ultra-oligotrophic conditions, long periods of ice cover and other conditions

peculiar to alpine lakes, that the same taxa might have slightly different pH optima. A further problem is that at some of the ALPE sites it is not easy to determine what the 'average pH' or any other average chemical conditions are. Given the large fluctuations in conditions in and around alpine lakes it is difficult to determine the ideal conditions under which to take measurements. For example during the period of ice and snow-melt there is a marked fall in pH at many lakes. At some of the lakes such as Etang d'Aube, remote from research laboratories involved in the project, it has only been possible to take a few water samples for chemical analyses.

5 CONCLUSIONS

5.1 LITHOSTRATIGRAPHIC AND RADIOMETRIC ANALYSES

Lithostratigraphic analyses of ALPE cores revealed two types of profile, fairly smooth dry weight and LOI profiles indicative of catchment stability and spiky profiles resulting from events of accelerated catchment erosion. Only at one site, Aube, did catchment inwash present a problem for constructing a core chronology. It is possible that further investigation of such inwash events in alpine lakes will be a useful part of the ALPE2 programme, given its aims in relation to the use of these lakes as early indicators of climatic change. At all six ALPE sites studied in the sediment investigation it was possible to produce useful chronologies based on radiometric measurements.

5.2 CARBONACEOUS PARTICLE ANALYSIS

Only one of the ALPE cores (Lochnagar) analysed for carbonaceous particles had a particle profile over 10 cm long. Of the other five, two of the profiles were 5 cm or less (Paione Superiore, Ovre Neådalsvatn) and that of Etang d'Aube was only longer than 5 cm because of a sediment inwash event. These remote oligotrophic mountain lakes have very low sediment accumulation rates and therefore the resolution possible in the carbonaceous particle record is equally low. In such instances it is difficult to tell whether a particle profile in a region is recording the history of increasing fossil-fuel combustion or whether the profile is just an artefact of the low accumulation. Faster accumulation rate sites whilst diluting the signal allow better resolution and would act as better (and earlier) indicators of increasing or decreasing atmospheric pollution.

However, as these are remote sites they have the advantage of recording national deposition trends of industrial pollutants rather than being influenced by local emissions and they are therefore valuable sites. Perhaps a better way of monitoring trends in atmospheric depositions (certainly of carbonaceous particles) in these low accumulation sites would be to implement a sediment trapping or re-coring programme. Sediment traps have the advantage of being deployed for a known, discrete time period and hence may act as better 'early response indicators' to changing deposition trends.

The use of national fossil-fuel combustion statistics and meteorological data enable the determination of possible regions of origin for the particles (and by implication other fossil-fuel combustion derivatives). This could be improved by the use of carbonaceous particle characterisation which is able to determine the fuel-type for particles extracted from lake sediments (Rose, 1991).

With the possible exception of Lochnagar and the Norwegian sites where other data already exist, the analysis of additional lake sediment cores from these regions is needed to confirm the results discussed above. This should be possible from ALPE 2. In addition, extra sites to those described were taken during ALPE 1 and it is hoped that before the conclusion of the ALPE programme it will be possible to analyse these cores for carbonaceous particles.

5.3 DIATOM ANALYSIS AND pH RECONSTRUCTION

Diatom analysis has been used successfully to reconstruct pH changes at all of the six sites studied in the ALPE sediment programme. At three sites: Stavsvatn in southern Norway; Lochnagar in the Cairngorm Mountains, Scotland, and at Paione Superiore in the Italian Alps a clear acidification signal was recorded. At Aube in the French Pyrenees there was evidence for a slight acidification. Øvre Neådalsvatn in mid-Norway was shown to be sensitive to acidification, but the effects of acid deposition in this relatively clean area are not detectable. At Milchsee, where lakewater had a high base cation content, pH changes indicated by the diatom assemblages were driven primarily by processes other than atmospheric sulphur deposition.

Considerable discrepancies occurred between the measured pH of the study lakes and the pH reconstructed from surface sediment diatom assemblages. This resulted partly from the use of the earlier SWAP diatom/pH calibration set (Stevenson *et al.* 1991) which did not include the ALPE site surface sediments in its database. Common taxa present in the ALPE sites were absent from this calibration set. It is also difficult, especially where sparse water chemistry measurements are available to estimate 'average pH' accurately.

As well as extending the network of high latitude and high altitude lakes involved in the first part of the ALPE study a primary aim of the ALPE2 sediment diatom programme will to be to improve the diatom/lakewater chemistry calibration set so that it is more appropriate for the lakes under investigation.

REFERENCES

Appleby, P.G. & F. Oldfield (1978) The calculation of ^{210}Pb dates assuming a constant rate of supply of unsupported ^{210}Pb to the sediment. *Catena*, 5: 1-8

Appleby, P.G., P.J. Nolan, D.W. Gifford, M.J. Godfrey, F. Oldfield, N.J. Anderson, & R.W. Battarbee (1986) ^{210}Pb dating by low background gamma counting. *Hydrobiologia*, 141: 21 -27

Appleby, P.G., N. Richardson & P.J. Nolan (1991) ^{241}Am dating of lake sediments. *Hydrobiologia*, 214: 35-42

Alcamo J., Shaw R. & Hordijk L. (eds.) (1990). *The RAINS model of acidification, science and strategies in Europe.* Kluwer Academic Publishers, Dordrecht, The Netherlands.

Battarbee, R.W. & M.J. Kneen (1982). The use of electronically counted microspheres in absolute diatom analysis. *Limnology & Oceanography*, 27: 184-188

Battarbee, R.W. (1986). Diatom analysis. *Handbook of Holocene Palaeoecology and Palaeohydrology* (ed. B.E. Berglund), pp. 527 - 570. Wiley, Chichester.

Battarbee, R.W., Mason, Sir J., Renberg, I. & Talling, J.F. (eds.) (1990). *Palaeolimnology and Lake Acidification.* Proceedings of a Royal Society Discussion Meeting held on 25 August 1989. Royal Society, London 219pp.

Bretschko, G. (1975). Annual benthic biomass distribution in a high-mountain lake (Vorderer Finstertaler See, Tyrol, Austria). *Verh. Internat. Verein. Limnol.* 19:1279-1285.

Brundin, L. (1949). Chironomiden und andere Bodentiere des südschwedischen Urgebirgsseen. Ein Beitrag zur Kenntnis der bodenfaunistischen Charakterzüge schwedischen oligotropher Seen. *Rep. Inst. Freshwat. Res. Drottningholm* 30:1-914.

Brundin, L. (1956). Die bodenfaunistischen Seetypen und ihre Anwendbarkeit auf die Südhalbkugel. Zugleich eine Theorie der produktionsbiologischen Bedeutung der glazialen Erosion. *Rep. Inst. Freshwat. Res. Drottningholm* 37:186-235.

Eliassen, A., Hor, T. Iversen, J. Saltbones & D. Simpson (1988). *Estimates of airbourne transboundary transport of sulphur and nitrogen over Europe.* EMEP/MSC-W report no. 1/88.

Flower, R.J. & V.J. Jones (1989). Taxonomic descriptions and occurrences of new Achnanthes taxa in acid lakes in the UK. *Diatom Research*, 4: 227-239

Flower, R.J., S. Politov, P.G. Appleby, B. Rippey, N.L. Rose & A.C. Stevenson (1993). A palaeolimnological evaluation of the extent and impact of atmospheric contamination and recent environmental change in a remote high mountain lake in Siberia (in preparation) Proceedings of the VIth International Symposium on Palaeolimnology

Glew, J.R. (1988). A portable extruding device for close interval sectioning of unconsolidated core samples. *Journal of Palaeolimnology* 1: 235-239

Glew, J.R. (1989). A new trigger mechanism for sediment samplers. *Journal of Palaeolimnology* 2: 241-243

Guilizzoni P., Lami A. & Marchetto A. (1992). Plant pigment ratios from lake sediments as indicators of recent acidification in alpine lakes. *Limnol. Oceanogr.* 37: 1565-1569.

Hofmann, W. (1986). Chironomid analysis. P. 715-727. In: B.E. Berglund (ed.): *Handbook on Holocene Palaeoecology and Palaeohydrology*. Wiley, Chichester.

Hofmann, W. (1988). The significance of chironomid analysis (Insecta: Diptera) for paleolimnological research. *Palaeogeography, Palaeoclimatology, Palaeoecology* 62:501-509.

Johannessen T.W. & Håland L. (1969). *Standard normals 1931 - 1960 of monthly wind summaries for Norway.* Climatological summaries for Norway. Det Norske Meteorologiske Institutt. Oslo.

Jones, V.J., R.J. Flower, P.G. Appleby, J. Natkanski, N. Richardson, B. Rippey, A.C. Stevenson & R.W. Battarbee (1993) Palaeolimnological evidence for the acidification of lochs in the Cairngorm and Lochnagar areas of Scotland. *Journal of Ecology* (In press)

Kreiser A.M., Anderson N.J., Appleby P.G., Battarbee R.W., Patrick S.T., Rippey B. & Rose N.L. (1992). *A palaeolimnological study of the water quality of lakes in the Vosges Mountains of France.* Environmental Change Research Centre, University College London. Research Paper No. 3.

Laville, H. & Vinçon, G. (1986). Inventaire 1986 des Chironomides (Diptera) connus des Pyrénées. Annls Limnol. 22:239-251.

Line, J.M. & Birks, H.J.B. (1990). WACALIB version 2.1 - a computer programme to reconstruct environmental variables from fossil assemblages by weighted averaging. *Journal of Paleolimnology* 3, 170-173.

Oldfield, F. & Appleby, P.G. (1984) *Empirical testing of ^{210}Pb dating models for lake sediments.* In **E.Y. Haworth & J.W.G. Lund** (eds.) *Lake sediments and environmental history*, 93-124. Leicester University Press.

Patrick S.T., Flower R.J., Appleby P.G., Oldfield F., Rippey B., Stevenson A.C., Darley J. & Battarbee R.W. (1989). *Palaeoecological evaluation of the recent acidification of Lochnagar, Scotland.* Palaeoecology Research Unit, University College London. Research Paper No. 34.

Pechlander, R. & Zaderer, P. (1985). Interrelations between brown trout and chironomids in the alpine lake Gossenköllesee (Tyrol). *Verh. Internat. Verein. Limnol.* 22:2620-2627.

Rose N.L. (1990). A method for the extraction of carbonaceous particles from lake sediment. *J. Paleolim.* 3: 45-53.

Rose N.L. (1991). *Fly-ash particles in lake sediments: Extraction, characterisation and distribution.* Unpublished PhD thesis. University of London.

Sæther, O.A. (1979). Chironomid communities as water quality indicators. *Holarctic Ecology* 2:65-74.

Schmidt, R. & R. Psenner (1992) Climatic changes and anthropogenic impacts as causes for pH fluctuations in remote high alpine lakes In R. Mosello, B.M. Wathne & G. Giussani (eds.) *Limnology on groups of remote lakes: ongoing and planned activities.* Documenta Ist. Ital. Idrobiol., 32: 31-57

Steinhauser, F. (1982). *Verteilung der Häufigkeiten der Windrichtungen und der Windstärken in Österreich zu verschiedenen Tages - und Jahreszeiten.* Arbeiten aus der Zentralanstalt für Meteorologie und Geodynamik, Wien. Publikation Nr. 260. Heft 53. [in German]

Stevenson, A.C., S. Juggins, H.J.B. Birks, D.S. Anderson, N.J. Anderson, R.W. Battarbee, F. Berge, R.B. Davis, R.J. Flower, E.Y. Haworth, V.J. Jones, J.C. Kingston, A.M. Kreiser, J.M. Line, M.A.R. Munro, & I. Renberg (1991). *The Surface Waters Acidification Project Palaeolimnology Programme: Modern Diatom/Lake-Water Chemistry Data-Set.* Ensis, London. pp. 86.

United Nations, 1952. World Energy Supplies in selected years 1929-1950. U.N. Statistical Papers. Series J. No. 1. New York.

United Nations Department of Economic and Social Affairs, 1976. World Energy Supplies 1950 - 1974. U.N. Statistical Papers. Series J. No. 19. New York.

United Nations Department of International Economic and Social Affairs, 1979. World Energy Supplies 1973 - 1978. U.N. Statistical Papers. Series J. No. 22. New York.

United Nations Department of International Economic and Social Affairs, 1981. 1980 Yearbook of World Energy Statistics. New York.

United Nations Department of International Economic and Social Affairs, 1986. 1984 Energy Statistics Yearbook. New York.

United Nations Department of International Economic and Social Affairs, 1990. 1988 Energy Statistics Yearbook. New York.

United Nations Department of International Economic and Social Affairs, 1991. 1989 Energy Statistics Yearbook. New York.

United Nations Department of International Economic and Social Affairs, 1992. 1990 Energy Statistics Yearbook. New York.

Walker, I.R. (1987). Chironomidae (Diptera) in palaeoecology. *Quarternary Sciences Reviews* 6:29-40.

Walker, I.R. & Paterson, C.G. (1983). Post-glacial chironomid succession in two small, humic lakes in the New Brunswick - Nova Scotia (Canada) border area. *Freshwater Invertebrate Biology* 2 (2):61-73.

Walker, I.R. & Paterson, C.G. (1985). Efficient separation of subfossil Chironomidae from lake sediments. *Hydrobiologia* 122:189-192.

Warwick, W.F. (1980). Palaeolimnology of the Bay of Quinte, Lake Ontario: 2800 years of cultural influence. *Canadian Bulletin of Fisheries and Aquatic Sciences* 206:1-117.

Wik M. (1989). Sedimentary records of particulate elemental carbon from the Scandinavian study sites. *Internal report to the Surface Waters Acidification Project (SWAP) meeting.* Lairdmannoch Lodge, 8-12 May 1989.

Wik M. & Natkanski J. (1990). British and Scandinavian lake sediment records of carbonaceous particles from fossil-fuel combustion. *Phil. Trans. R. Soc. Lond.* B327: 319-323.

ETANG D AUBE

FIG. 3.1.1

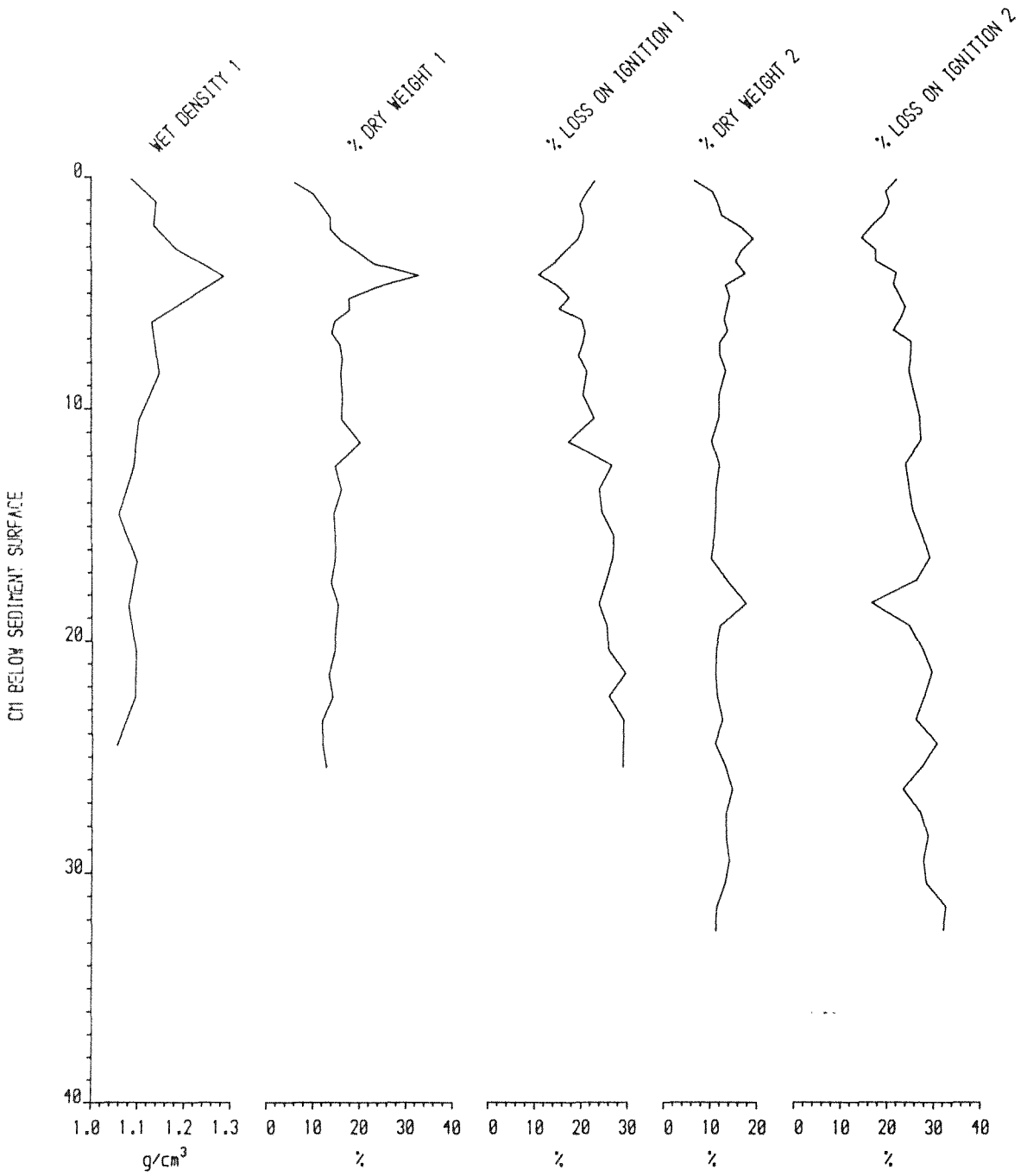

FIG. 3.1.2

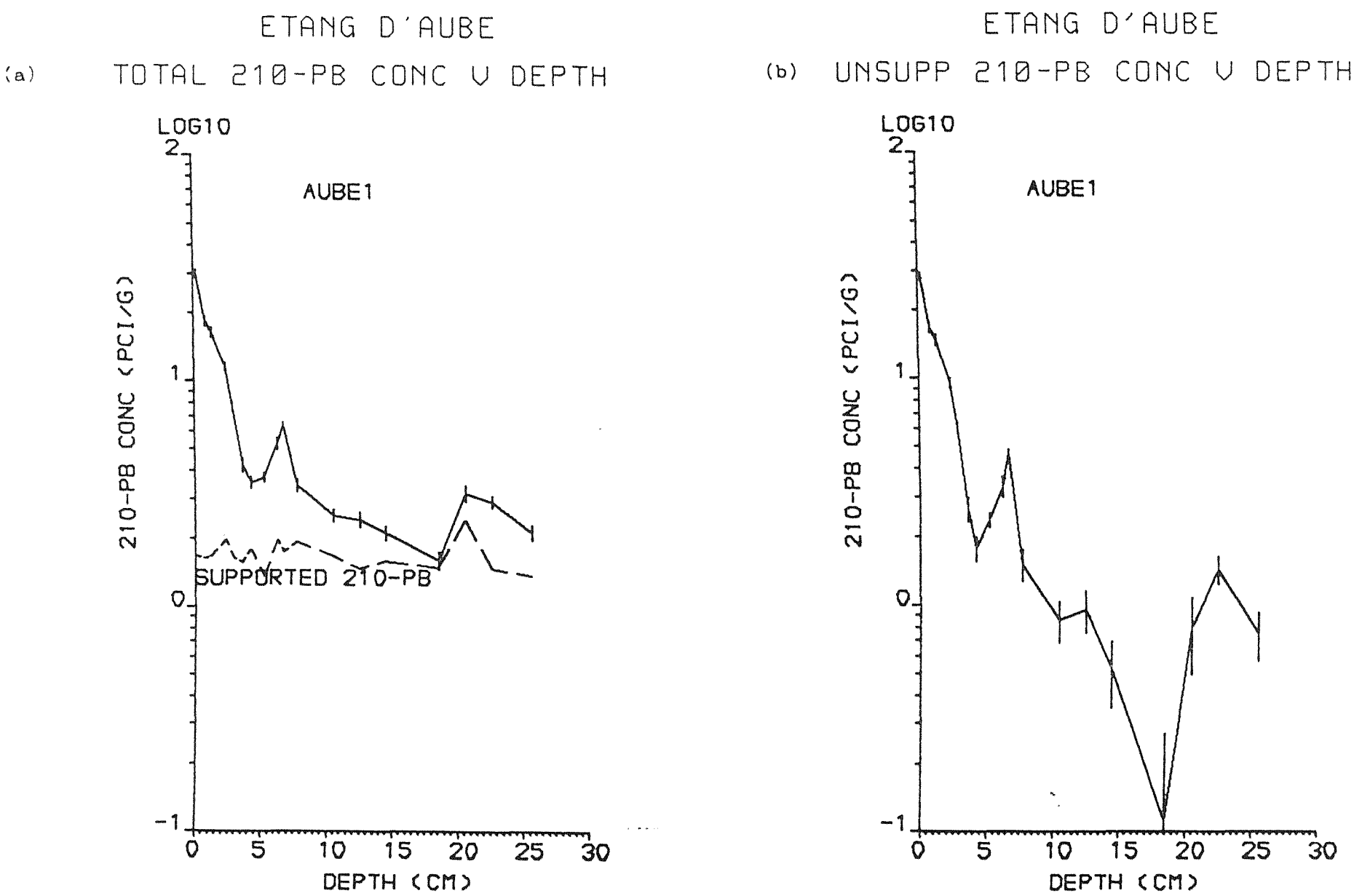
ETANG D'AUBE
(a) TOTAL 210-PB CONC V DEPTH
LOG10
AUBE1
210-PB CONC (PCI/G)
SUPPORTED 210-PB
DEPTH (CM)
ETANG D'AUBE
(b) UNSUPP 210-PB CONC V DEPTH
LOG10
AUBE1
210-PB CONC (PCI/G)
DEPTH (CM)

FIG. 3.1.3

(a) ETANG D'AUBE
CS-137 CONC V DEPTH

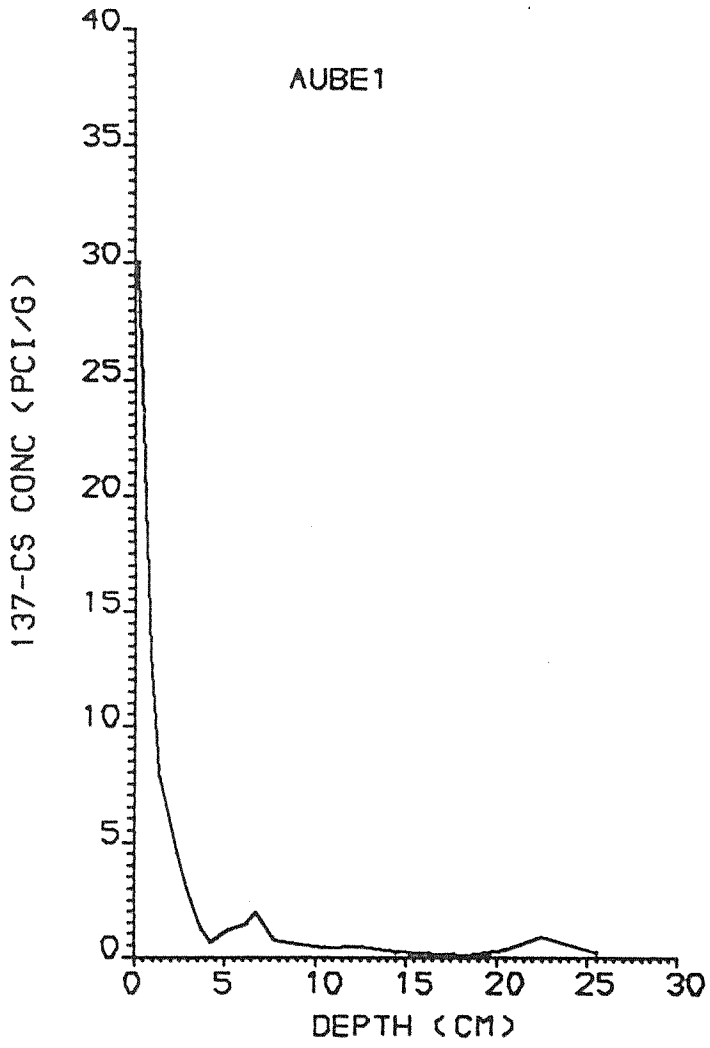

(b) ETANG D'AUBE
AM-241 CONC V DEPTH

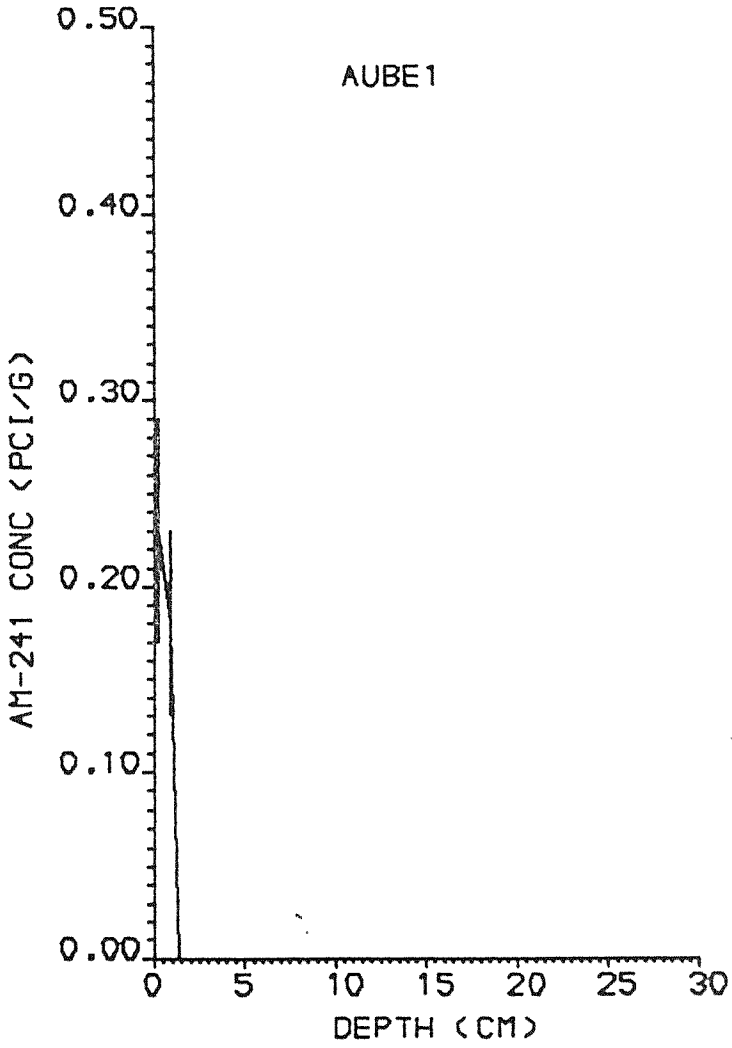

FIG. 3.1.4

ETANG D'AUBE

DEPTH V AGE

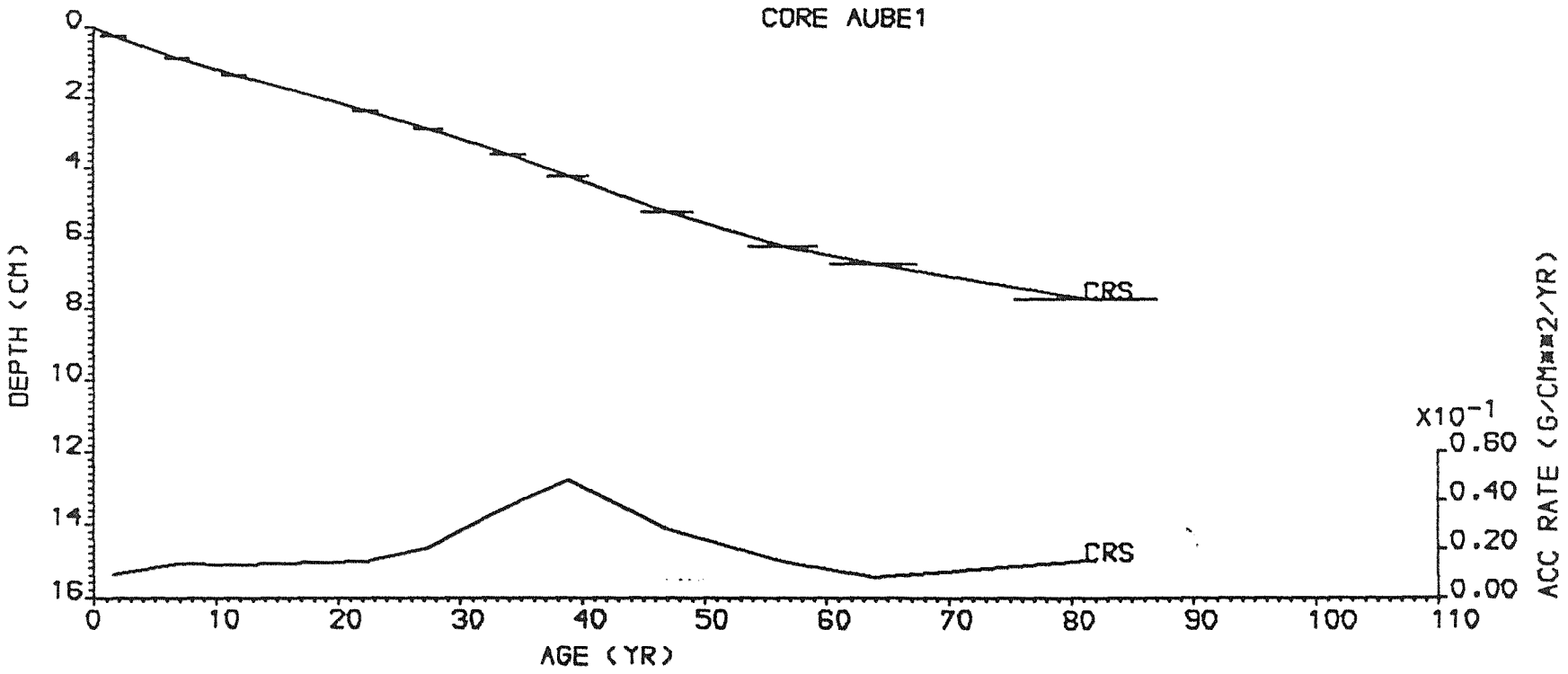

Carbonaceous Particle Concentration and Flux Profiles

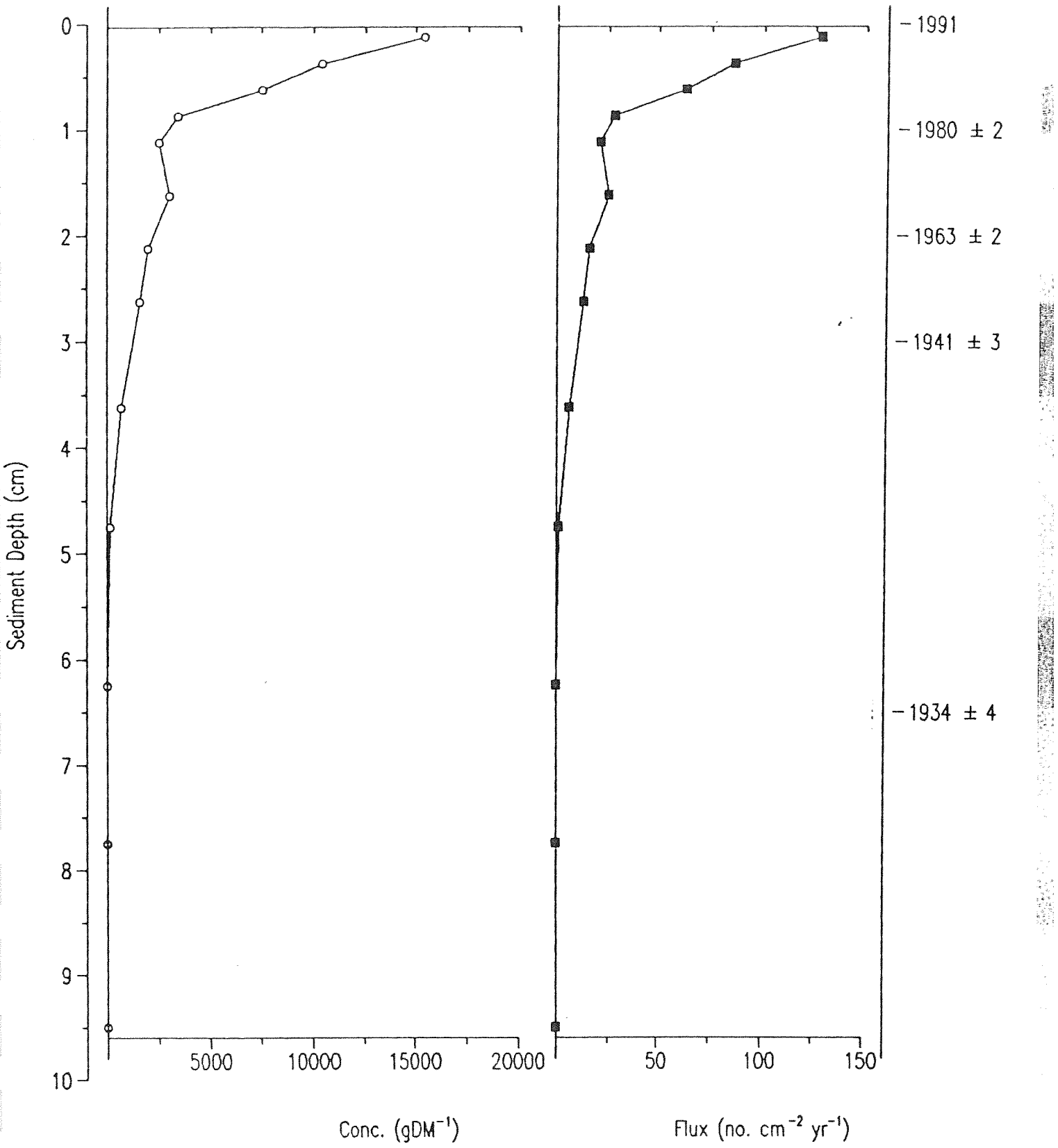

AUBET, diatom cell concentration

FIG. 5.1.6

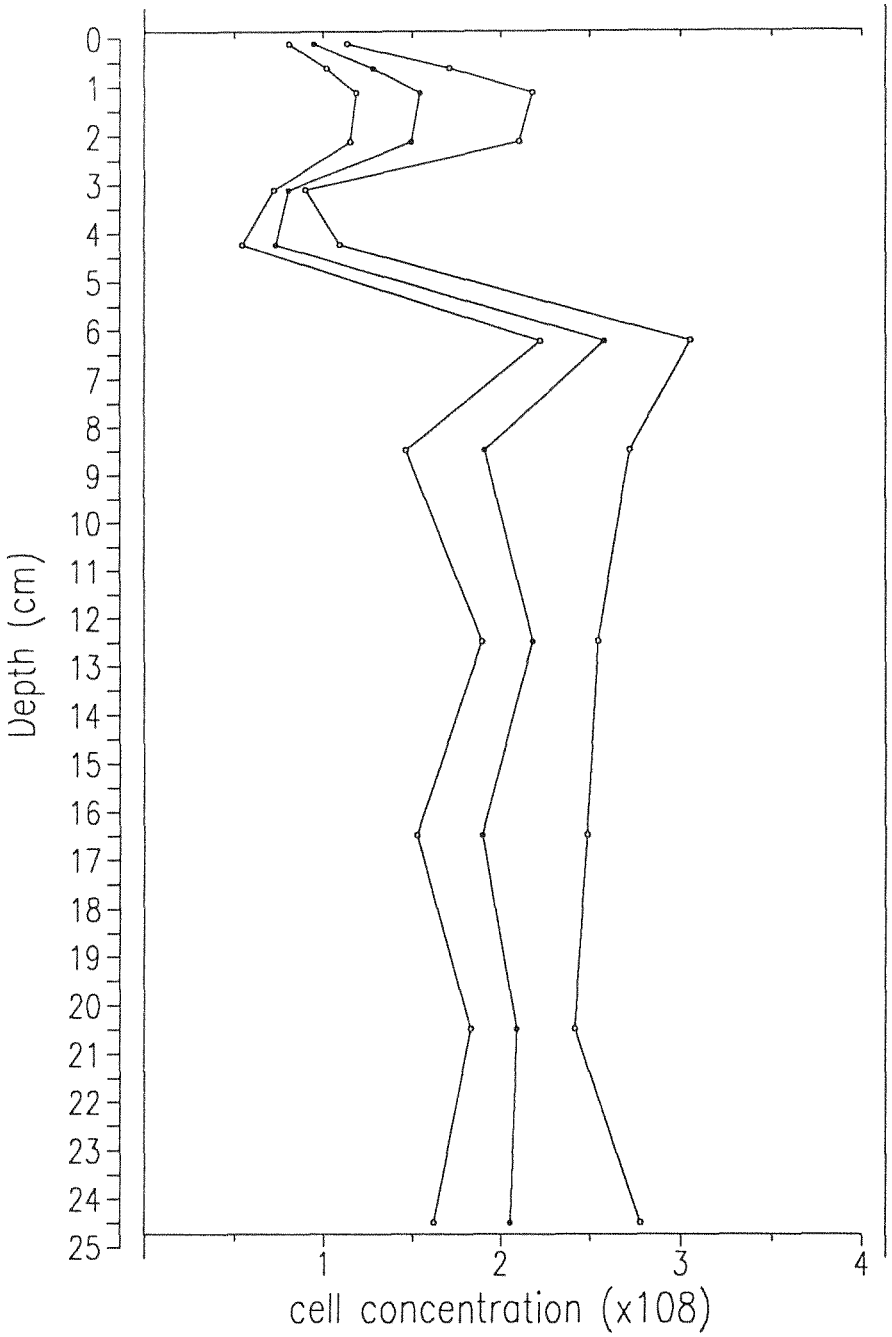

:tang a Aube, AUBE1 summary percentage diatom diagram FIG. 3.1.7

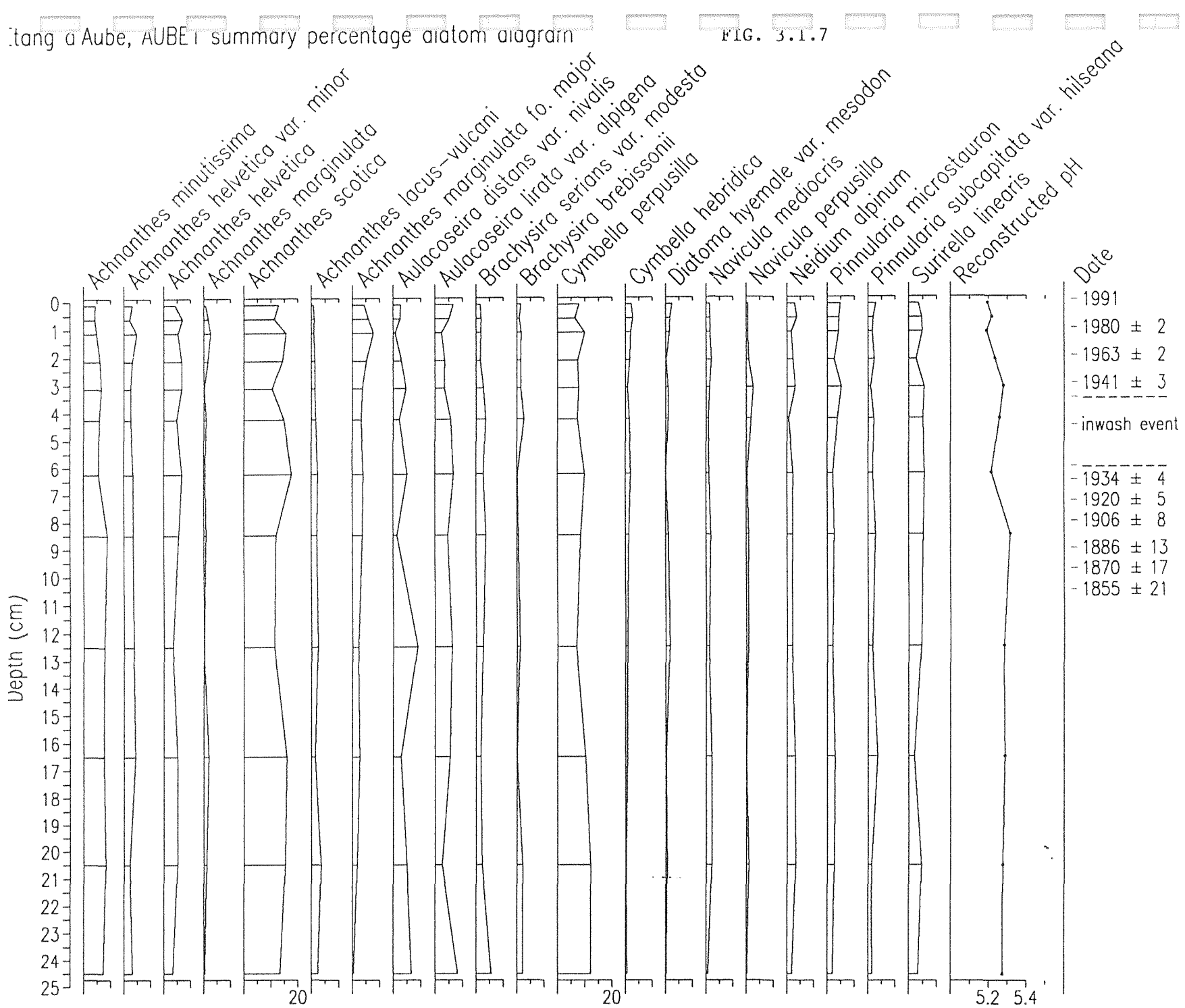

TABLE 3.1.1 Etang d'Aube: ^{210}Pb Data Core 1

Depth	Dry Mass	^{210}Pb Concentration Total		^{210}Pb Concentration Unsupp		^{226}Ra Concentration	
cm	gcm^{-2}	$pCig^{-1}$	±	$pCig^{-1}$	±	$pCig^{-1}$	±
0.25	0.017	29.98	1.17	28.32	1.19	1.66	0.24
0.875	0.077	18.28	0.89	16.64	0.90	1.64	0.16
1.375	0.141	16.35	0.86	14.67	0.87	1.68	0.15
2.375	0.294	11.45	0.50	9.48	0.51	1.97	0.12
2.875	0.384	7.66	0.36	6.01	0.37	1.65	0.07
3.625	0.556	4.21	0.33	2.64	0.34	1.57	0.08
4.25	0.762	3.53	0.21	1.76	0.22	1.77	0.06
5.25	1.060	3.71	0.18	2.35	0.18	1.36	0.04
6.25	1.255	5.26	0.34	3.29	0.35	1.97	0.09
6.75	1.339	6.34	0.23	4.60	0.24	1.74	0.06
7.75	1.519	3.43	0.23	1.50	0.24	1.93	0.06
10.50	2.032	2.52	0.17	0.86	0.18	1.66	0.06
12.50	2.430	2.42	0.19	0.95	0.20	1.47	0.06
14.50	2.767	2.10	0.16	0.52	0.17	1.58	0.06
18.50	3.411	1.59	0.15	0.11	0.16	1.48	0.05
20.50	3.741	3.17	0.27	0.78	0.29	2.39	0.10
22.50	4.050	2.89	0.19	1.42	0.20	1.47	0.05
25.50	4.459	2.11	0.17	0.74	0.18	1.37	0.06

TABLE 3.1.2 Etang d'Aube: ^{137}Cs and ^{241}Am Data Core 1

Depth	^{137}Cs conc		^{241}Am conc	
cm	$pCig^{-1}$	±	$pCig^{-1}$	±
0.25	29.67	0.39	0.23	0.06
0.88	13.07	0.26	0.18	0.05
1.38	7.93	0.21	0.00	0.00
2.38	4.57	0.11	0.00	0.00
2.88	2.98	0.08	0.00	0.00
3.63	1.28	0.07	0.00	0.00
4.25	0.62	0.04	0.00	0.00
5.25	1.15	0.03	0.00	0.00
6.25	1.42	0.07	0.00	0.00
6.75	1.92	0.06	0.00	0.00
7.75	0.69	0.04	0.00	0.00
10.50	0.41	0.04	0.00	0.00
12.50	0.42	0.04	0.00	0.00
14.50	0.20	0.04	0.00	0.00
18.50	0.07	0.03	0.00	0.00
20.50	0.27	0.06	0.00	0.00
22.50	0.84	0.04	0.00	0.00
25.50	0.19	0.04	0.00	0.00
Inventories:	6.28±0.12 $pCicm^{-2}$		0.02±0.01 $pCicm^{-2}$	

TABLE 3.1.3 Etang d'Aube: ^{210}Pb Chronology for Core 1

Depth	Cum Dry Mass	Chronology Date	Age		Sedimentation Rate		
cm	gcm^{-2}	AD	yr	±	$gcm^{-2}yr^{-1}$	$cmyr^{-1}$	±
0.00	0.000	1991	0				
0.25	0.017	1989	2	1			
0.50	0.040	1986	5	1		0.091	
0.75	0.064	1983	8	2			
1.00	0.092	1980	11	2			
1.25	0.124	1976	15	2			
1.50	0.159	1972	19	2	0.0083		~6%
1.75	0.197	1967	24	2			
2.00	0.236	1963	28	2		0.051	
2.25	0.274	1958	33	2			
2.50	0.315	1953	38	3			
2.75	0.360	1948	43	3			
3.00	0.411	1941	50	3			
3.50	0.526						
4.00	0.679						
4.50	0.836		Inwash event?				
5.00	0.985						
5.50	1.107						
6.00	1.206						
6.50	1.297	1934	57	4			
6.75	1.339	1930	61	4			
7.00	1.384	1925	66	5			
7.25	1.429	1920	71	5			
7.50	1.474	1915	76	6			
7.75	1.519	1911	80	6			
8.00	1.566	1906	85	8			
8.25	1.612	1901	90	9			
8.50	1.659	1896	95	10			
8.75	1.706	1891	100	12	0.0093	0.050	~27%
9.00	1.752	1886	105	13			
9.25	1.799	1881	110	14			
9.50	1.845	1875	116	15			
9.75	1.892	1870	121	17			
10.00	1.939	1865	126	18			
10.25	1.985	1860	131	19			
10.50	2.032	1855	136	21			

OVRE NEADALSVATN

FIG. 3.2.1

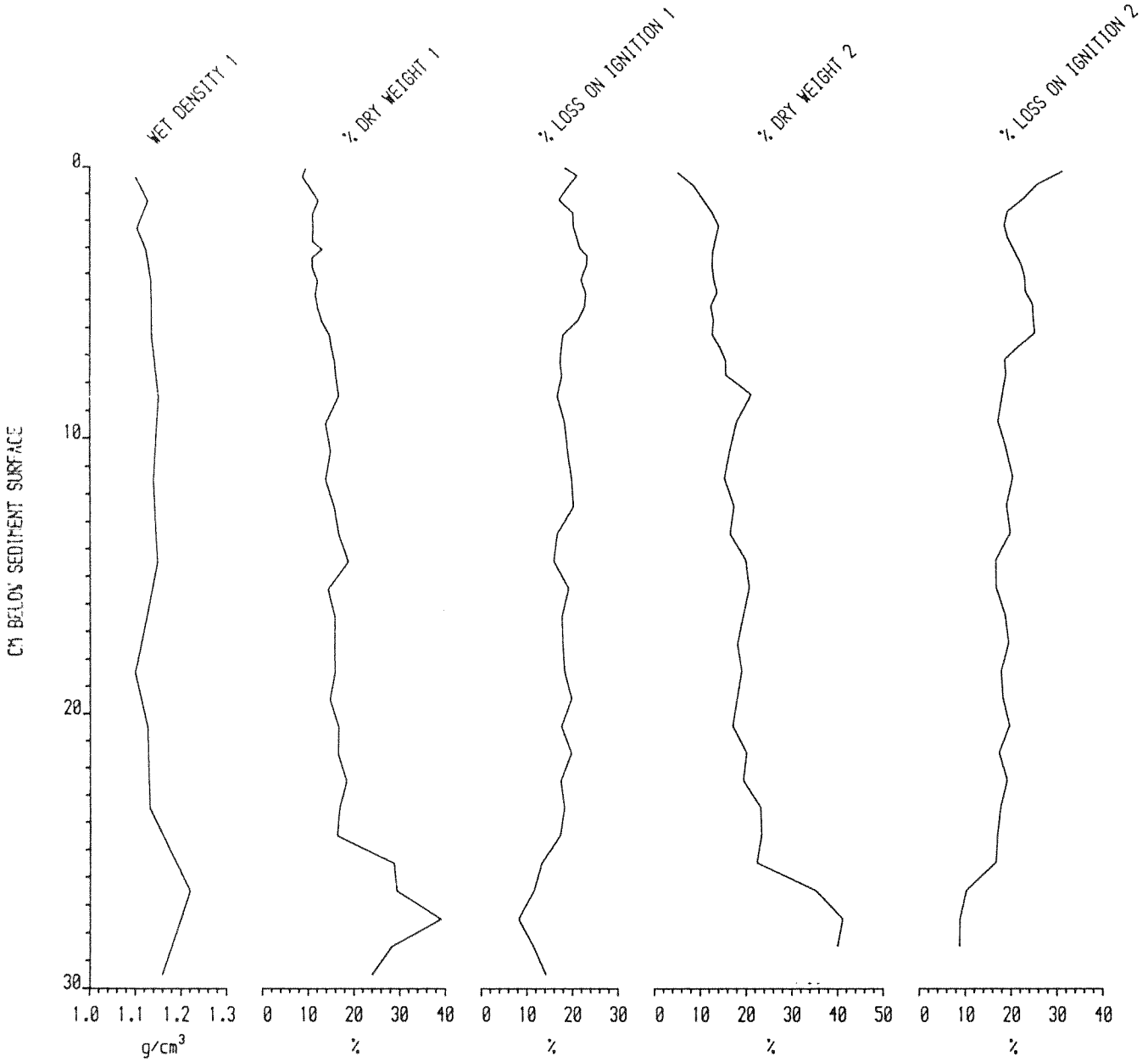

FIG. 3.2.2

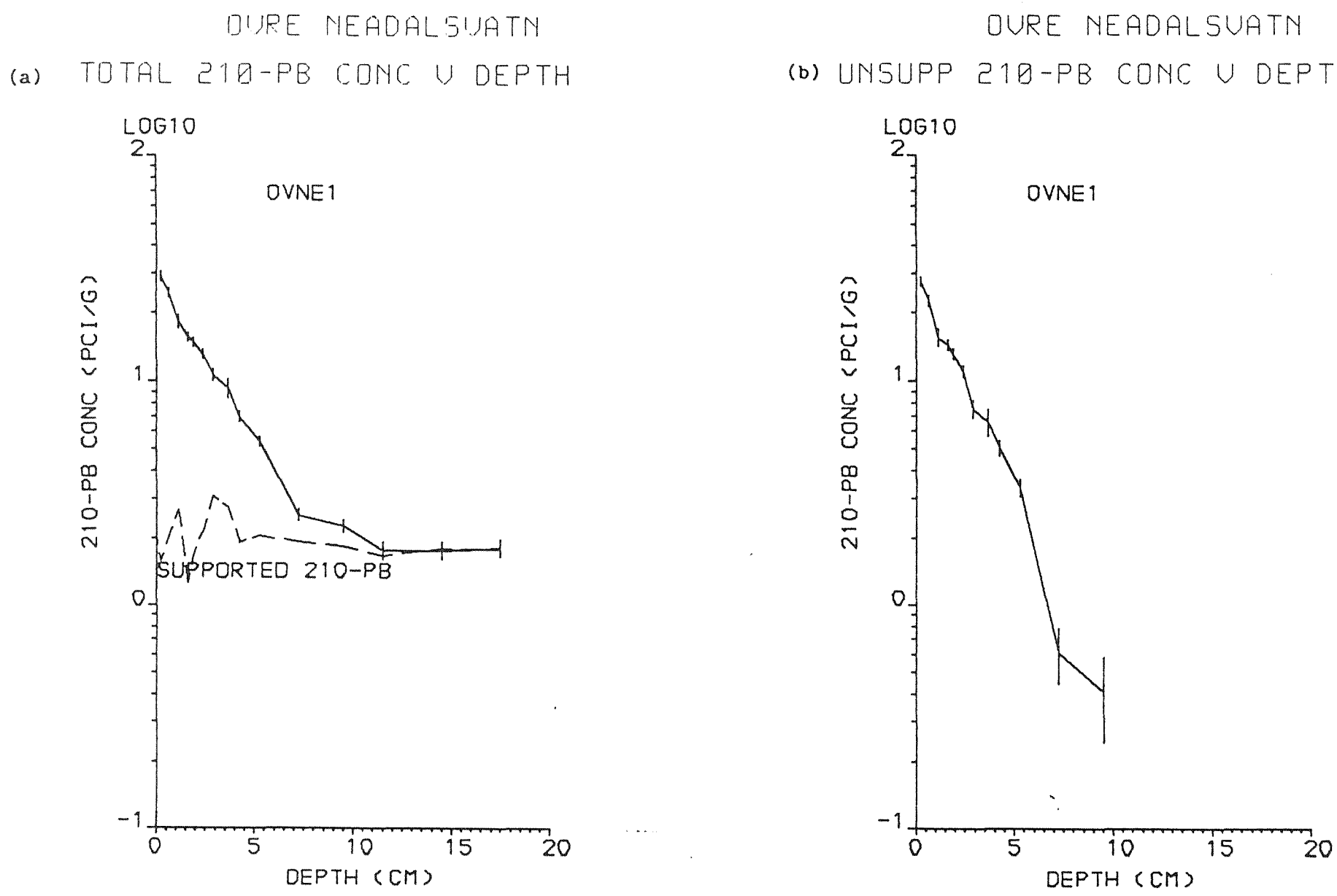
ØVRE NEADALSVATN
(a) TOTAL 210-PB CONC V DEPTH
LOG10
2
1
0
-1
ØVNE1
210-PB CONC (PCI/G)
SUPPORTED 210-PB
0
5
10
15
20
DEPTH (CM)
ØVRE NEADALSVATN
(b) UNSUPP 210-PB CONC V DEPTH
LOG10
2
1
0
-1
ØVNE1
210-PB CONC (PCI/G)
0
5
10
15
20
DEPTH (CM)

FIG. 3.2.3

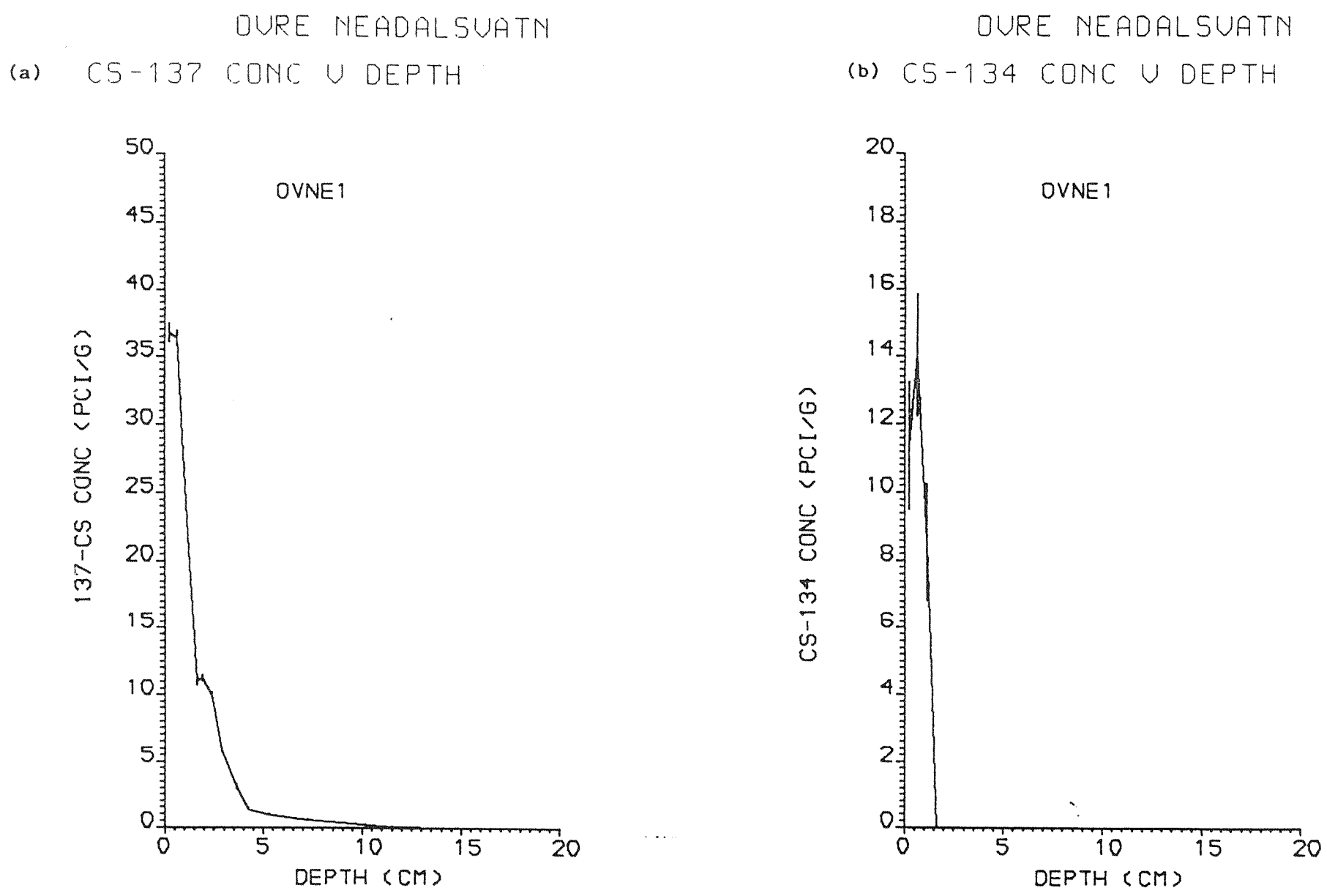
OVRE NEADALSVATN
(a) CS-137 CONC V DEPTH
OVNE1
137-CS CONC (PCI/G)
DEPTH (CM)
0
5
10
15
20
25
30
35
40
45
50
OVRE NEADALSVATN
(b) CS-134 CONC V DEPTH
OVNE1
CS-134 CONC (PCI/G)
DEPTH (CM)
0
2
4
6
8
10
12
14
16
18
20

FIG. 3.2.4

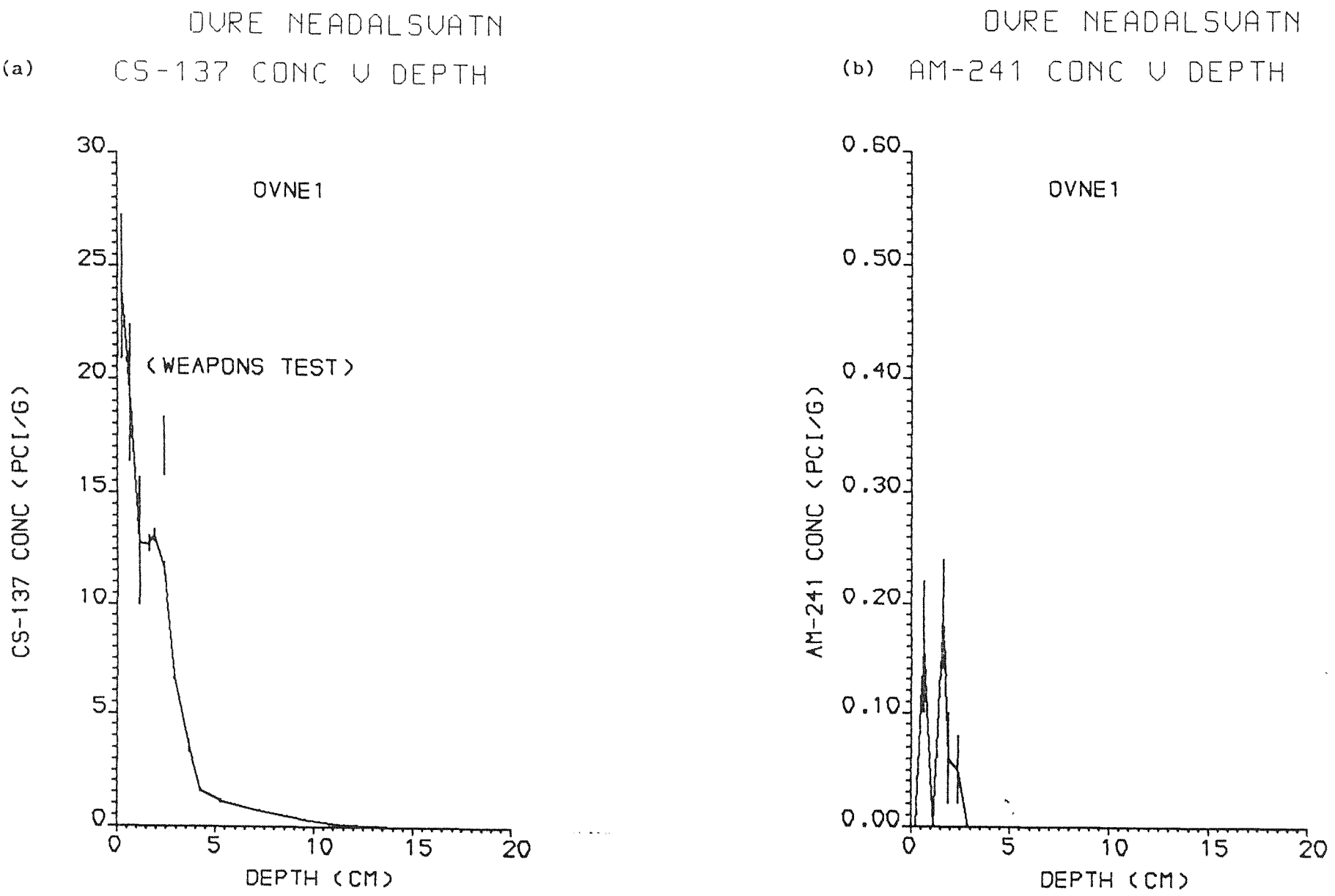
OVRE NEADALSVATN
(a) CS-137 CONC V DEPTH
OVNE1
(WEAPONS TEST)
CS-137 CONC (PCI/G)
DEPTH (CM)
0
5
10
15
20
25
30
OVRE NEADALSVATN
(b) AM-241 CONC V DEPTH
OVNE1
AM-241 CONC (PCI/G)
DEPTH (CM)
0.00
0.10
0.20
0.30
0.40
0.50
0.60

FIG. 3.2.5

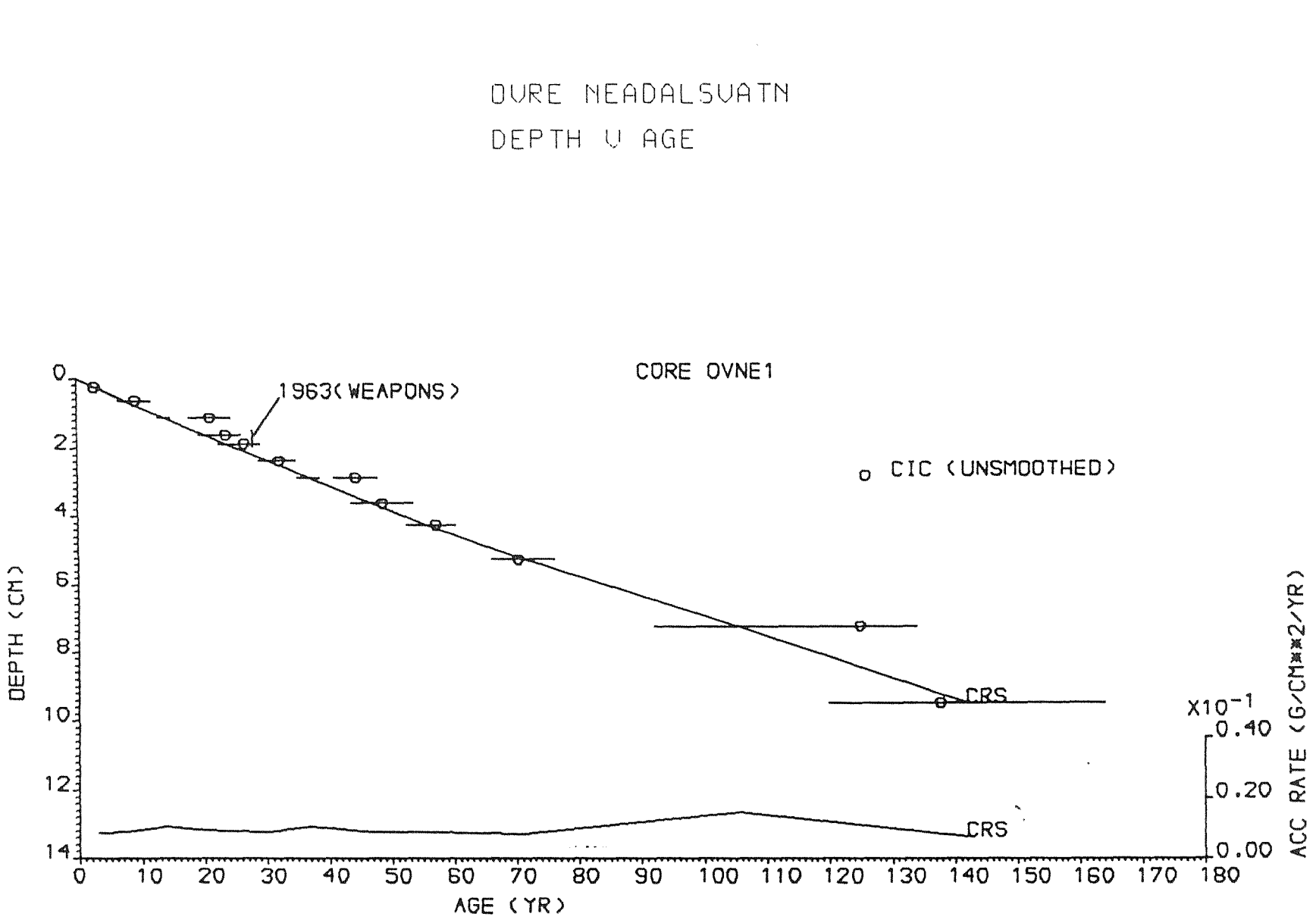
ØVRE NEADALSVATN
DEPTH V AGE
CORE ØVNE1
1963(WEAPONS)
CIC (UNSMOOTHED)
CRS
CRS
DEPTH (CM)
AGE (YR)
X10⁻¹
ACC RATE (G/CM**2/YR)
0
2
4
6
8
10
12
14
0
10
20
30
40
50
60
70
80
90
100
110
120
130
140
150
160
170
180
0.40
0.20
0.00

Carbonaceous Particle Concentration and Flux Profiles

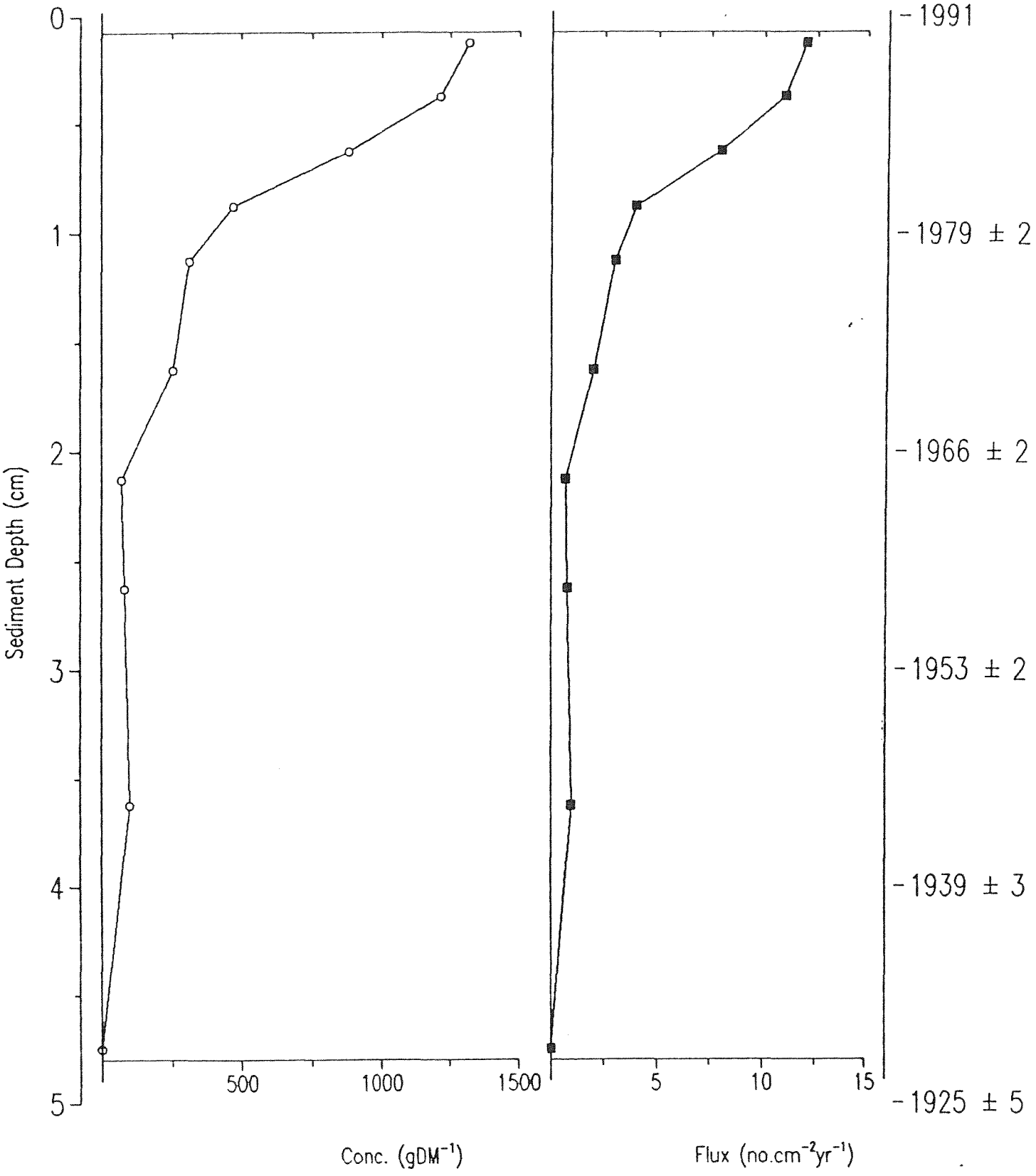

)VNET, diatom cell concentration

FIG. 3.2.7

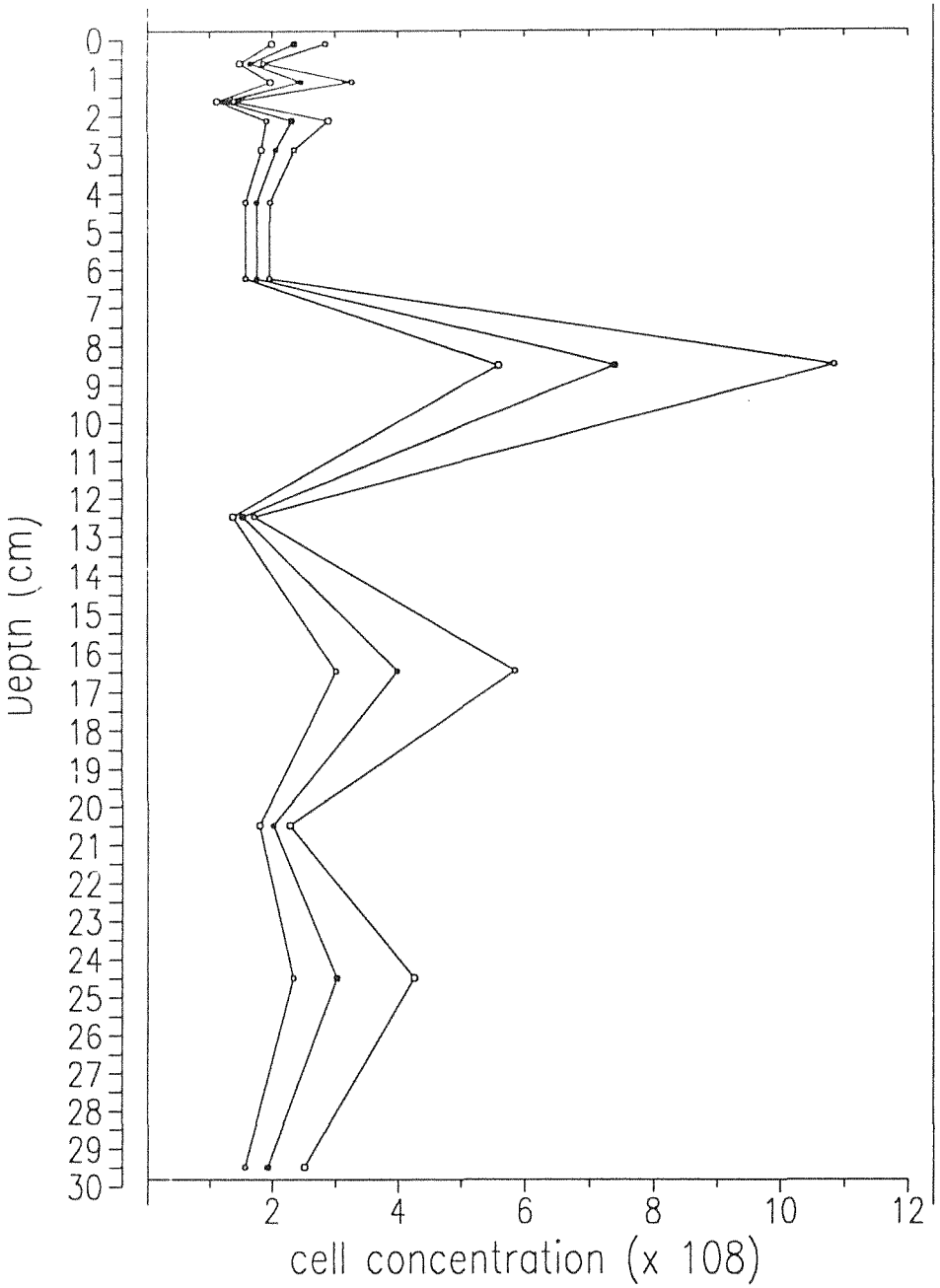

vre Neadalsvatn, OVNE1 summary percentage diatom diagram FIG. 3.2.8

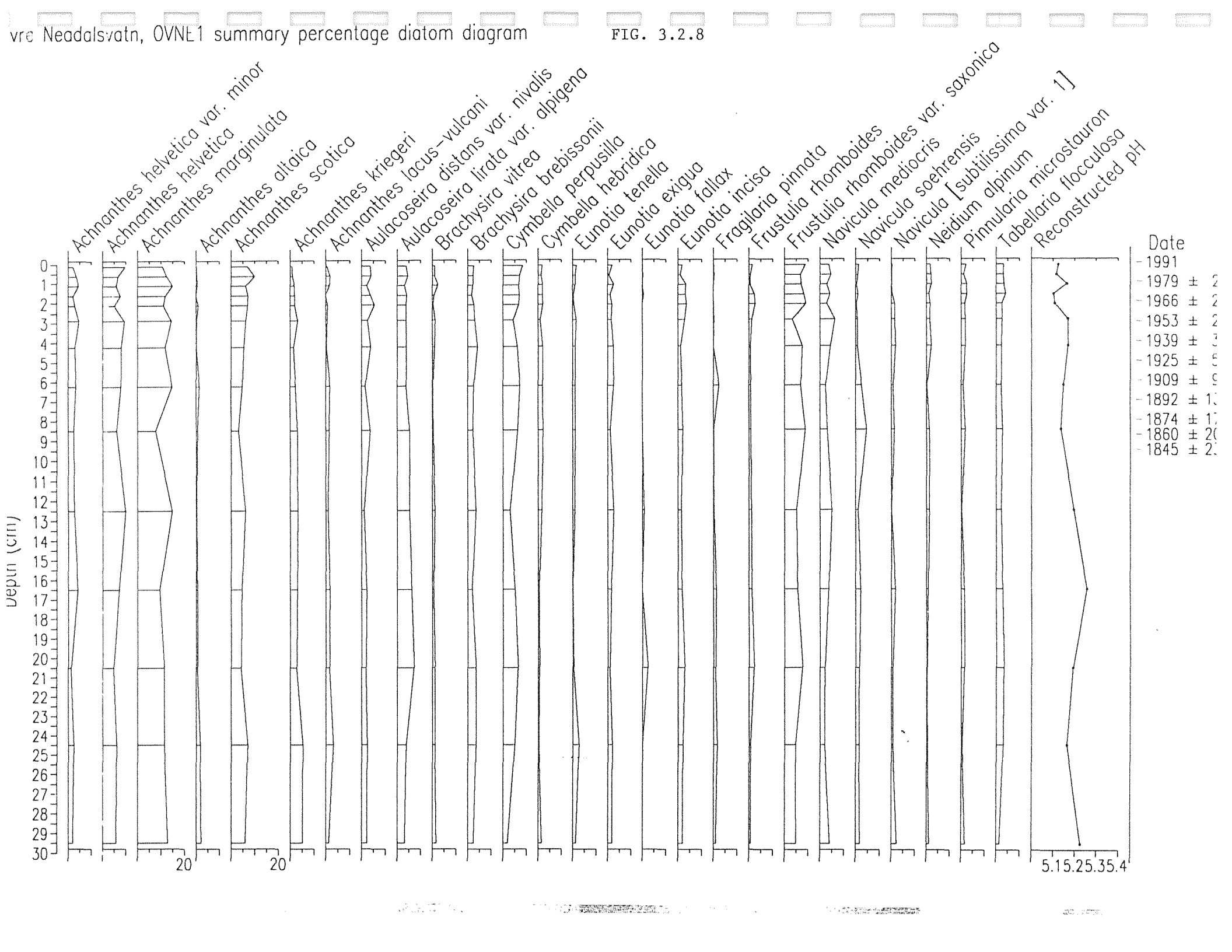

TABLE 3.2.1 Ovre Neådalsvatn: ^{210}Pb Data for Core OVNE1

Depth	Dry Mass	^{210}Pb Concentration				^{226}Ra Concentration	
		Total		Unsupp			
cm	gcm^{-2}	$pCig^{-1}$	±	$pCig^{-1}$	±	$pCig^{-1}$	±
0.25	0.025	29.05	1.49	27.48	1.53	1.57	0.35
0.625	0.064	24.51	1.30	22.49	1.35	2.02	0.35
1.125	0.124	18.15	1.30	15.49	1.35	2.66	0.37
1.625	0.187	15.59	0.79	14.34	0.83	1.25	0.24
1.875	0.219	14.73	0.74	13.06	0.77	1.67	0.21
2.375	0.279	13.08	0.69	10.97	0.72	2.11	0.20
2.875	0.341	10.58	0.67	7.51	0.70	3.07	0.21
3.625	0.437	9.29	0.92	6.56	0.95	2.73	0.25
4.25	0.515	6.95	0.39	5.04	0.41	1.91	0.11
5.25	0.645	5.40	0.29	3.34	0.30	2.06	0.09
7.25	0.963	2.53	0.16	0.61	0.17	1.92	0.06
9.50	1.363	2.26	0.16	0.41	0.17	1.85	0.06
11.50	1.684	1.76	0.17	0.09	0.18	1.67	0.05
14.50	2.234	1.76	0.16	-0.04	0.17	1.80	0.06
17.50	2.768	1.81	0.17	0.01	0.18	1.80	0.06

TABLE 3.2.2 Ovre Neådalsvatn: ^{137}Cs, ^{134}Cs and ^{241}Am Data for Core OVNE1

Depth	^{137}Cs Conc		^{134}Cs Conc		^{241}Am Conc	
cm	$pCig^{-1}$	±	$pCig^{-1}$	±	$pCig^{-1}$	±
0.25	36.75	0.73	11.36	1.88	0.00	0.00
0.625	36.33	0.63	14.03	1.81	0.16	0.06
1.125	22.95	0.49	8.51	1.72	0.00	0.00
1.625	10.97	0.32	0.00	0.00	0.19	0.05
1.875	11.25	0.25	0.00	0.00	0.06	0.04
2.375	9.96	0.26	0.00	0.00	0.05	0.03
2.875	5.82	0.20	0.00	0.00	0.00	0.00
3.625	3.05	0.23	0.00	0.00	0.00	0.00
4.25	1.36	0.08	0.00	0.00	0.00	0.00
5.25	0.96	0.06	0.00	0.00	0.00	0.00
7.25	0.58	0.03	0.00	0.00	0.00	0.00
9.50	0.25	0.04	0.00	0.00	0.00	0.00
11.50	0.04	0.03	0.00	0.00	0.00	0.00
14.50	0.00	0.00	0.00	0.00	0.00	0.00
17.50	0.00	0.00	0.00	0.00	0.00	0.00
Inventories:	7.88±0.16 $pCicm^{-2}$		1.72±0.17 $pCicm^{-2}$		0.02±0.01 $pCicm^{-2}$	

TABLE 3.2.3 Ovre Neådalsvatn: ^{210}Pb chronology for Core OVNE1

Depth	Dry Mass	Date	Age		Sedimentation Rate		
cm	gcm^{-2}	AD	yr	±	$gcm^{-2}yr^{-1}$	$cmyr^{-1}$	
0.00	0.000	1991	0				
0.25	0.025	1988	3	2			
0.50	0.050	1986	5	2			
0.75	0.078	1983	8	2			
1.00	0.108	1979	12	2			
1.25	0.139	1976	15	2			
1.50	0.171	1973	18	2			
1.75	0.202	1969	22	2			
2.00	0.233	1966	25	2			
2.25	0.263	1963	28	2		0.076	
2.50	0.294	1960	31	2			
2.75	0.325	1956	35	2			
3.00	0.356	1953	38	2			
3.25	0.388	1949	42	3			
3.50	0.420	1946	45	3			
3.75	0.452	1943	48	3			
4.00	0.484	1939	52	3			
4.25	0.515	1936	55	4			
4.50	0.547	1932	59	4	0.0094		±10.1%
4.75	0.580	1929	62	5			
5.00	0.613	1925	66	5			
5.25	0.645	1922	69	6			
5.50	0.685	1918	73	7			
5.75	0.725	1914	77	8			
6.00	0.764	1909	82	9			
6.25	0.804	1905	86	10			
6.50	0.844	1901	90	11			
6.75	0.883	1897	94	12			
7.00	0.923	1892	99	13		0.057	
7.25	0.963	1888	103	14			
7.50	1.007	1883	108	15			
7.75	1.052	1879	112	16			
8.00	1.096	1874	117	17			
8.25	1.141	1869	122	18			
8.50	1.185	1864	127	19			
8.75	1.230	1860	131	20			
9.00	1.274	1855	136	21			
9.25	1.318	1850	141	22			
9.50	1.363	1845	146	23			

STAVSVATN

FIG. 3.3.1

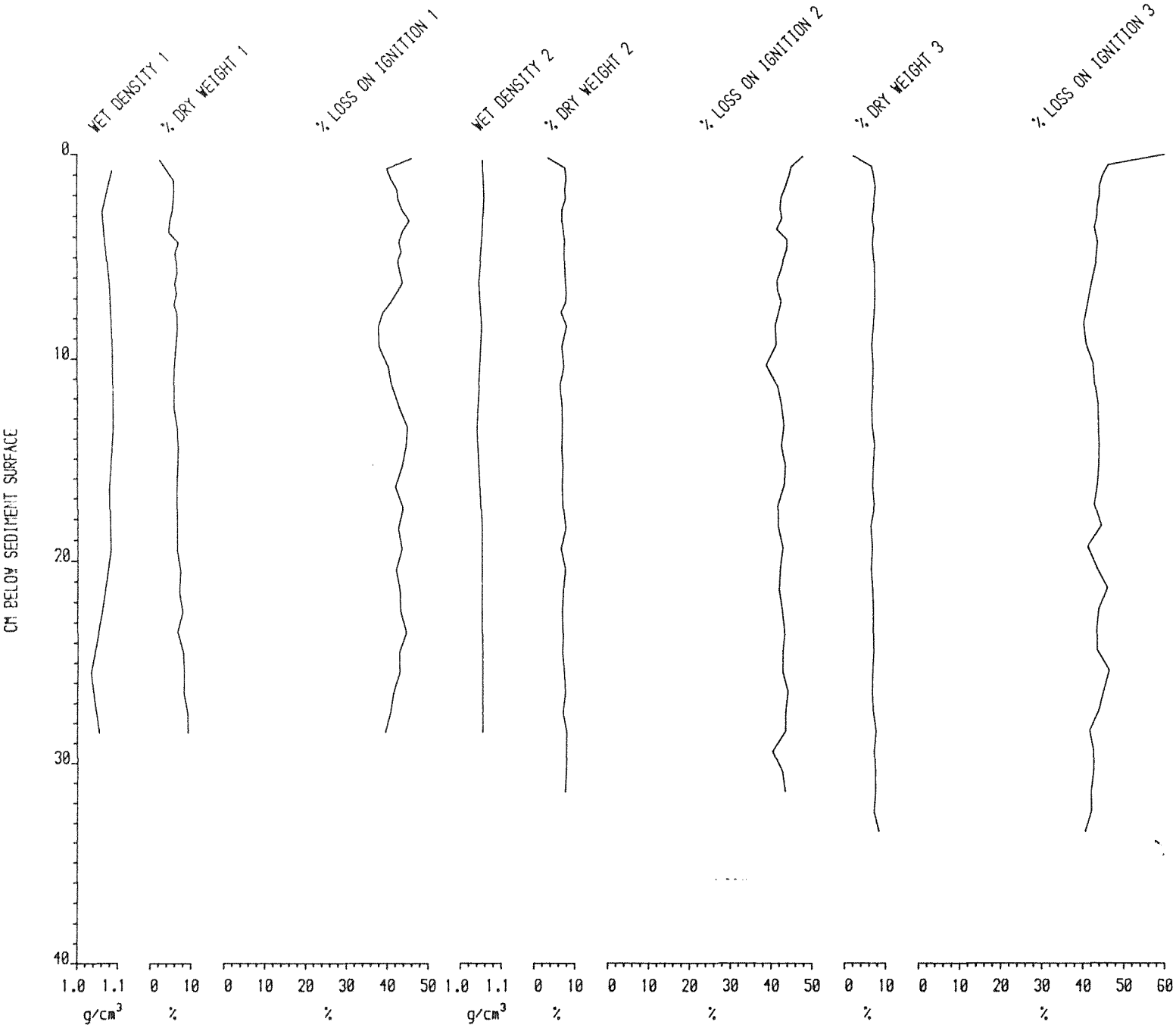

FIG. 3.3.2

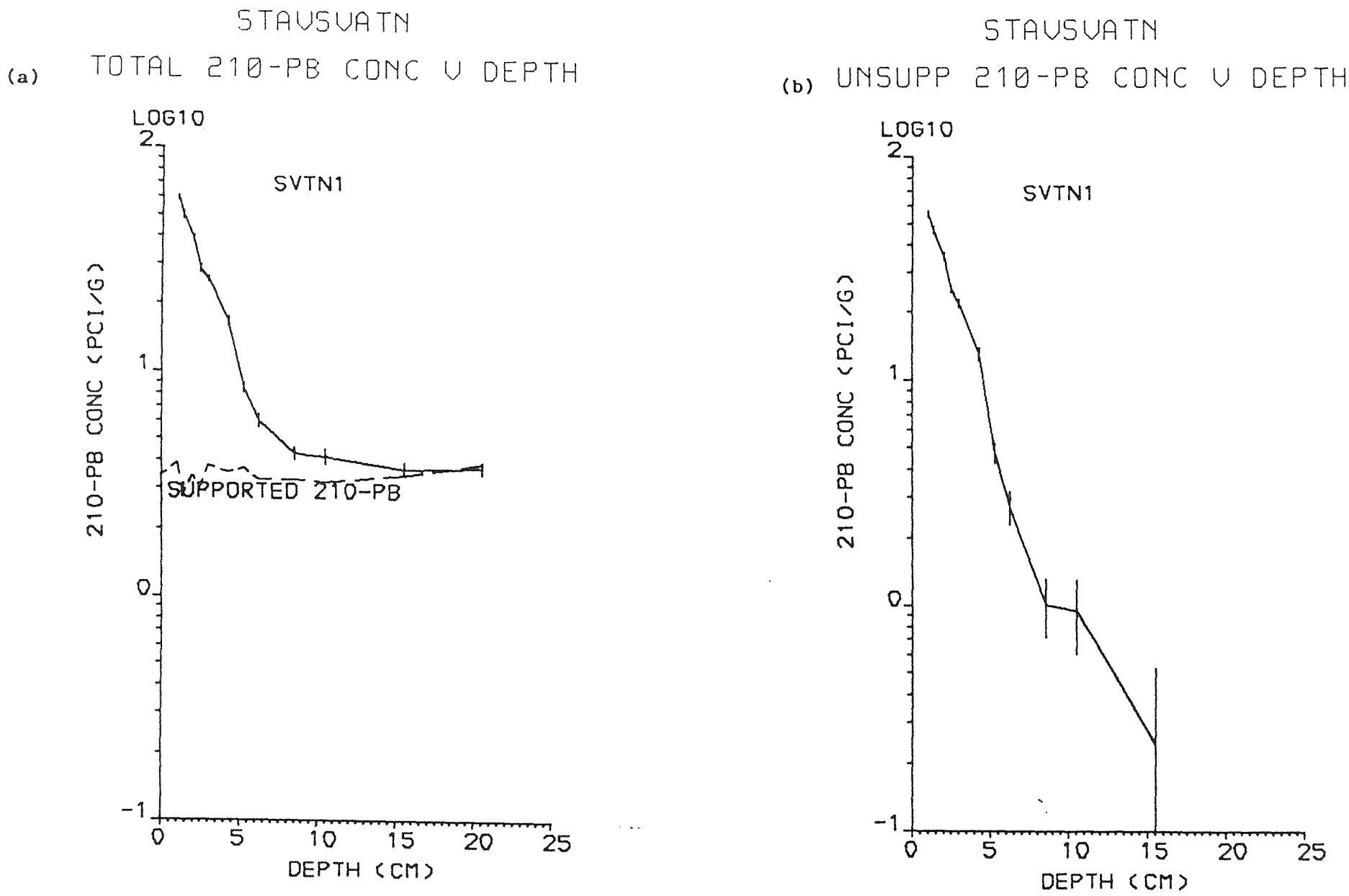
STAVSVATN
(a) TOTAL 210-PB CONC V DEPTH
LOG10
SVTN1
210-PB CONC (PCI/G)
SUPPORTED 210-PB
DEPTH (CM)
STAVSVATN
(b) UNSUPP 210-PB CONC V DEPTH
LOG10
SVTN1
210-PB CONC (PCI/G)
DEPTH (CM)

FIG. 3.3.3

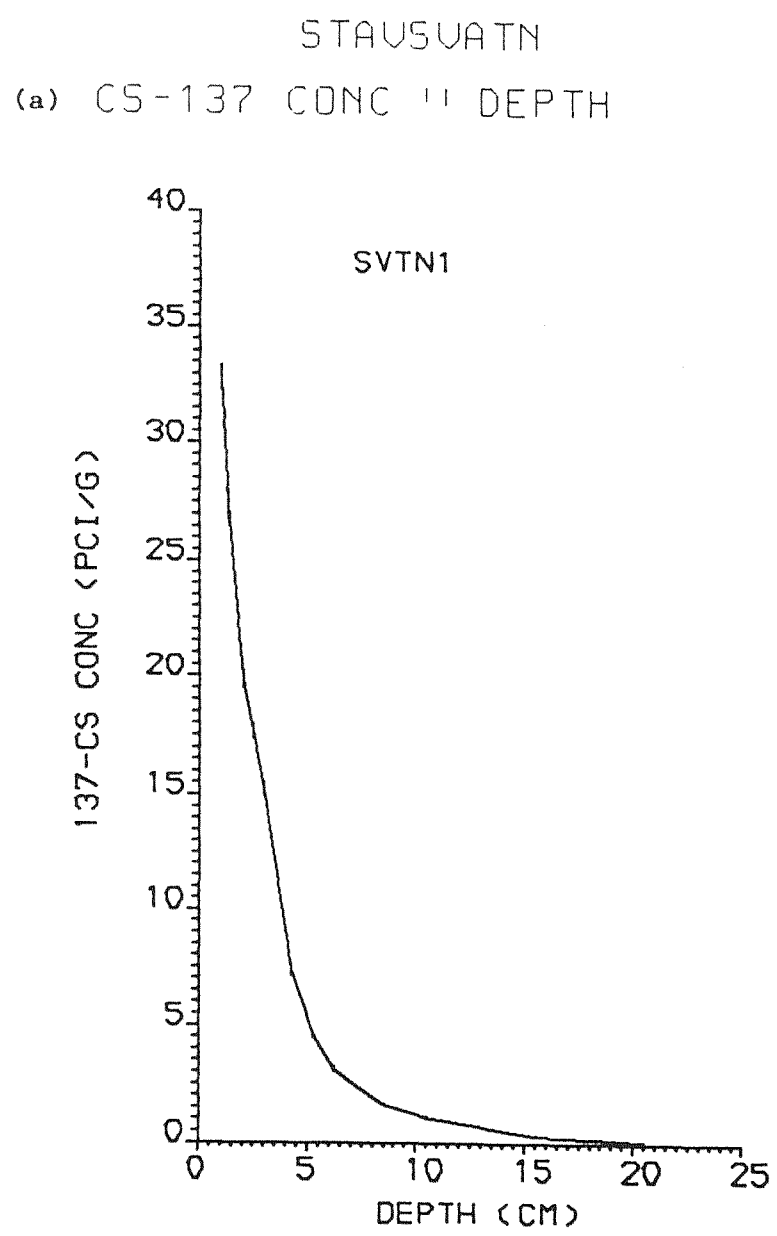
STAVSVATN
(a) CS-137 CONC V DEPTH
SVTN1
137-CS CONC (PCI/G)
DEPTH (CM)
0
5
10
15
20
25
30
35
40

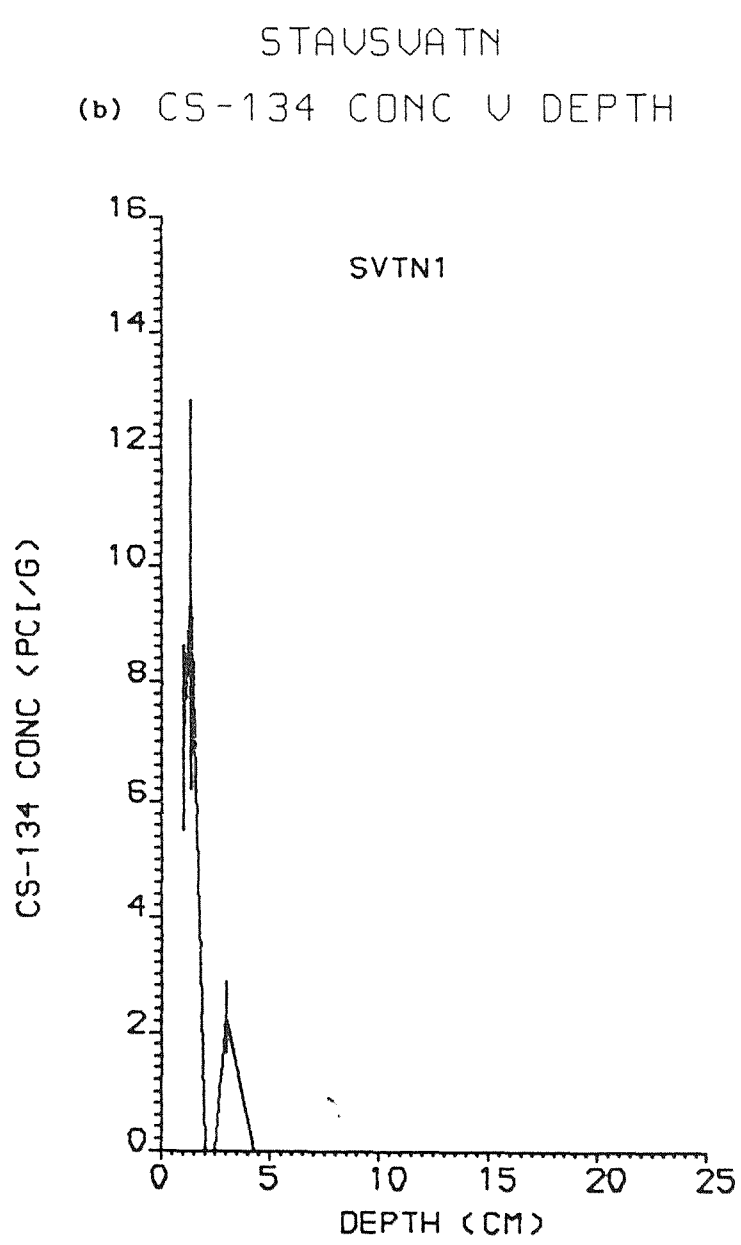
STAVSVATN
(b) CS-134 CONC V DEPTH
SVTN1
CS-134 CONC (PCI/G)
DEPTH (CM)
0
2
4
6
8
10
12
14
16
5
15
20
25

FIG. 3.3.4

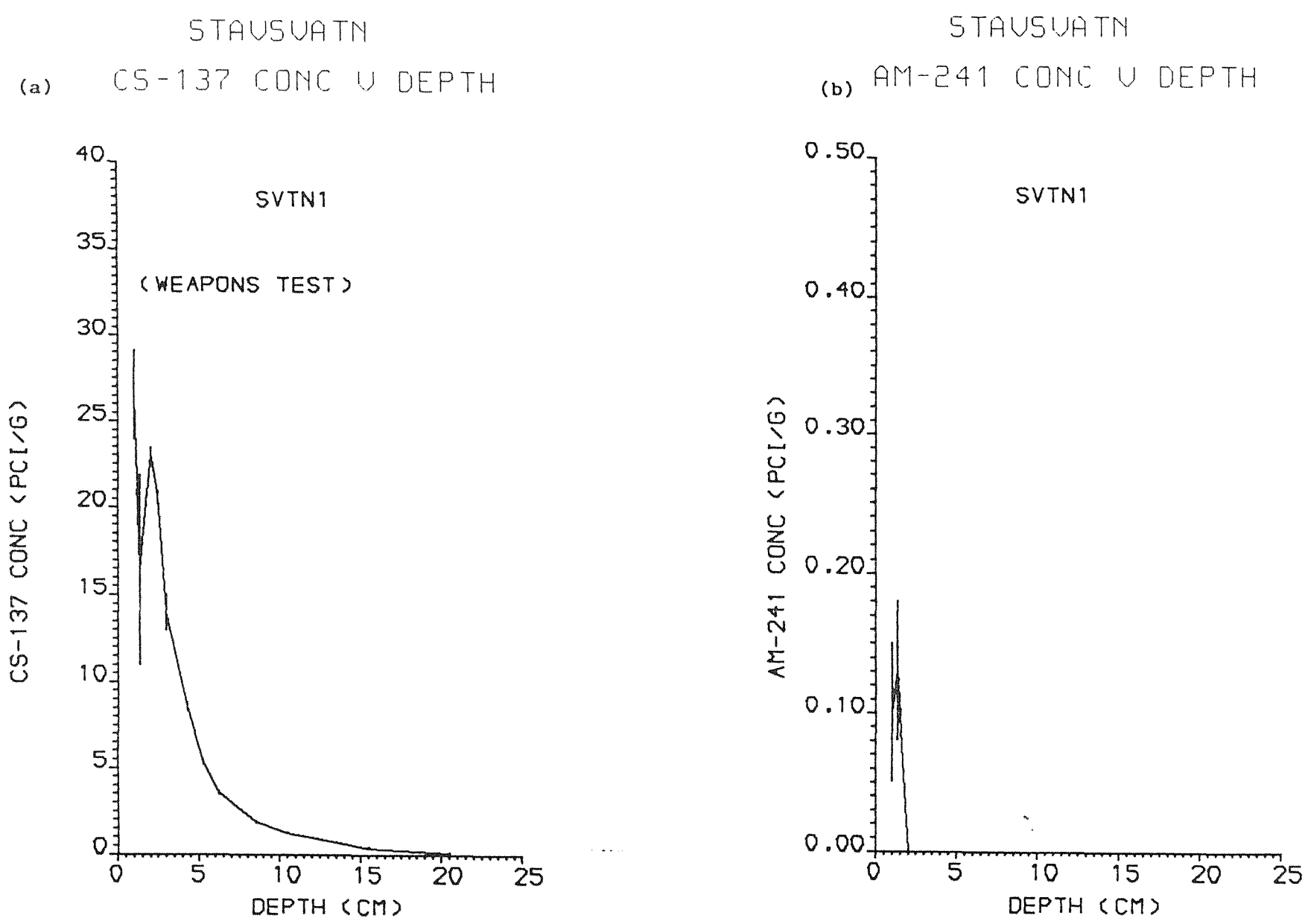
STAVSVATN
(a) CS-137 CONC V DEPTH
SVTN1
(WEAPONS TEST)
CS-137 CONC (PCI/G)
DEPTH (CM)
0
5
10
15
20
25
30
35
40
STAVSVATN
(b) AM-241 CONC V DEPTH
SVTN1
AM-241 CONC (PCI/G)
DEPTH (CM)
0.00
0.10
0.20
0.30
0.40
0.50

FIG. 3.3.5

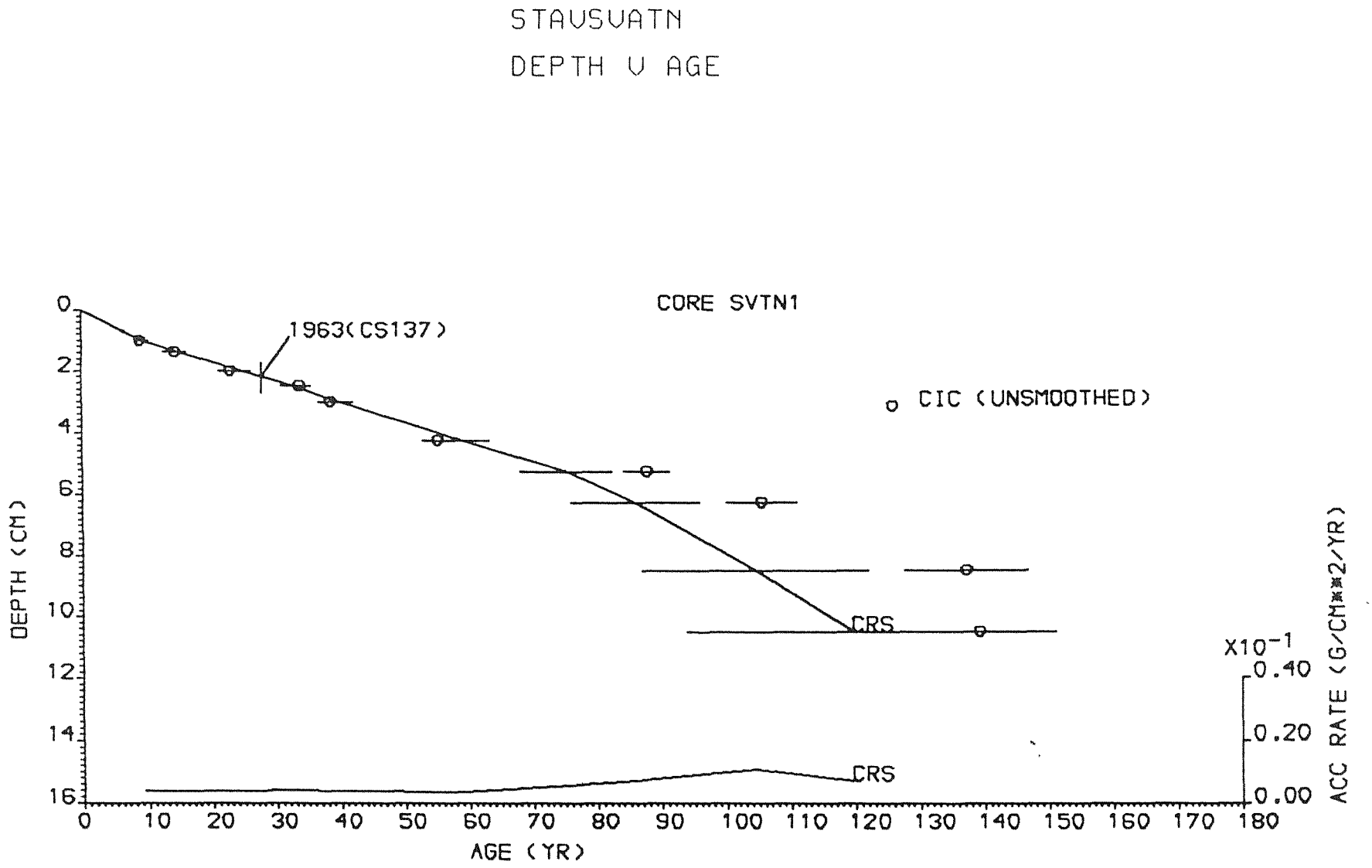
STAVSVATN
DEPTH V AGE
CORE SVTN1
1963(CS137)
CIC (UNSMOOTHED)
CRS
CRS
DEPTH (CM)
AGE (YR)
ACC RATE (G/CM**2/YR)
X10-1
0.40
0.20
0.00
0
2
4
6
8
10
12
14
16
0
10
20
30
40
50
60
70
80
90
100
110
120
130
140
150
160
170
180

Carbonaceous Particle Concentration and Flux Profiles

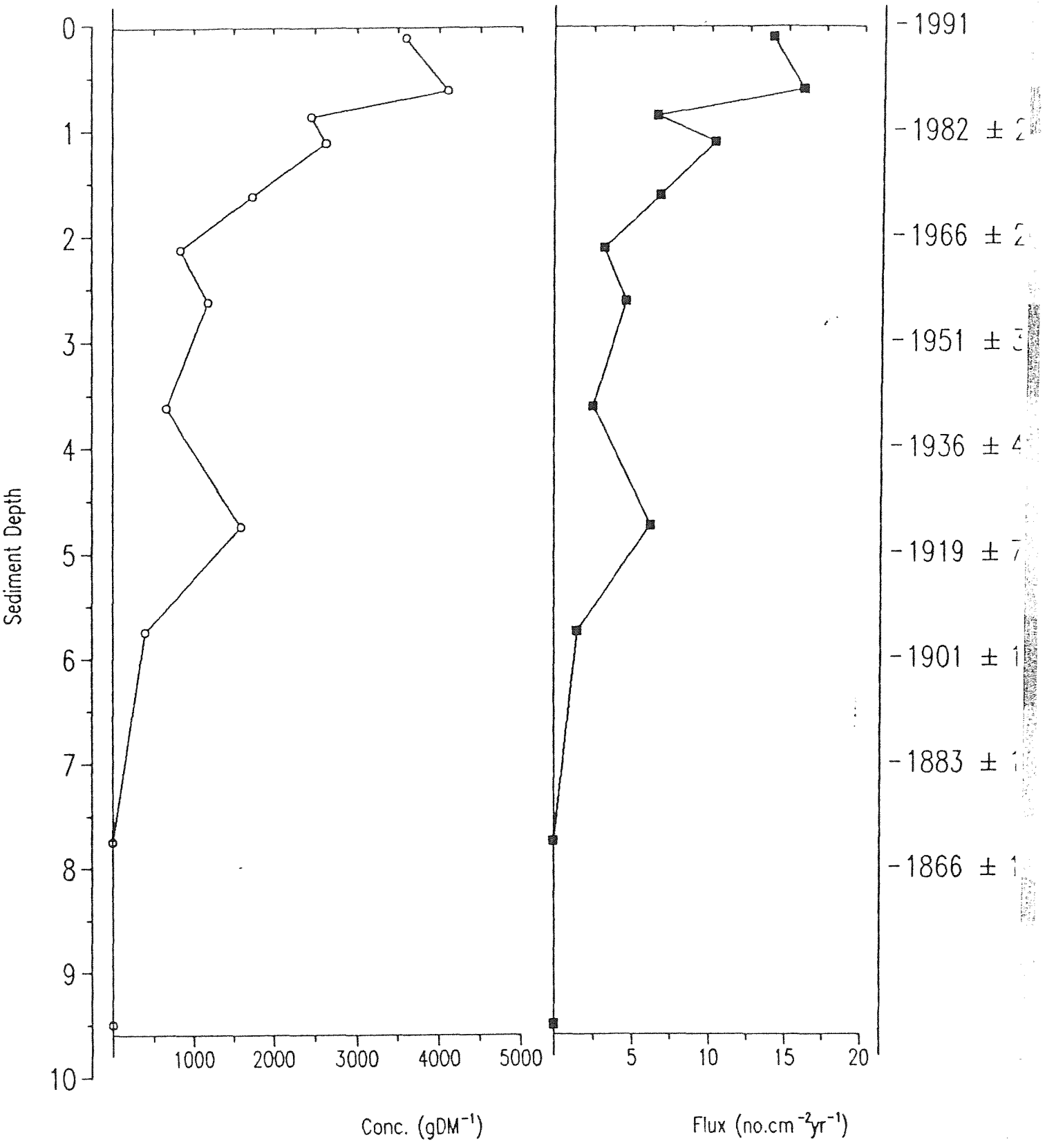

VINT, diatom cell concentration

FIG. 3.3.7

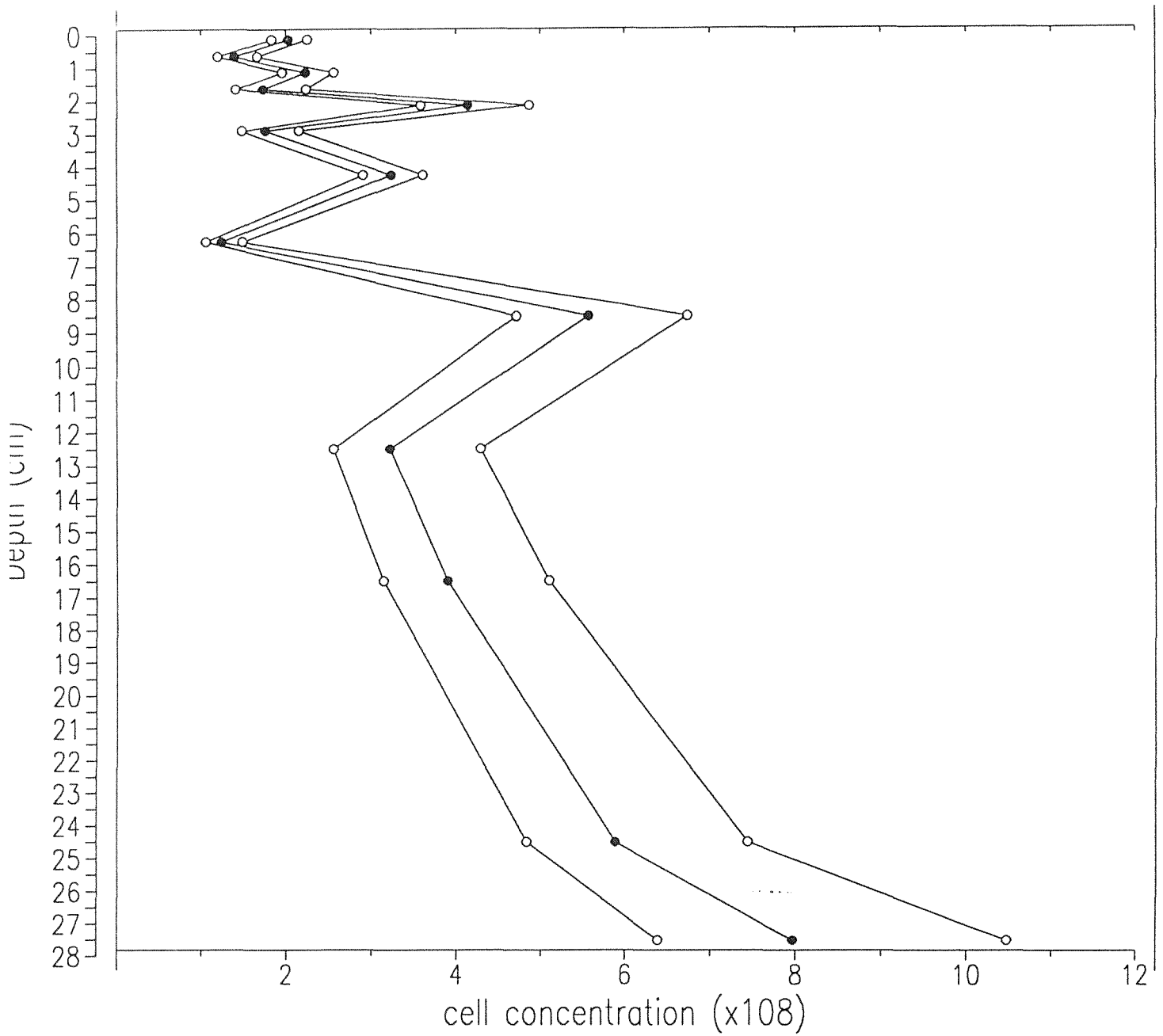

avsvatn, SVINT summary percentage diatom diagram

FIG. 3.3.8

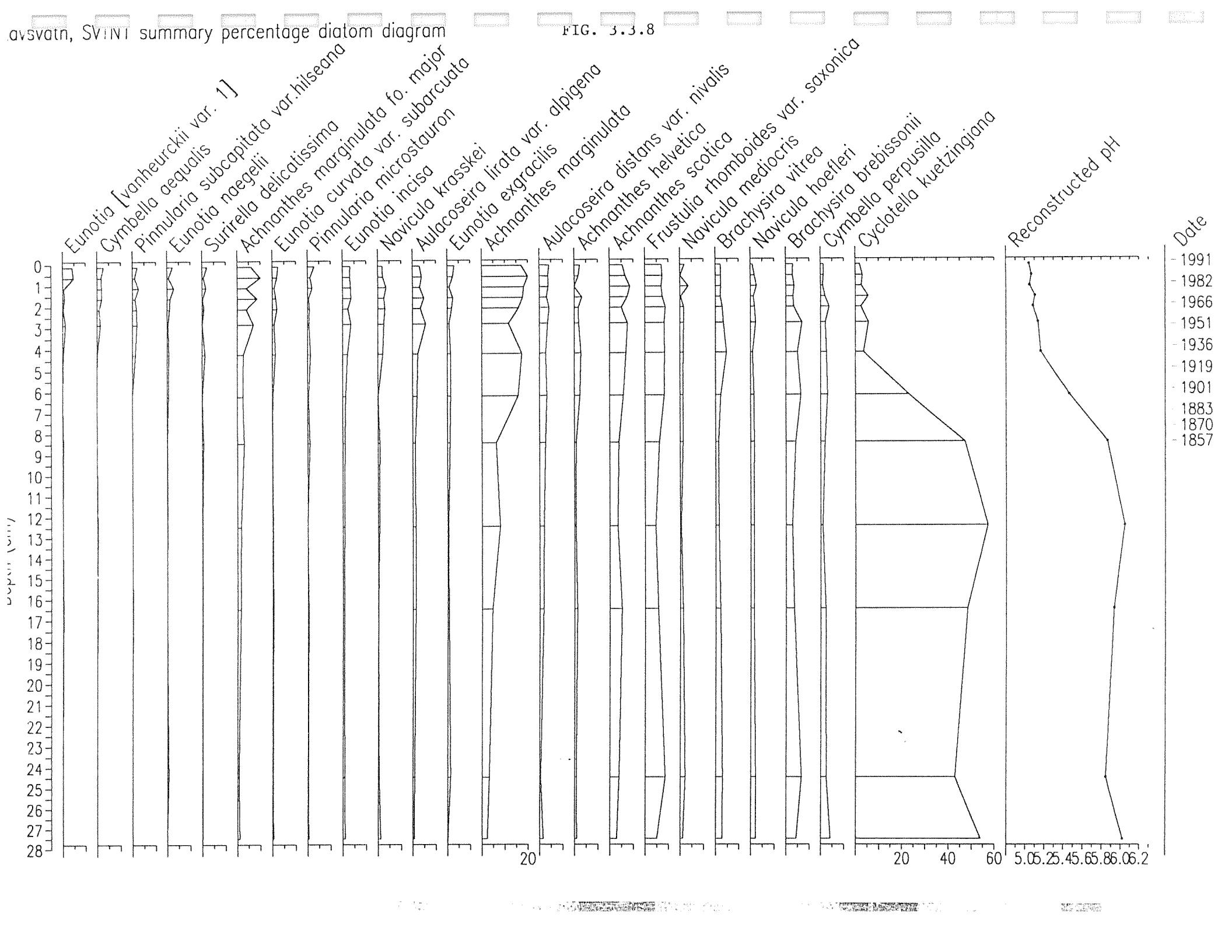

TABLE 3.3.1 Stavsvatn: ^{210}Pb chronology for Core SVTN1

Depth cm	Dry Mass gcm^{-2}	Date AD	Age yr	±	Sedimentation Rate $gcm^{-2}yr^{-1}$	Sedimentation Rate $cmyr^{-1}$	
0.00	0.000	1991	0				
0.25	0.009	1989	2	1			
0.50	0.018	1986	5	1		0.11	
0.75	0.027	1984	7	1			
1.00	0.036	1982	9	2			
1.25	0.050	1978	13	2			
1.50	0.065	1974	17	2			
1.75	0.081	1970	21	2			
2.00	0.096	1966	25	2			
2.25	0.112	1962	29	2			
2.50	0.127	1958	33	2			
2.75	0.141	1955	36	3		0.064	
3.00	0.155	1951	40	3			
3.25	0.169	1947	44	3			
3.50	0.183	1943	48	4			
3.75	0.197	1939	52	4			
4.00	0.211	1936	55	4			
4.25	0.225	1932	59	5	0.0039		~11.6%
4.50	0.243	1928	63	5			
4.75	0.260	1923	68	6			
5.00	0.277	1919	72	7			
5.25	0.294	1915	76	8			
5.50	0.312	1910	81	8			
5.75	0.329	1906	85	9			
6.00	0.346	1901	90	10			
6.25	0.363	1897	94	10			
6.50	0.380	1892	99	11			
6.75	0.397	1888	103	12		0.057	
7.00	0.414	1883	108	13			
7.25	0.431	1879	112	14			
7.50	0.449	1875	116	15			
7.75	0.466	1870	121	16			
8.00	0.483	1866	125	16			
8.25	0.500	1861	130	17			
8.50	0.517	1857	134	18			

TABLE 3.3.2 · Stavsvatn: ^{210}Pb Data for Core STAV1

Depth	Dry Mass	^{210}Pb Concentration Total		^{210}Pb Concentration Unsupp		^{226}Ra Concentration	
cm	gcm^{-2}	$pCig^{-1}$	±	$pCig^{-1}$	±	$pCig^{-1}$	±
1.00	0.036	58.85	1.66	55.01	1.86	3.84	0.85
1.375	0.058	49.16	1.80	46.45	1.84	2.71	0.38
2.00	0.096	38.76	1.23	35.38	1.42	3.38	0.70
2.50	0.127	28.29	1.08	25.32	1.09	2.97	0.16
3.00	0.155	25.57	0.84	21.80	0.96	3.77	0.46
4.25	0.225	16.49	0.82	12.98	0.84	3.51	0.20
5.25	0.294	8.36	0.47	4.72	0.49	3.64	0.12
6.25	0.363	5.96	0.43	2.71	0.45	3.25	0.12
8.50	0.517	4.26	0.29	1.01	0.30	3.25	0.09
10.50	0.653	4.12	0.33	0.95	0.35	3.17	0.11
15.50	0.992	3.63	0.27	0.24	0.28	3.39	0.09
20.50	1.347	3.68	0.25	-0.16	0.27	3.84	0.09

TABLE 3.3.3 Stavsvatn: ^{137}Cs, ^{134}Cs and ^{241}Am Data for Core STAV1

Depth	^{137}Cs Conc		^{134}Cs Conc		^{241}Am Conc	
cm	$pCig^{-1}$	±	$pCig^{-1}$	±	$pCig^{-1}$	±
1.00	32.75	0.60	7.06	1.57	0.10	0.05
1.375	27.36	0.64	9.51	3.32	0.13	0.05
2.00	19.81	0.40	0.00	0.00	0.00	0.00
2.50	17.63	0.35	0.00	0.00	0.00	0.00
3.00	15.19	0.30	2.25	0.00	0.00	0.00
4.25	7.32	0.22	0.00	0.00	0.00	0.00
5.25	4.55	0.12	0.00	0.00	0.00	0.00
6.25	3.07	0.11	0.00	0.00	0.00	0.00
8.50	1.58	0.06	0.00	0.00	0.00	0.00
10.50	1.05	0.07	0.00	0.00	0.00	0.00
15.50	0.31	0.06	0.00	0.00	0.00	0.00
20.50	0.05	0.05	0.00	0.00	0.00	0.00
Inventories:	6.07±0.12 $pCicm^{-2}$		0.73±0.13 $pCicm^{-2}$		0.01±0.005 $pCicm^{-2}$	

PAIONE SUPERIORE

FIG. 3.4.1

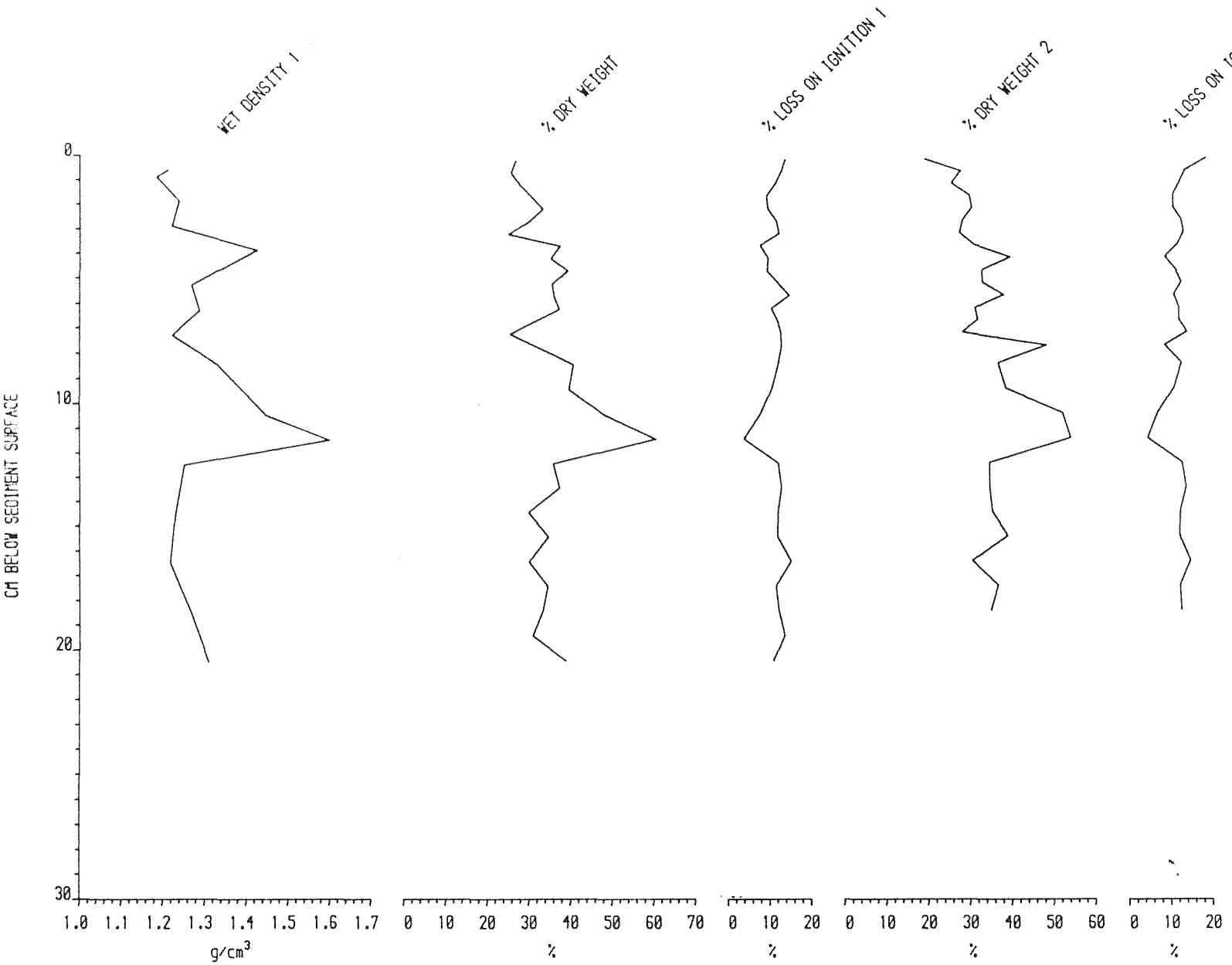

FIG. 3.4.2

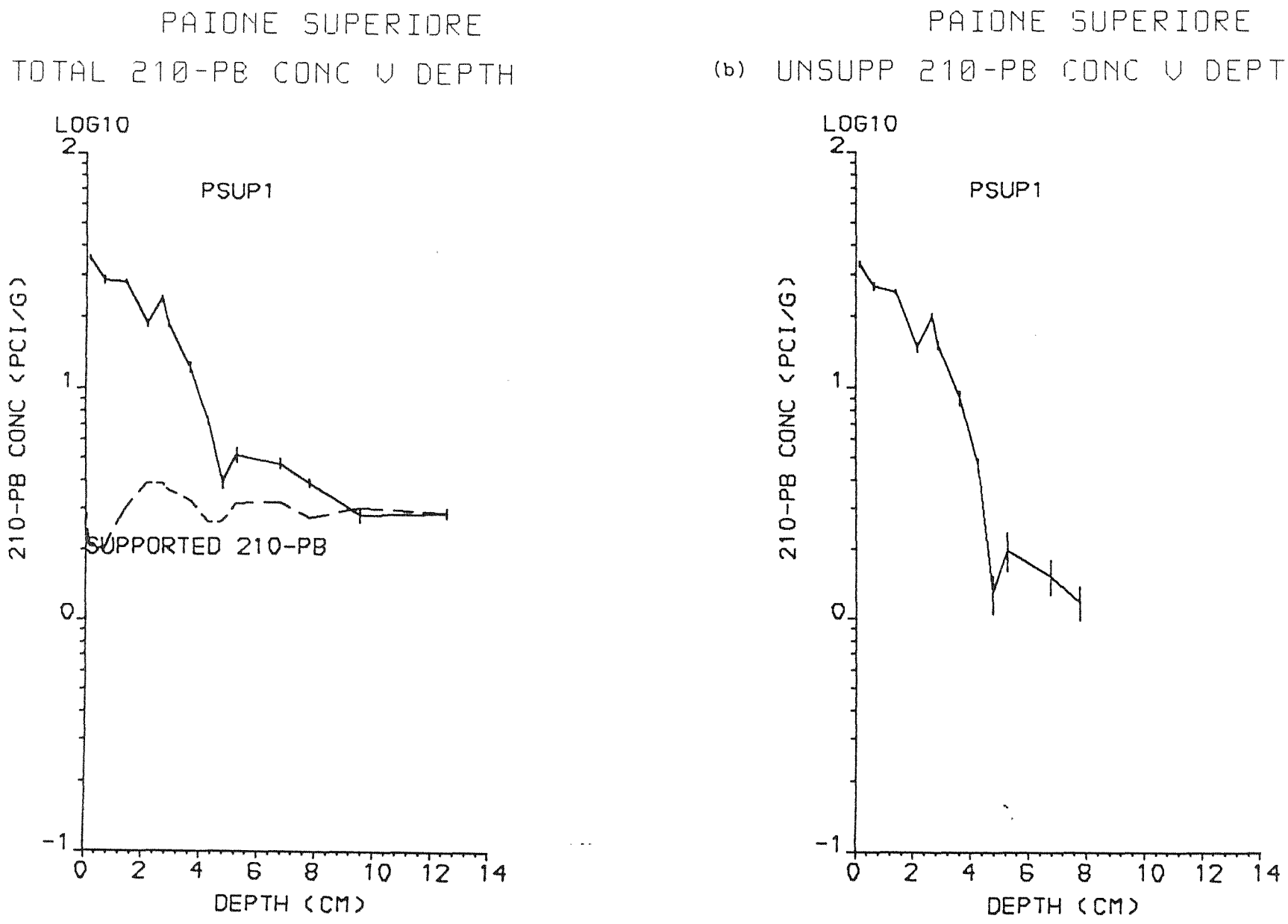
PAIONE SUPERIORE
(a) TOTAL 210-PB CONC V DEPTH
LOG10
PSUP1
210-PB CONC (PCI/G)
SUPPORTED 210-PB
DEPTH (CM)
PAIONE SUPERIORE
(b) UNSUPP 210-PB CONC V DEPTH
LOG10
PSUP1
210-PB CONC (PCI/G)
DEPTH (CM)

FIG. 3.4.3

PAIONE SUPERIORE

(a) CS-137 CONC V DEPTH

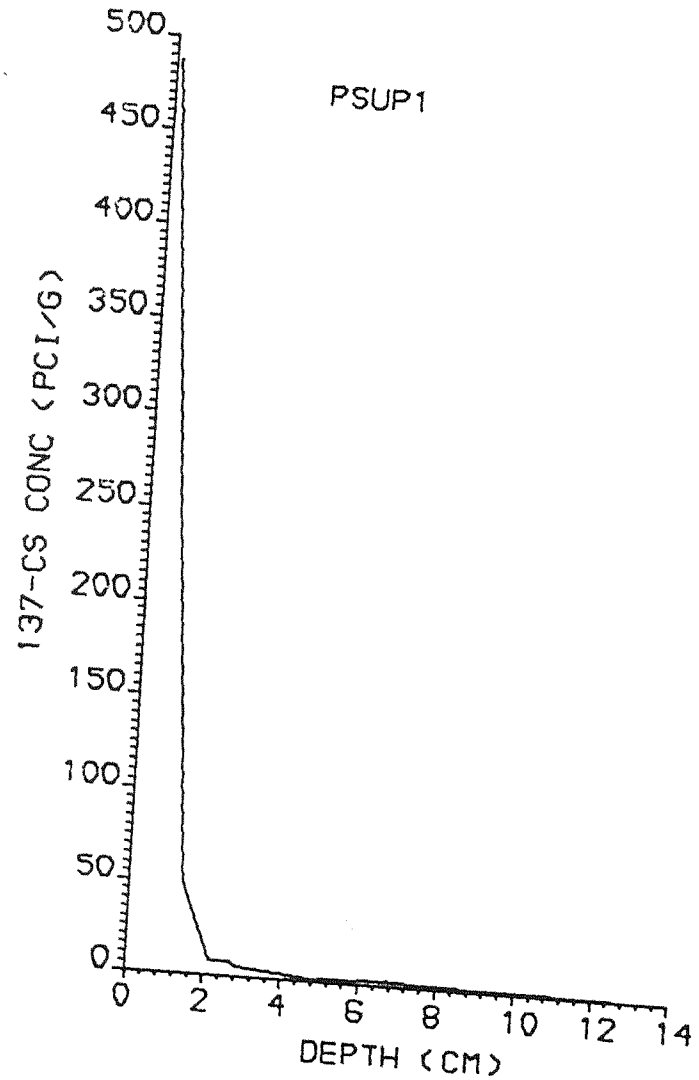

PAIONE SUPERIORE

(b) CS-134 CONC V DEPTH

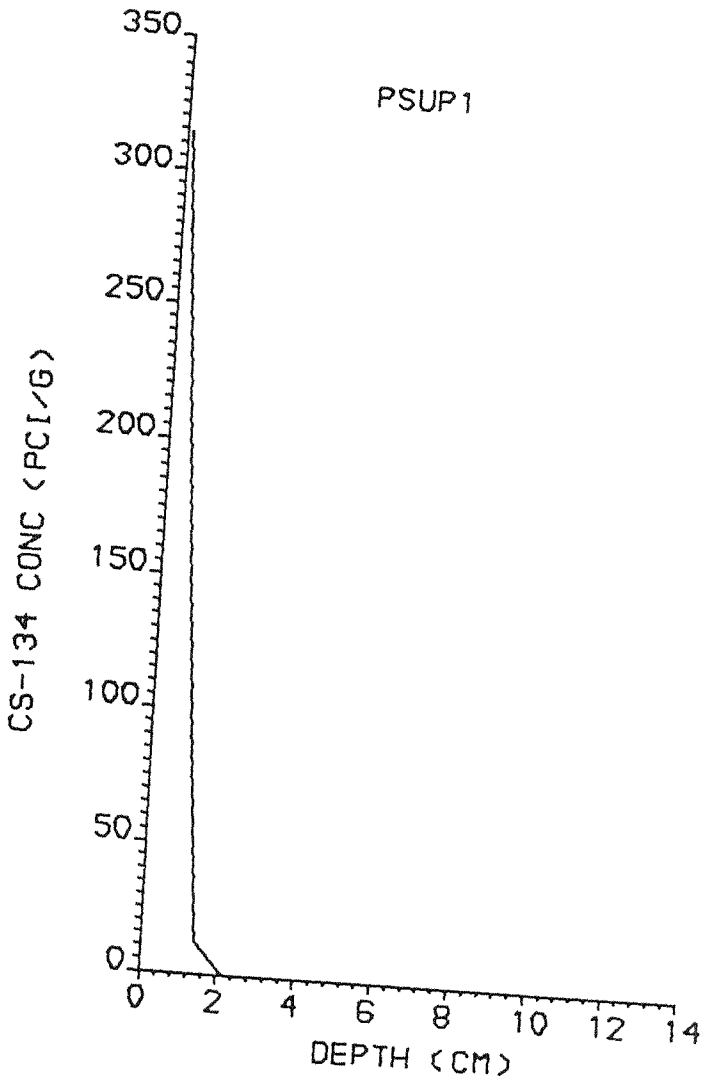

FIG. 3.4.4

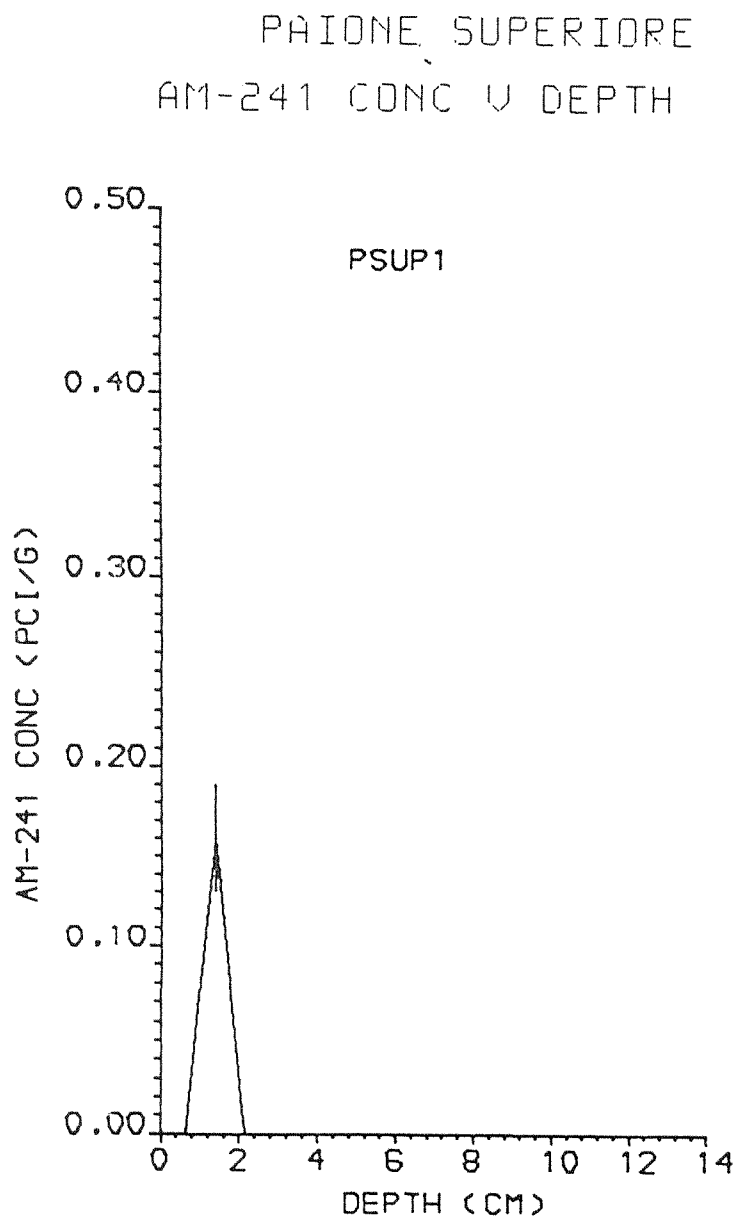
PAIONE SUPERIORE
AM-241 CONC V DEPTH
PSUP1
AM-241 CONC (PCI/G)
0.50
0.40
0.30
0.20
0.10
0.00
0
2
4
6
8
10
12
14
DEPTH (CM)

FIG. 3.4.5

PAIONE SUPERIORE

DEPTH V AGE

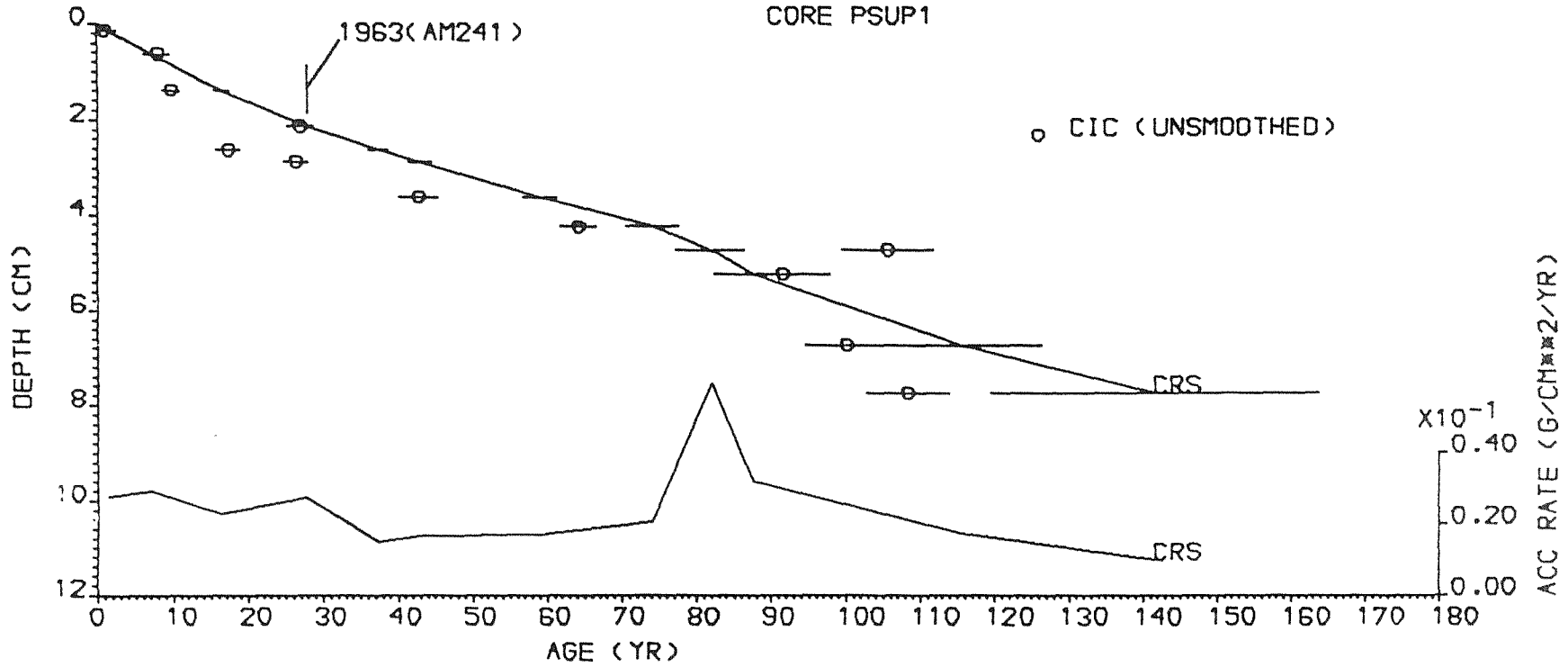

Palone Superiore (PSUP 1) 1991 FIG. 3.4.6

Carbonaceous Particle Concentration and Flux Profiles

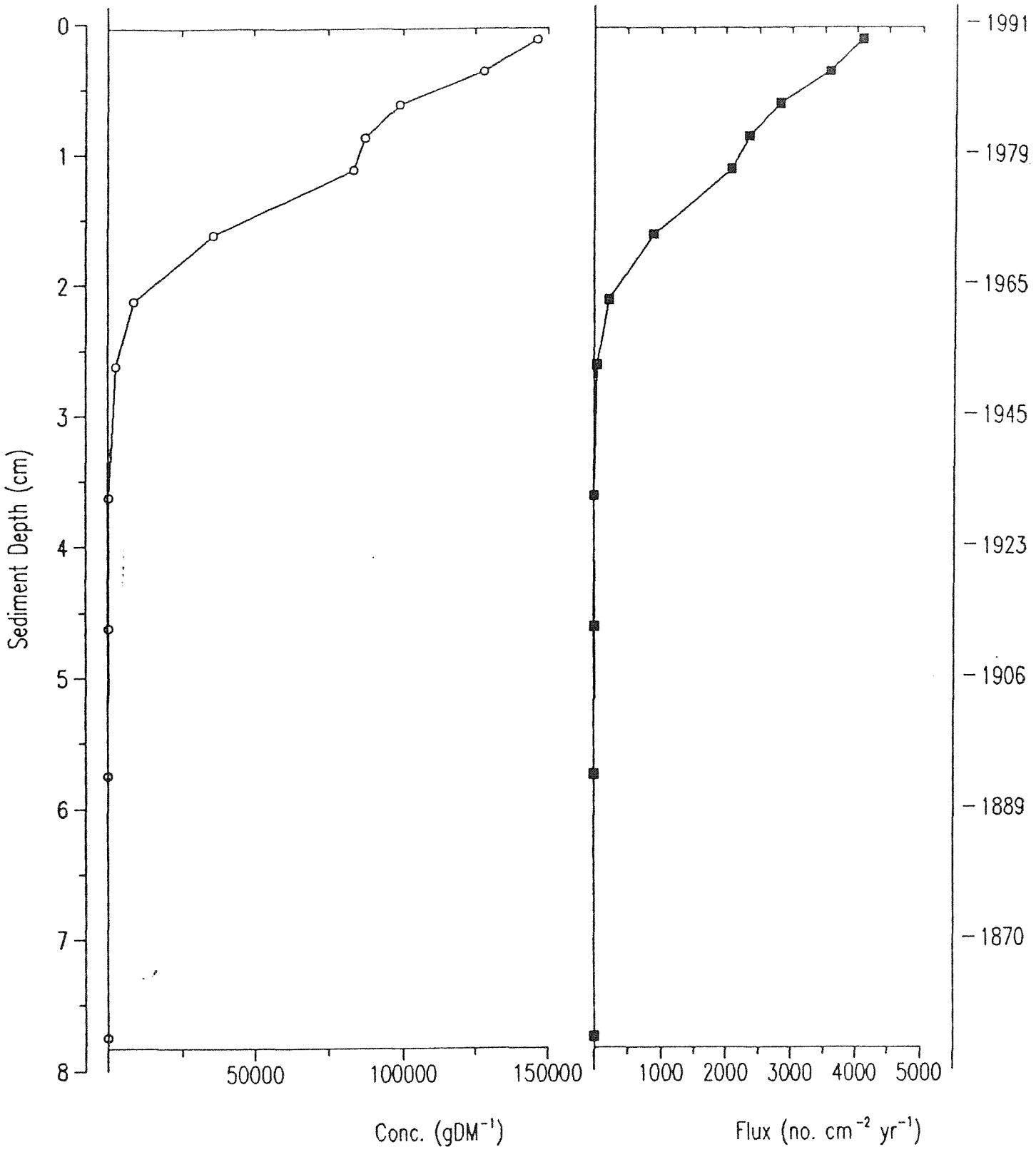

UP1, diatom cell concentration

FIG. 3.4.7

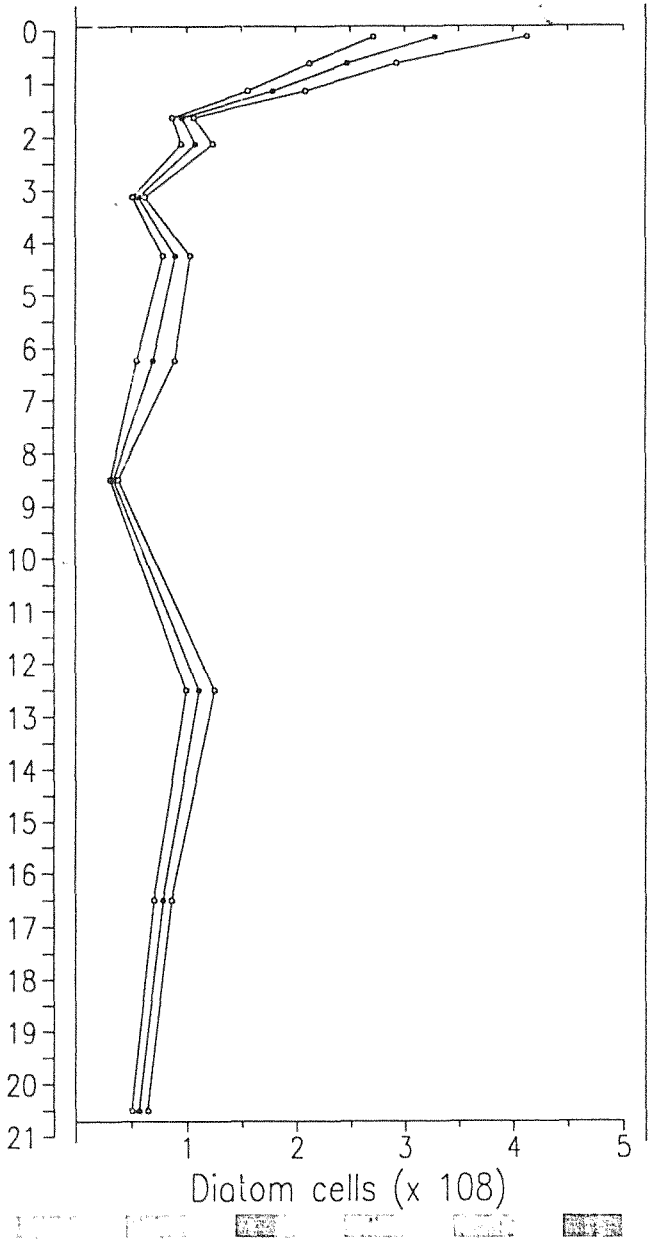

e Superiore, PSUP1 summary percentage diatom diagram

FIG. 3.4.8

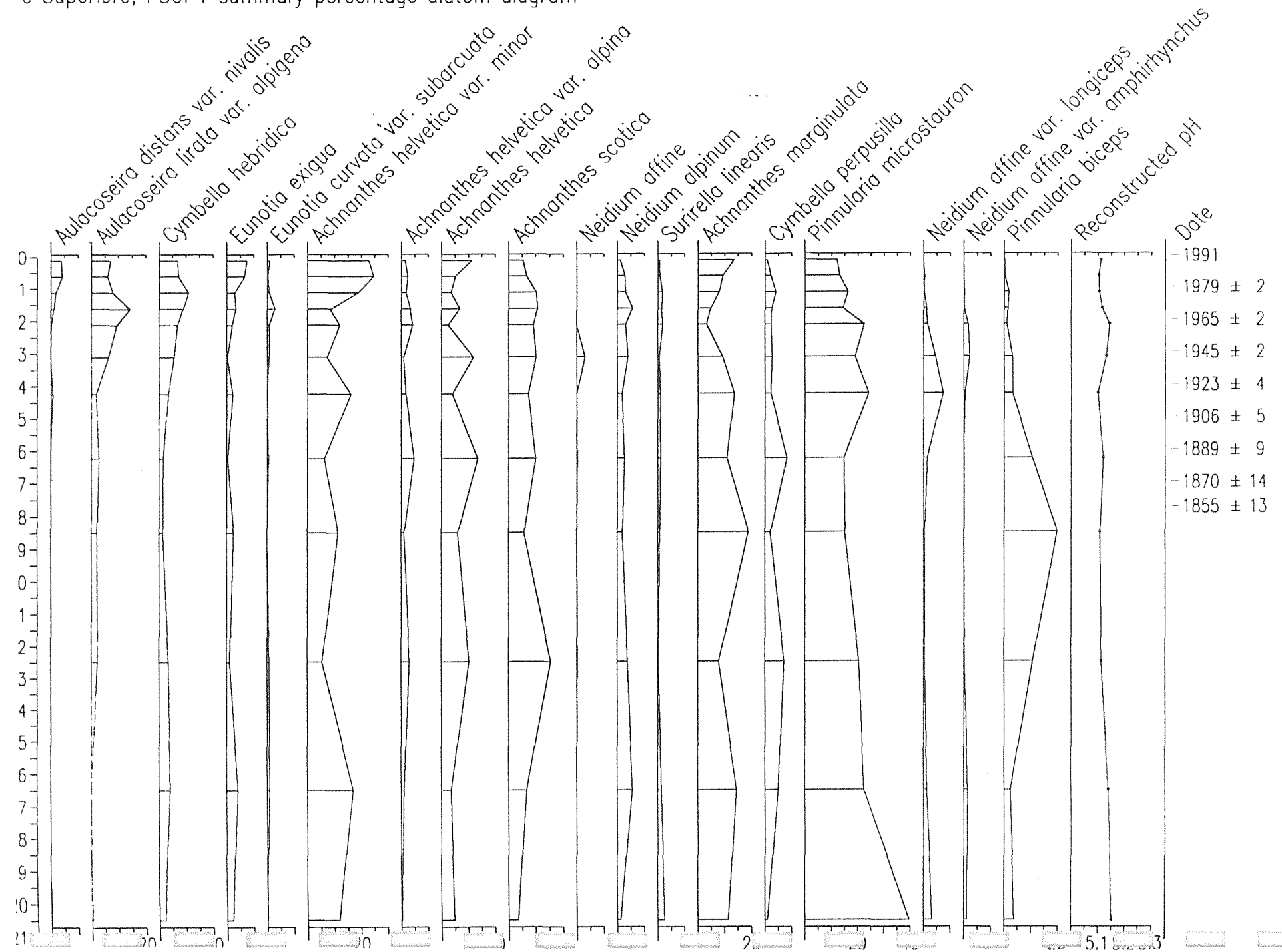

TABLE 3.4.1 . Lake Palone Superiore: ^{210}Pb chronology for Core PSUP1

Depth	Dry Mass	Date	Age		Sedimentation Rate		
cm	gcm^{-2}	AD	yr	±	$gcm^{-2}yr^{-1}$	$cmyr^{-1}$	
0.00	0.00	1991	0				
0.25	0.08	1988	3	2	0.028	0.089	4.0
0.50	0.16	1985	6	2	0.029	0.090	4.4
0.75	0.24	1982	9	2	0.028	0.087	4.5
1.00	0.32	1979	12	2	0.026	0.078	4.3
1.25	0.40	1976	15	2	0.024	0.070	4.0
1.50	0.49	1973	18	2	0.024	0.067	4.2
1.75	0.58	1969	22	2	0.025	0.069	4.8
2.00	0.68	1965	26	2	0.027	0.071	5.5
2.25	0.77	1961	30	2	0.025	0.064	5.9
2.50	0.87	1956	35	2	0.019	0.048	6.1
2.75	0.97	1951	40	2	0.016	0.043	6.3
3.00	1.06	1945	46	2	0.017	0.046	7.1
3.25	1.15	1940	51	2	0.017	0.045	8.2
3.50	1.24	1935	56	3	0.017	0.043	9.4
3.75	1.34	1929	62	3	0.018	0.043	10.6
4.00	1.45	1923	68	4	0.019	0.044	12.1
4.25	1.57	1917	74	4	0.021	0.045	13.5
4.50	1.69	1913	78	5	0.040	0.083	18.5
4.75	1.81	1909	82	5	0.059	0.122	23.5
5.00	1.93	1906	85	5	0.046	0.096	22.1
5.25	2.05	1903	88	6	0.032	0.070	20.8
5.50	2.17	1899	92	7	0.030	0.065	23.3
5.75	2.28	1894	97	8	0.027	0.060	25.9
6.00	2.40	1889	102	9	0.025	0.056	28.5
6.25	2.51	1885	106	9	0.022	0.051	31.0
6.50	2.62	1880	111	10	0.020	0.047	33.6
6.75	2.74	1875	116	11	↑	↑	
7.00	2.83	1870	121	14			
7.25	2.91	1865	126	17	0.018	0.050	
7.50	3.00	1860	131	20			
7.75	3.09	1855	136	23	↓	↓	

TABLE 3.4.2 Lake Palone Superiore: ^{210}Pb Data for Core PSUP1

Depth	Dry Mass	^{210}Pb Concentration				^{226}Ra Concentration	
		Total		Unsupp			
cm	gcm^{-2}	$pCig^{-1}$	±	$pCig^{-1}$	±	$pCig^{-1}$	±
0.125	0.04	35.29	0.93	33.15	0.96	2.14	0.24
0.625	0.20	28.63	1.09	26.64	1.12	1.99	0.26
1.375	0.44	28.19	0.61	25.22	0.62	2.97	0.13
2.125	0.73	18.64	0.67	14.74	0.69	3.90	0.16
2.625	0.93	23.78	0.75	19.89	0.77	3.89	0.17
2.875	1.02	18.62	0.58	15.00	0.60	3.62	0.14
3.625	1.29	12.23	0.68	8.98	0.70	3.25	0.16
4.25	1.57	7.24	0.31	4.62	0.32	2.62	0.09
4.75	1.81	3.90	0.23	1.27	0.24	2.63	0.06
5.25	2.05	5.14	0.38	1.97	0.39	3.17	0.10
6.75	2.74	4.71	0.25	1.51	0.26	3.20	0.07
7.75	3.09	3.90	0.19	1.17	0.20	2.73	0.05
9.50	3.99	2.81	0.21	-0.22	0.22	3.03	0.07
12.50	6.15	2.87	0.16	-0.02	0.17	2.89	0.05

TABLE 3.4.3 Lake Palone Superiore: ^{137}Cs, ^{134}Cs and ^{241}Am Data for Core PSUP1

Depth	^{137}Cs Conc		^{134}Cs Conc		^{241}Am Conc	
cm	$pCig^{-1}$	±	$pCig^{-1}$	±	$pCig^{-1}$	±
0.125	486.4	1.0	310.8	2.8	0.00	0.00
0.625	316.0	0.9	186.2	2.4	0.00	0.00
1.375	48.4	0.3	11.9	0.6	0.16	0.03
2.125	7.5	0.2	0.0	0.0	0.00	0.00
2.625	7.5	0.2	0.0	0.0	0.00	0.00
2.875	4.9					
cm	pCig	±	$pCig^{-1}$	±	$pCig^{-1}$	±
0.125	486.4	1.0	310.8	2.8	0.00	0.00
0.625	316.0	0.9	186.2	2.4	0.00	0.00
1.375	48.4	0.3	11.9	0.6	0.16	0.03
2.125	7.5	0.2	0.0	0.0	0.00	0.00
2.625	7.5	0.2	0.0	0.0	0.00	0.00
2.875	4.9	0.0	0.0	0.00	0.00	
12.50	0.1	0.02	0.0	0.0	0.00	0.00
Inventories:	145.6 ± 4.0 $pCicm^{-2}$		78.1 ± 2.5 $pCicm^{-2}$		0.04±0.01 $pCicm^{-2}$	

MILCHSEE (LAGO DI LATTE)

FIG. 3.5.1

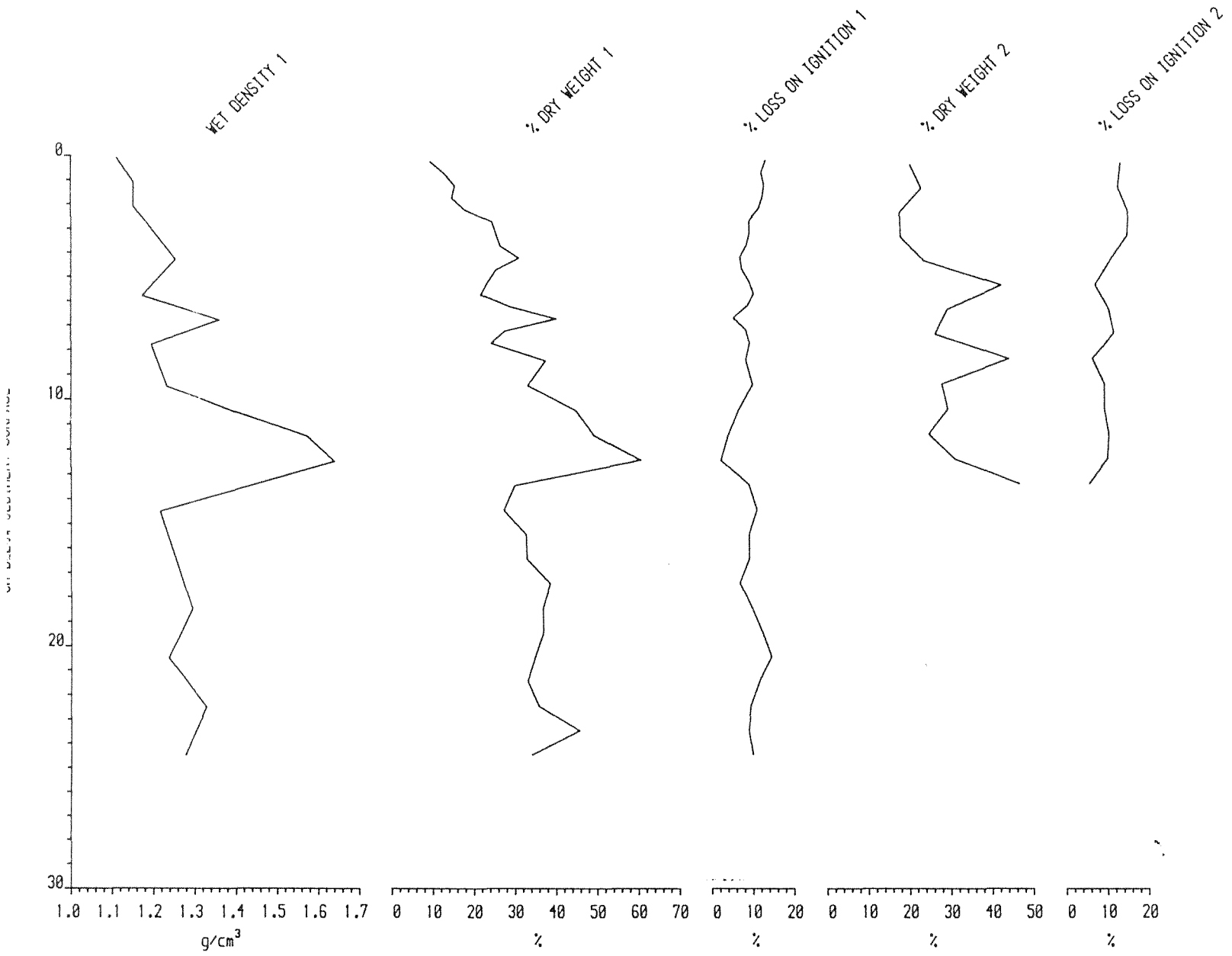

FIG. 3.5.2

MILCHSEE (LAGO DI LATTE)

(a) TOTAL 210-PB CONC V DEPTH

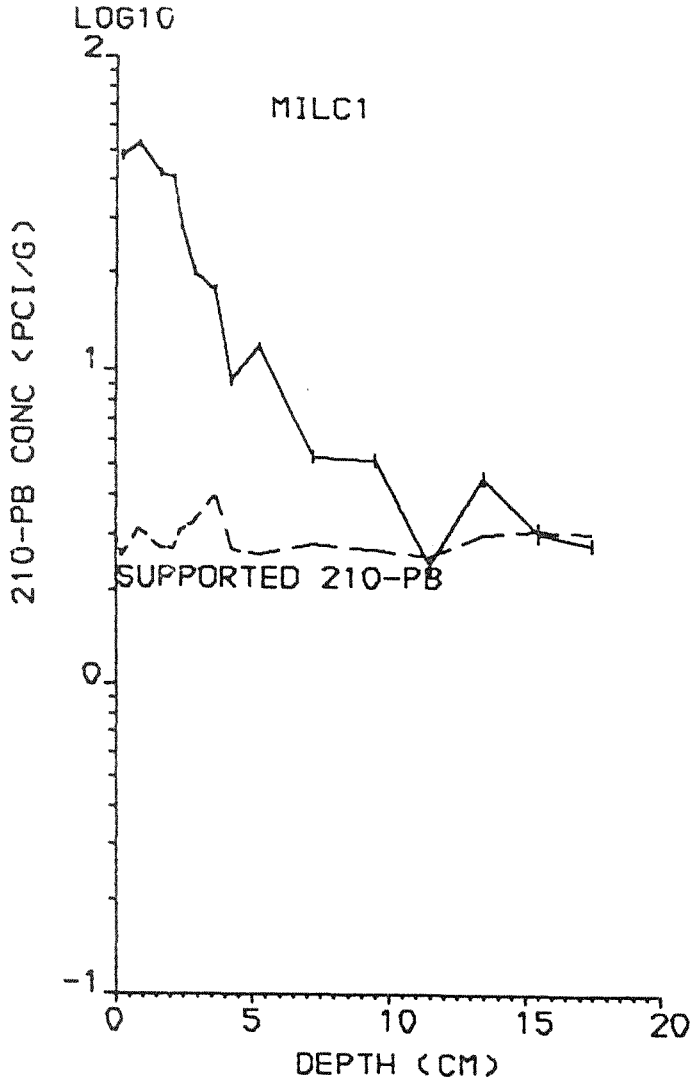

MILCHSEE (LAGO DI LATTE

(b) UNSUPP 210-PB CONC V DEPTH

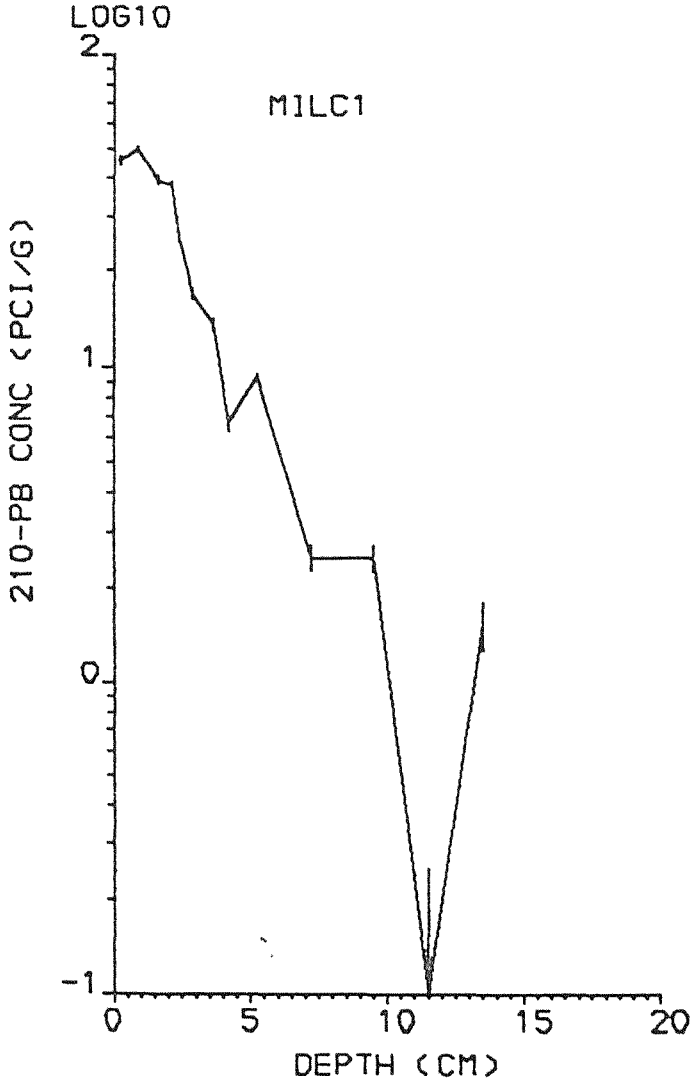

FIG. 3.5.3

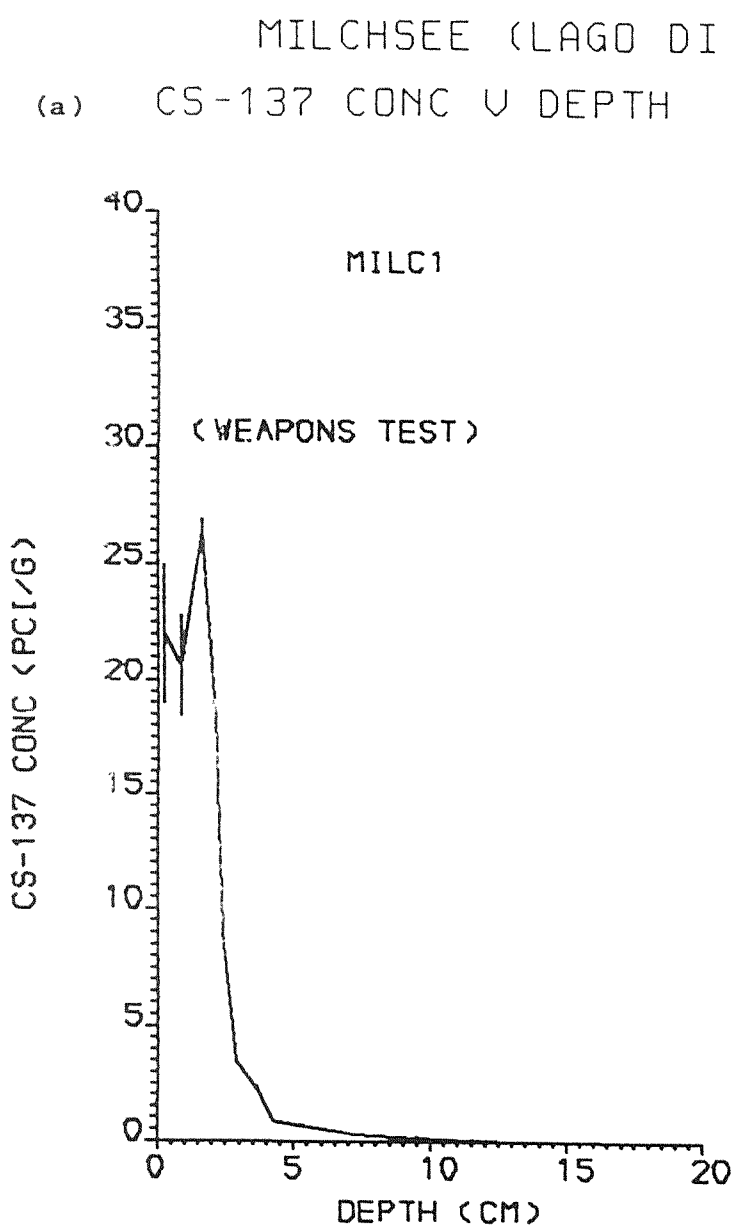
MILCHSEE (LAGO DI LATTE)
(a) CS-137 CONC V DEPTH
MILC1
(WEAPONS TEST)
CS-137 CONC (PCI/G)
DEPTH (CM)
0
5
10
15
20
25
30
35
40

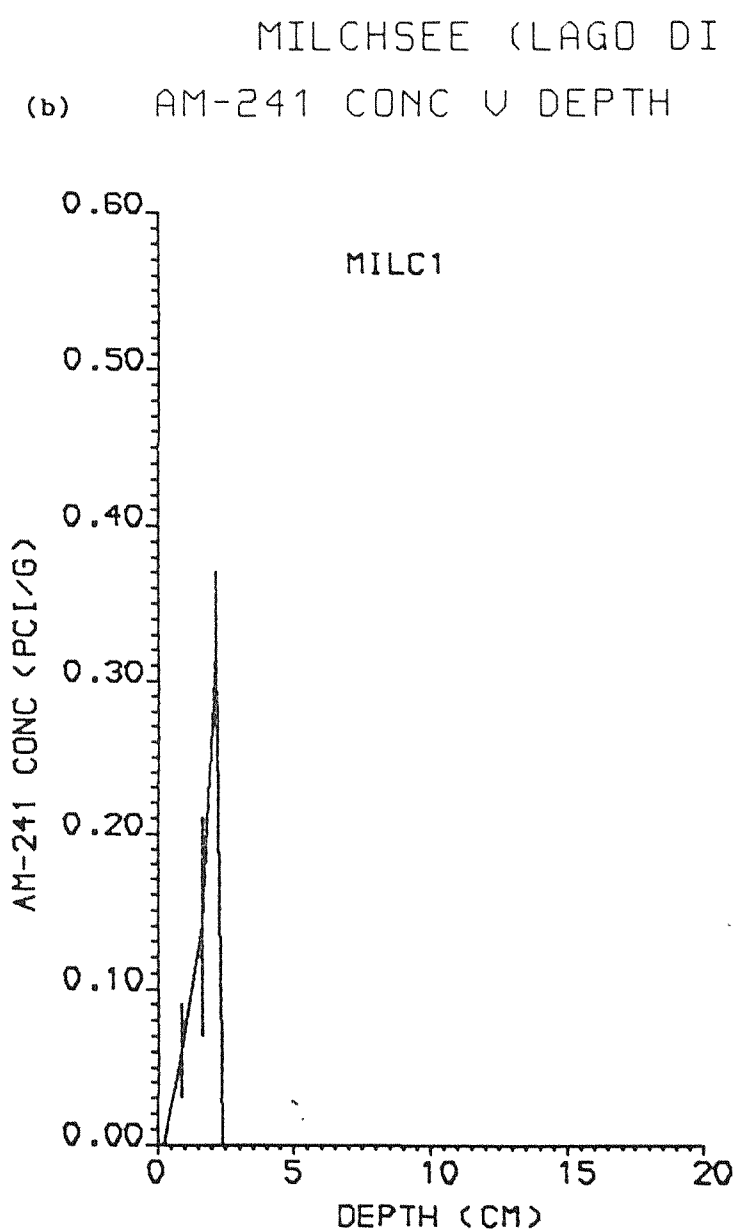
MILCHSEE (LAGO DI LATT
(b) AM-241 CONC V DEPTH
MILC1
AM-241 CONC (PCI/G)
DEPTH (CM)
0.00
0.10
0.20
0.30
0.40
0.50
0.60
0
5
10
15
20

FIG. 3.5.4

MILCHSEE (LAGO DI LATTE)

(a) CS-137 CONC V DEPTH

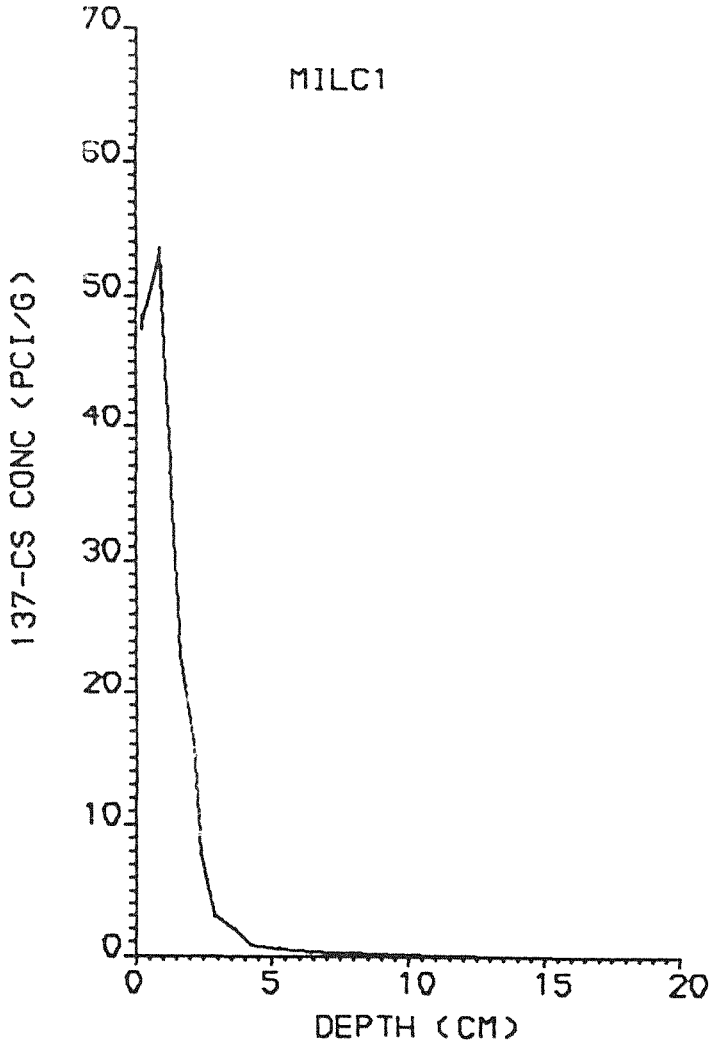

MILCHSEE (LAGO DI LAT

(b) CS-134 CONC V DEPTH

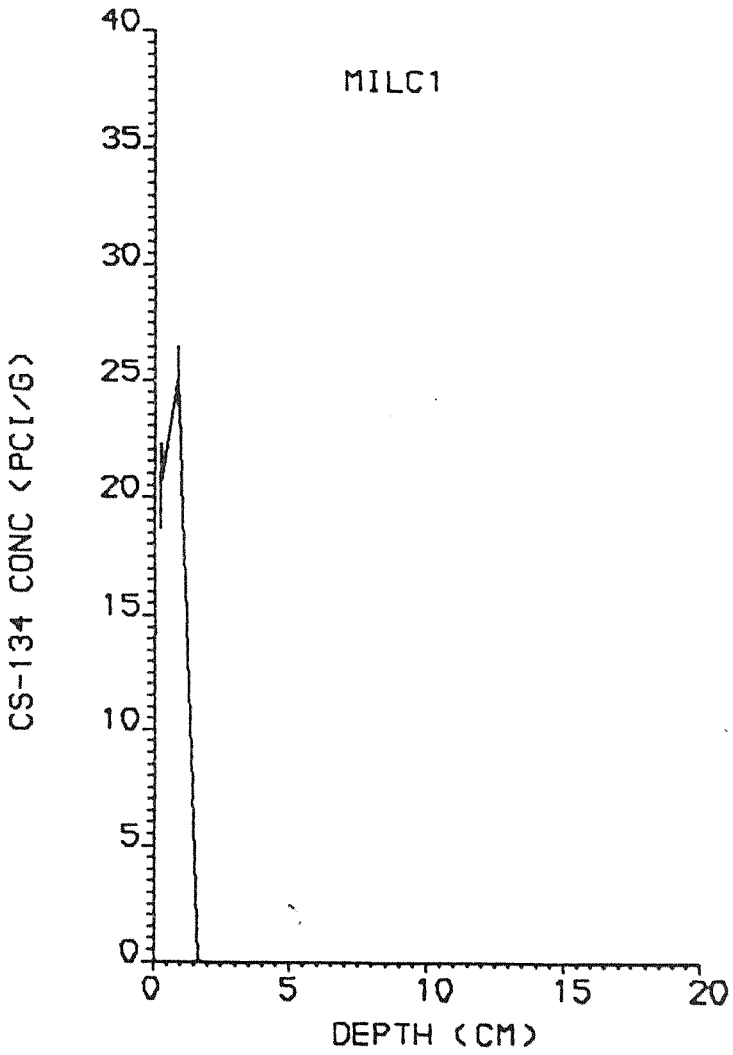

FIG. 3.5.5

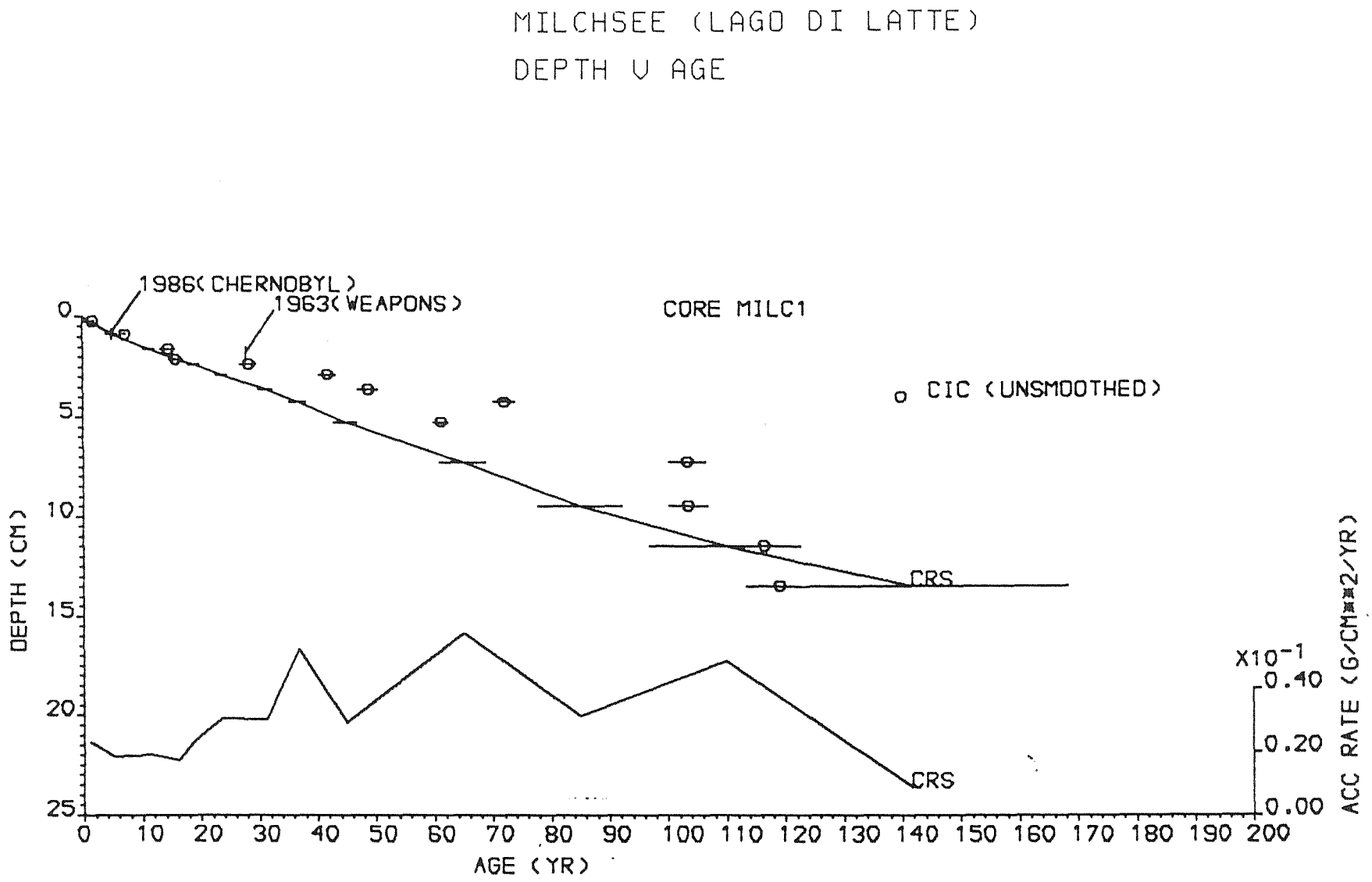
MILCHSEE (LAGO DI LATTE)
DEPTH V AGE
1986(CHERNOBYL)
1963(WEAPONS)
CORE MILC1
CIC (UNSMOOTHED)
CRS
CRS
DEPTH (CM)
AGE (YR)
ACC RATE (G/CM**2/YR)
X10**-1
0.40
0.20
0.00
0
5
10
15
20
25
0 10 20 30 40 50 60 70 80 90 100 110 120 130 140 150 160 170 180 190 200

Carbonaceous Particle Concentration and Flux Profiles

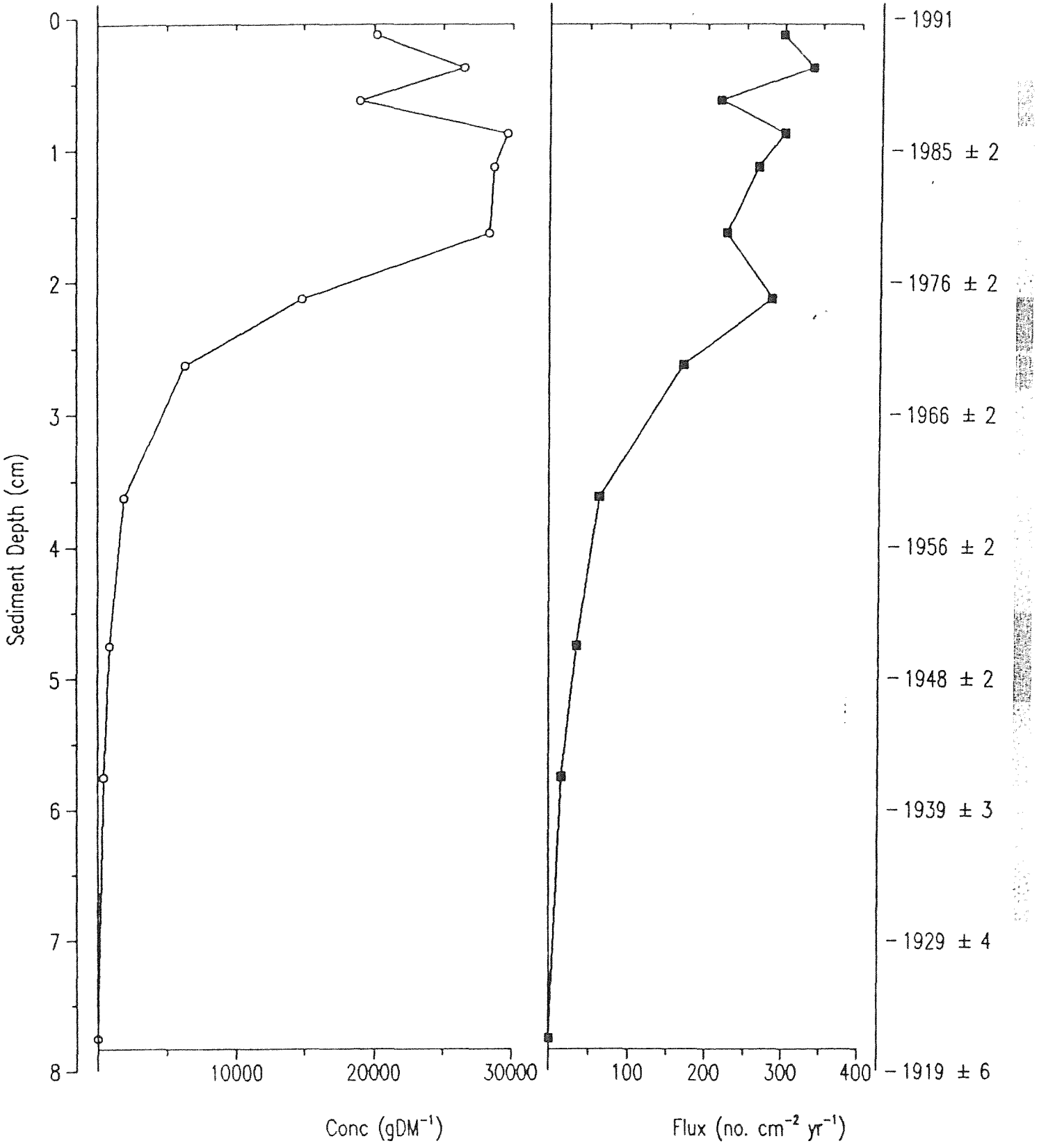

ECT, diatom cell concentration

FIG. 3.5.7

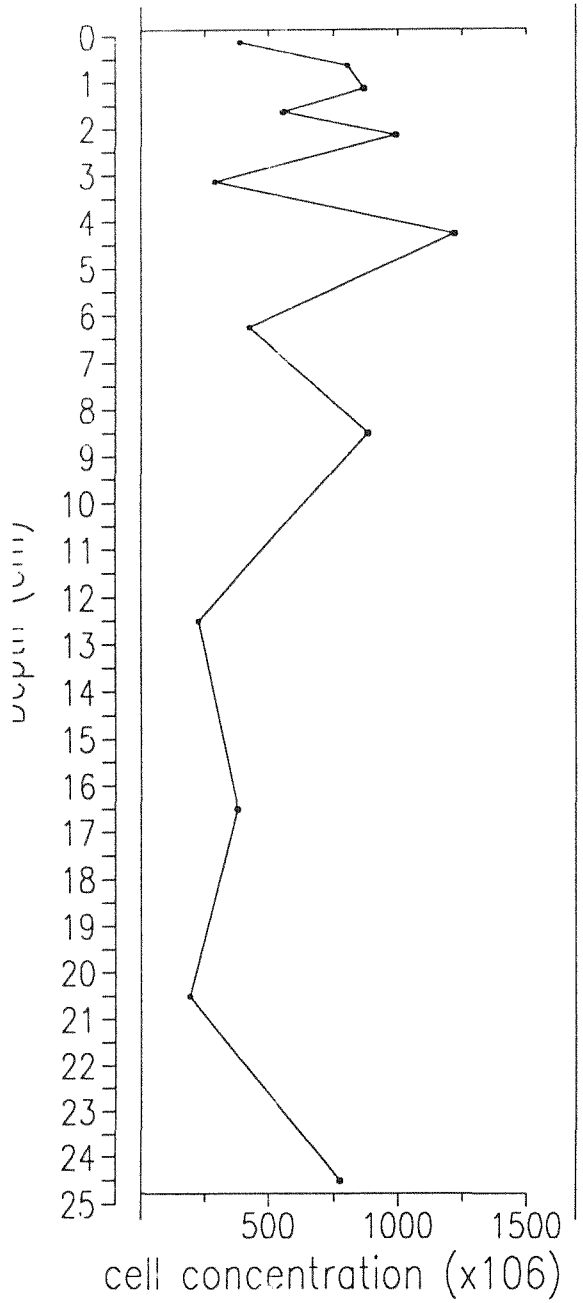

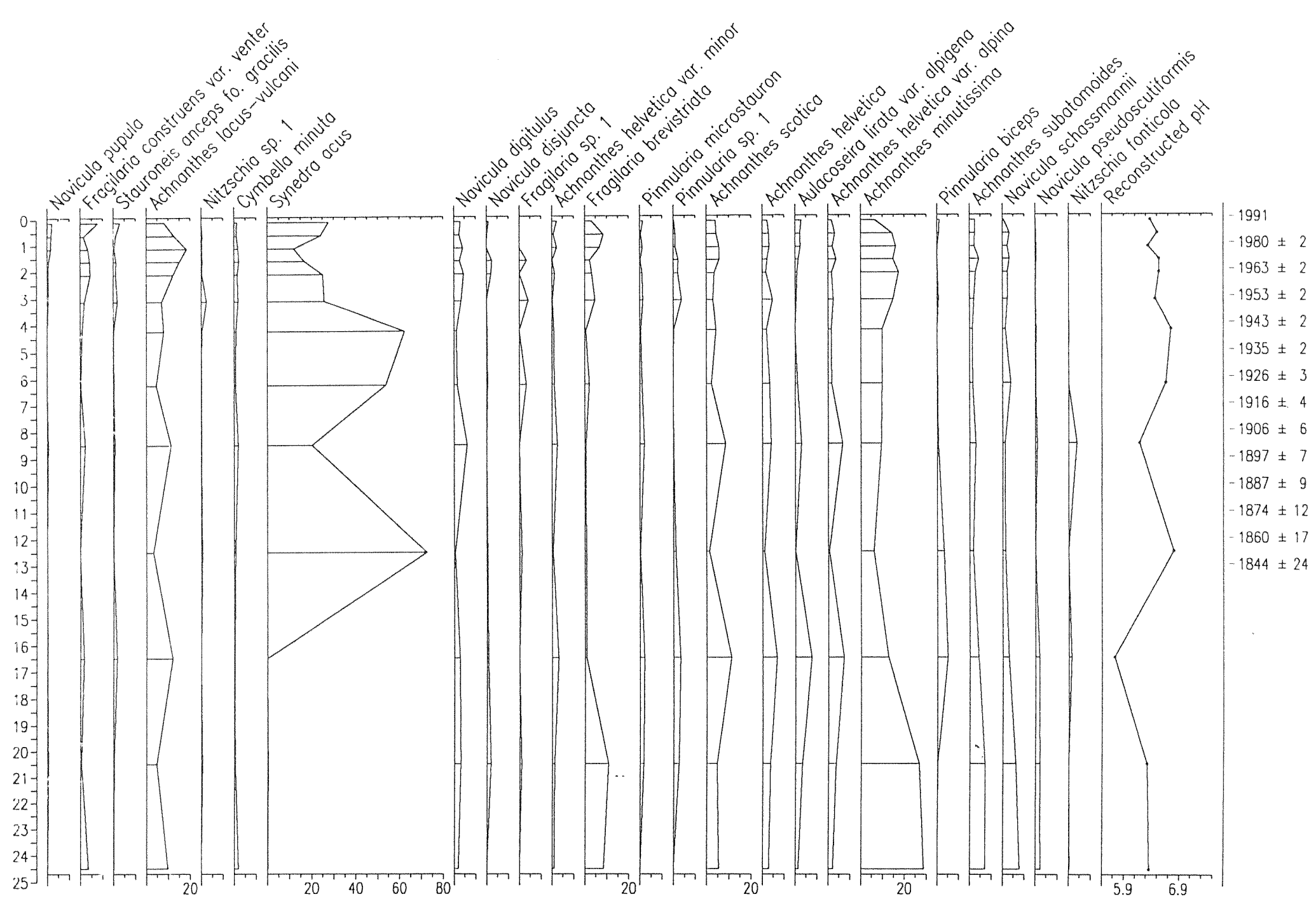
Navicula pupula
Fragilaria construens var. venter
Stauroneis anceps fo. gracilis
Achnanthes lacus-vulcani
Nitzschia sp. 1
Cymbella minuta
Synedra acus
Navicula digitulus
Navicula disjuncta
Fragilaria sp. 1
Achnanthes helvetica var. minor
Fragilaria brevistriata
Pinnularia microstauron
Pinnularia sp. 1
Achnanthes scotica
Achnanthes helvetica
Aulacoseira lirata var. alpigena
Achnanthes helvetica var. alpina
Achnanthes minutissima
Pinnularia biceps
Achnanthes subatomoides
Navicula schassmannii
Navicula pseudoscutiformis
Nitzschia fonticola
Reconstructed pH
0 1 2 3 4 5 6 7 8 9 10 11 12 13 14 15 16 17 18 19 20 21 22 23 24 25
20
20 40 60 80
20
20
20
5.9 6.9
1991
1980 ± 2
1963 ± 2
1953 ± 2
1943 ± 2
1935 ± 2
1926 ± 3
1916 ± 4
1906 ± 6
1897 ± 7
1887 ± 9
1874 ± 12
1860 ± 17
1844 ± 24

TABLE 3.5.1 Milchsee (Lago di Latte): ^{210}Pb Data for Core MILC1

Depth	Dry Mass	^{210}Pb Concentration Total		^{210}Pb Concentration Unsupp		^{226}Ra Concentration	
cm	gcm^{-2}	$pCig^{-1}$	±	$pCig^{-1}$	±	$pCig^{-1}$	±
0.25	0.025	48.00	1.57	45.43	1.60	2.57	0.31
0.875	0.107	52.67	1.04	49.54	1.06	3.13	0.21
1.625	0.228	42.14	1.34	39.39	1.37	2.75	0.27
2.125	0.318	40.66	0.96	37.94	0.98	2.72	0.19
2.375	0.372	28.74	0.92	25.64	0.94	3.10	0.18
2.875	0.502	20.10	0.65	16.82	0.67	3.28	0.17
3.625	0.732	17.50	0.60	13.54	0.62	3.96	0.14
4.25	0.947	9.26	0.34	6.56	0.35	2.70	0.09
5.25	1.271	11.81	0.29	9.19	0.30	2.62	0.08
7.25	2.012	5.29	0.23	2.48	0.24	2.81	0.07
9.50	2.882	5.18	0.24	2.47	0.25	2.71	0.07
11.50	4.010	2.38	0.14	-0.18	0.15	2.56	0.05
13.50	5.696	4.55	0.25	1.52	0.27	3.03	0.09
15.50	6.443	3.06	0.22	-0.04	0.23	3.10	0.07
17.50	7.304	2.81	0.15	-0.25	0.16	3.06	0.06

TABLE 3.5.2

Milchsee (Lago di Latte): ^{137}Cs, ^{134}Cs and ^{241}Am Data for Core MILC1

Depth	^{137}Cs Conc		^{134}Cs Conc		^{241}Am Conc	
cm	$pCig^{-1}$	±	$pCig^{-1}$	±	$pCig^{-1}$	±
0.25	47.92	0.58	20.46	1.79	0.00	0.00
0.875	53.09	0.47	25.16	1.31	0.06	0.03
1.625	22.88	0.39	0.00	0.00	0.14	0.07
2.125	15.87	0.30	0.00	0.00	0.32	0.05
2.375	7.73	0.19	0.00	0.00	0.00	0.00
2.875	3.02	0.12	0.00	0.00	0.00	0.00
3.625	1.93	0.10	0.00	0.00	0.00	0.00
4.25	0.74	0.05	0.00	0.00	0.00	0.00
5.25	0.54	0.05	0.00	0.00	0.00	0.00
7.25	0.22	0.03	0.00	0.00	0.00	0.00
9.50	0.13	0.03	0.00	0.00	0.00	0.00
11.50	0.03	0.02	0.00	0.00	0.00	0.00
13.50	0.00	0.00	0.00	0.00	0.00	0.00
15.50	0.00	0.00	0.00	0.00	0.00	0.00
17.50	0.00	0.00	0.00	0.00	0.00	0.00
Inventories:	14.18 ± 0.35 $pCicm^{-2}$		3.90 ± 0.22 $pCicm^{-2}$		0.04 ± 0.01 $pCicm^{-2}$	

TABLE 3.5.3 Milchsee (Lago di Latte): ^{210}Pb chronology for Core MILC1

(a) Raw CRS model dates

Depth	Dry Mass	Date	Age		Sedimentation Rate		
cm	gcm^{-2}	AD	yr	±	$gcm^{-2}yr^{-1}$	$cmyr^{-1}$	
0.00	0.000	1991	0				
0.25	0.0253	1990	1	2	0.0232	0.192	4.3
0.50	0.0575	1988	3	2	0.0215	0.167	4.0
0.75	0.0897	1987	4	2	0.0198	0.141	3.7
1.00	0.1260	1985	6	2	0.0190	0.126	3.7
1.25	0.1666	1983	8	2	0.0192	0.122	4.1
1.50	0.2073	1981	10	2	0.0194	0.117	4.5
1.75	0.2499	1978	13	2	0.0190	0.109	4.7
2.00	0.2948	1976	15	2	0.0179	0.097	4.6
2.25	0.3441	1973	18	2	0.0204	0.093	4.9
2.50	0.4034	1971	20	2	0.0254	0.099	5.4
2.75	0.4685	1968	23	2	0.0290	0.105	5.7
3.00	0.5391	1966	25	2	0.0309	0.105	6.0
3.25	0.6156	1964	27	2	0.0307	0.101	6.4
3.50	0.6920	1961	30	2	0.0305	0.096	6.8
3.75	0.7734	1959	32	2	0.0348	0.107	7.2
4.00	0.8601	1956	35	2	0.0439	0.133	7.7
4.25	0.9468	1954	37	2	0.0531	0.159	8.2
4.50	1.0278	1952	39	2	0.0471	0.140	8.2
4.75	1.1087	1950	41	2	0.0412	0.121	8.3
5.00	1.1897	1948	43	2	0.0352	0.102	8.4
5.25	1.2707	1946	45	3	0.0293	0.082	8.4
5.50	1.3634	1944	47	3	0.0329	0.091	9.3
5.75	1.4561	1941	50	3	0.0365	0.100	10.3
6.00	1.5488	1939	52	3	0.0401	0.109	11.2
6.25	1.6414	1936	55	4	0.0437	0.118	12.1
6.50	1.7341	1934	57	4	0.0474	0.127	13.0
6.75	1.8268	1931	60	4	0.0510	0.136	13.9
7.00	1.9195	1929	62	4	0.0546	0.145	14.8
7.25	2.0122	1926	65	4	0.0582	0.154	15.8
7.50	2.1088	1924	67	5	0.0552	0.144	16.6
7.75	2.2054	1922	69	5	0.0522	0.134	17.5
8.00	2.3020	1919	72	6	0.0492	0.124	18.4
8.25	2.3986	1917	74	6	0.0463	0.114	19.3
8.50	2.4952	1915	76	6	0.0433	0.104	20.2
8.75	2.5918	1913	78	7	0.0403	0.094	21.0
9.00	2.6884	1910	81	7	0.0373	0.084	21.9
9.25	2.7850	1908	83	7	0.0343	0.074	22.8
9.50	2.8816	1906	85	8	0.0313	0.064	23.7
9.75	3.0339	1903	88	8	0.0336	0.065	25.0
10.00	3.1861	1900	91	9	0.0358	0.065	26.2
10.50	3.4907	1894	97	11	0.0403	0.067	28.8
11.00	3.7953	1887	104	12	0.0447	0.068	31.4
11.50	4.0998	1881	110	13	0.0492	0.070	34.0
12.00	4.4988	1873	118	17	0.0391	0.056	37.6
12.50	4.8977	1865	126	20	0.0290	0.042	41.1
13.00	5.2966	1857	134	24	0.0188	0.029	44.7

(b) Adjusted CRS model dates

Depth	Dry Mass	Date	Age		Sedimentation Rate		
cm	gcm^{-2}	AD	yr	±	$gcm^{-2}yr^{-1}$	$cmyr^{-1}$	
0.00	0.0000	1991	0				
0.25	0.0253	1989	2	2	0.0134	0.111	4.1
0.50	0.0575	1986	5	2	0.0120	0.093	3.8
0.75	0.0897	1983	8	2	0.0106	0.076	3.5
1.00	0.1260	1980	11	2	0.0096	0.064	3.5
1.25	0.1666	1975	16	2	0.0090	0.058	3.8
1.50	0.2073	1971	20	2	0.0084	0.051	4.1
1.75	0.2499	1965	26	2	0.0075	0.043	4.3
2.00	0.2948	1963	28	2	0.0179	0.097	4.6
2.25	0.3441	1960	31	2	0.0204	0.093	4.9
2.50	0.4034	1958	33	2	0.0254	0.099	5.4
2.75	0.4685	1955	36	2	0.0290	0.105	5.7
3.00	0.5391	1953	38	2	0.0309	0.105	6.0
3.25	0.6156	1951	40	2	0.0307	0.101	6.4
3.50	0.6920	1948	43	2	0.0305	0.096	6.8
3.75	0.7734	1946	45	2	0.0348	0.107	7.2
4.00	0.8601	1943	48	2	0.0439	0.133	7.7
4.25	0.9468	1941	50	2	0.0531	0.159	8.2
4.50	1.0278	1939	52	2	0.0471	0.140	8.2
4.75	1.1087	1937	54	2	0.0412	0.121	8.3
5.00	1.1897	1935	56	2	0.0352	0.102	8.4
5.25	1.2707	1933	58	3	0.0293	0.082	8.4
5.50	1.3634	1931	60	3	0.0329	0.091	9.3
5.75	1.4561	1928	63	3	0.0365	0.100	10.3
6.00	1.5488	1926	65	3	0.0401	0.109	11.2
6.25	1.6414	1923	68	4	0.0437	0.118	12.1
6.50	1.7341	1921	70	4	0.0474	0.127	13.0
6.75	1.8268	1918	73	4	0.0510	0.136	13.9
7.00	1.9195	1916	75	4	0.0546	0.145	14.8
7.25	2.0122	1913	78	4	0.0582	0.154	15.8
7.50	2.1088	1911	80	5	0.0552	0.144	16.6
7.75	2.2054	1909	82	5	0.0522	0.134	17.5
8.00	2.3020	1906	85	6	0.0492	0.124	18.4
8.25	2.3986	1904	87	6	0.0463	0.114	19.3
8.50	2.4952	1902	89	6	0.0433	0.104	20.2
8.75	2.5918	1900	91	7	0.0403	0.094	21.0
9.00	2.6884	1897	94	7	0.0373	0.084	21.9
9.25	2.7850	1895	96	7	0.0343	0.074	22.8
9.50	2.8816	1893	98	8	0.0313	0.064	23.7
9.75	3.0339	1890	101	8	0.0336	0.065	25.0
10.00	3.1861	1887	104	9	0.0358	0.065	26.2
10.50	3.4907	1881	110	11	0.0403	0.067	28.8
11.00	3.7953	1874	117	12	0.0447	0.068	31.4
11.50	4.0998	1868	123	13	0.0492	0.070	34.0
12.00	4.4988	1860	131	17	0.0391	0.056	37.6
12.50	4.8977	1852	139	20	0.0290	0.042	41.1
13.00	5.2966	1844	147	24	0.0188	0.029	44.7

LOCHNAGAR

FIG. 3.6.1

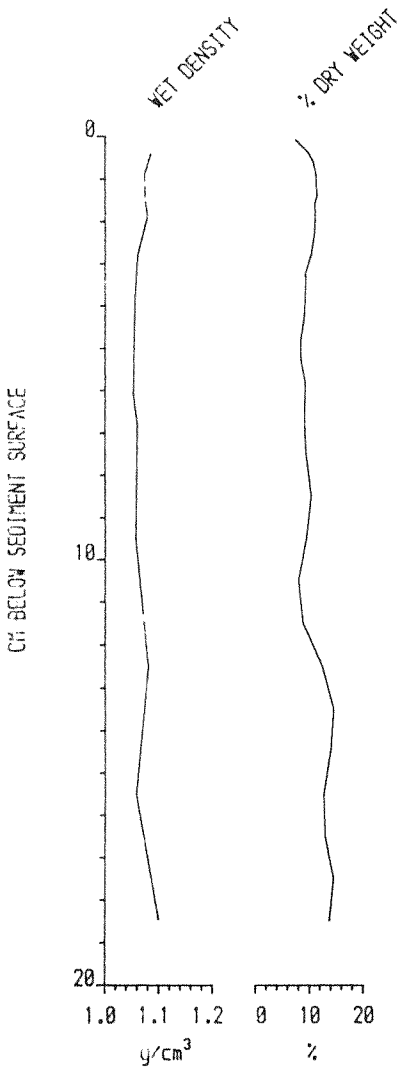

FIG. 3.6.2

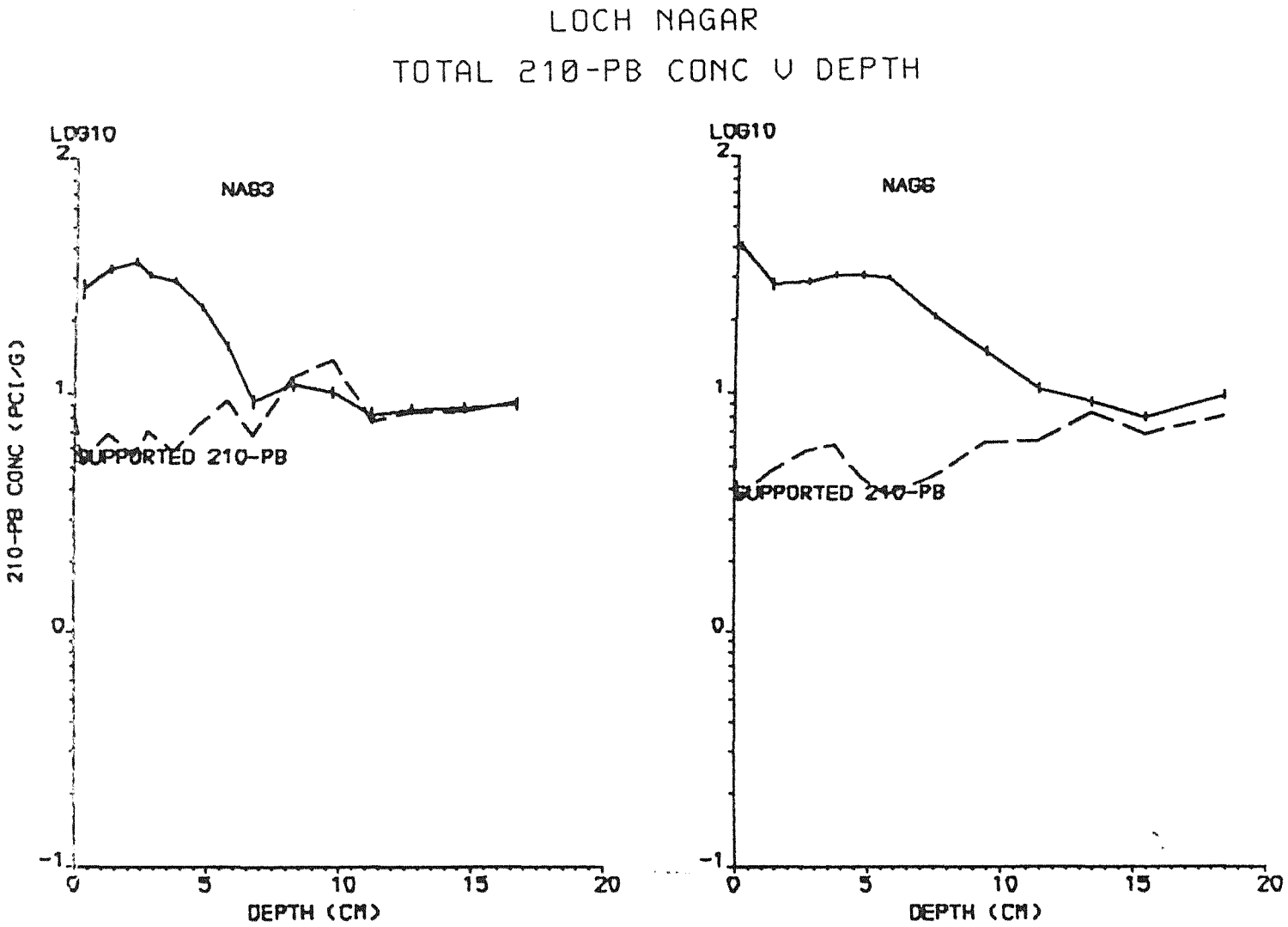
LOCH NAGAR
TOTAL 210-PB CONC V DEPTH
LOG10
2
1
0
-1
NA83
SUPPORTED 210-PB
210-PB CONC (PCI/G)
0
5
10
15
20
DEPTH (CM)
LOG10
2
1
0
-1
NA66
SUPPORTED 210-PB
0
5
10
15
20
DEPTH (CM)

FIG. 3.6.3

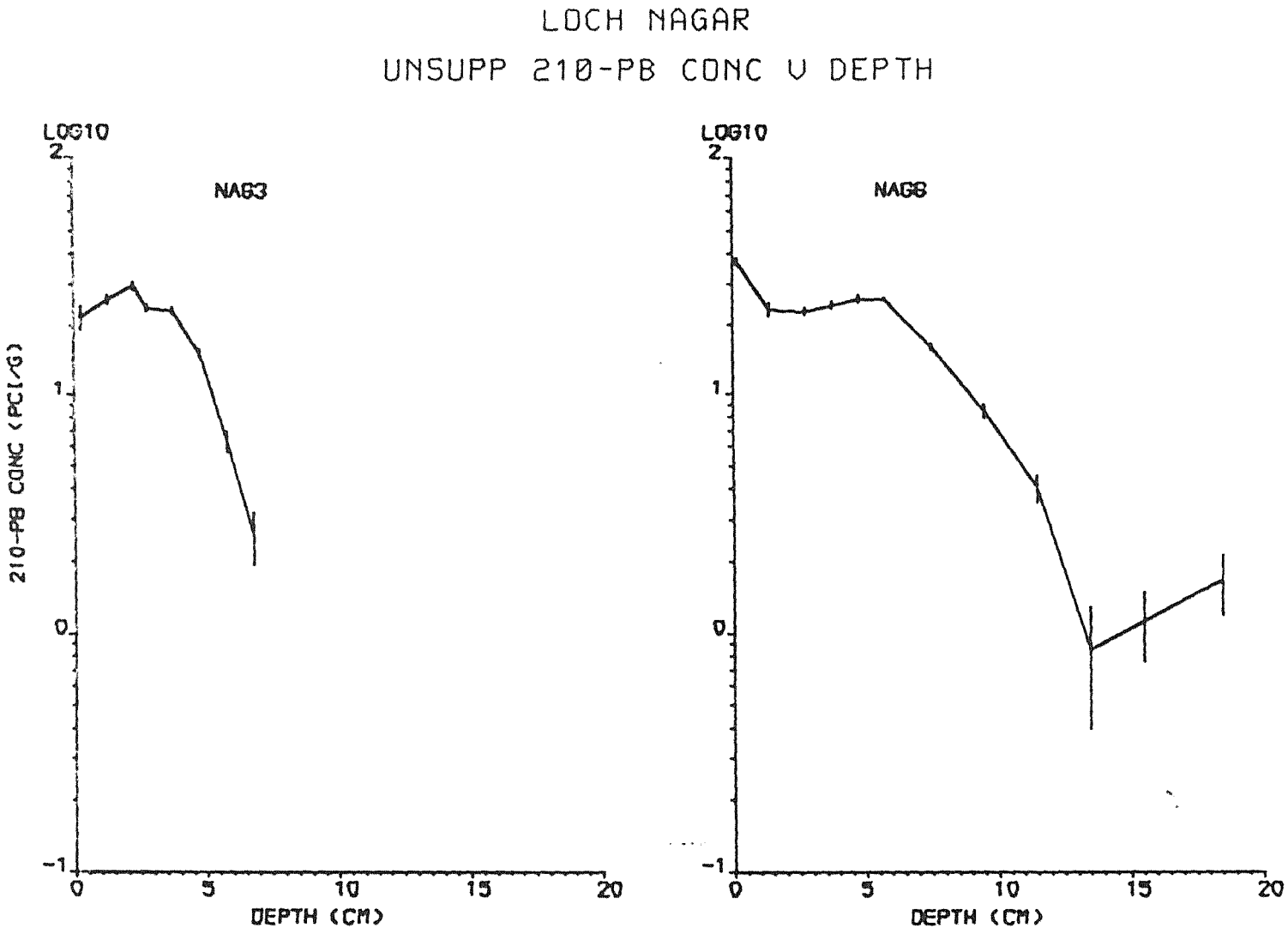
LOCH NAGAR
UNSUPP 210-PB CONC V DEPTH
LOG10
NAG3
210-PB CONC (PCI/G)
2
1
0
-1
0
5
10
15
20
DEPTH (CM)
LOG10
NAG8
2
1
0
-1
0
5
10
15
20
DEPTH (CM)

FIG. 3.6.4

LOCH NAGAR

CS-137 CONC V DEPTH

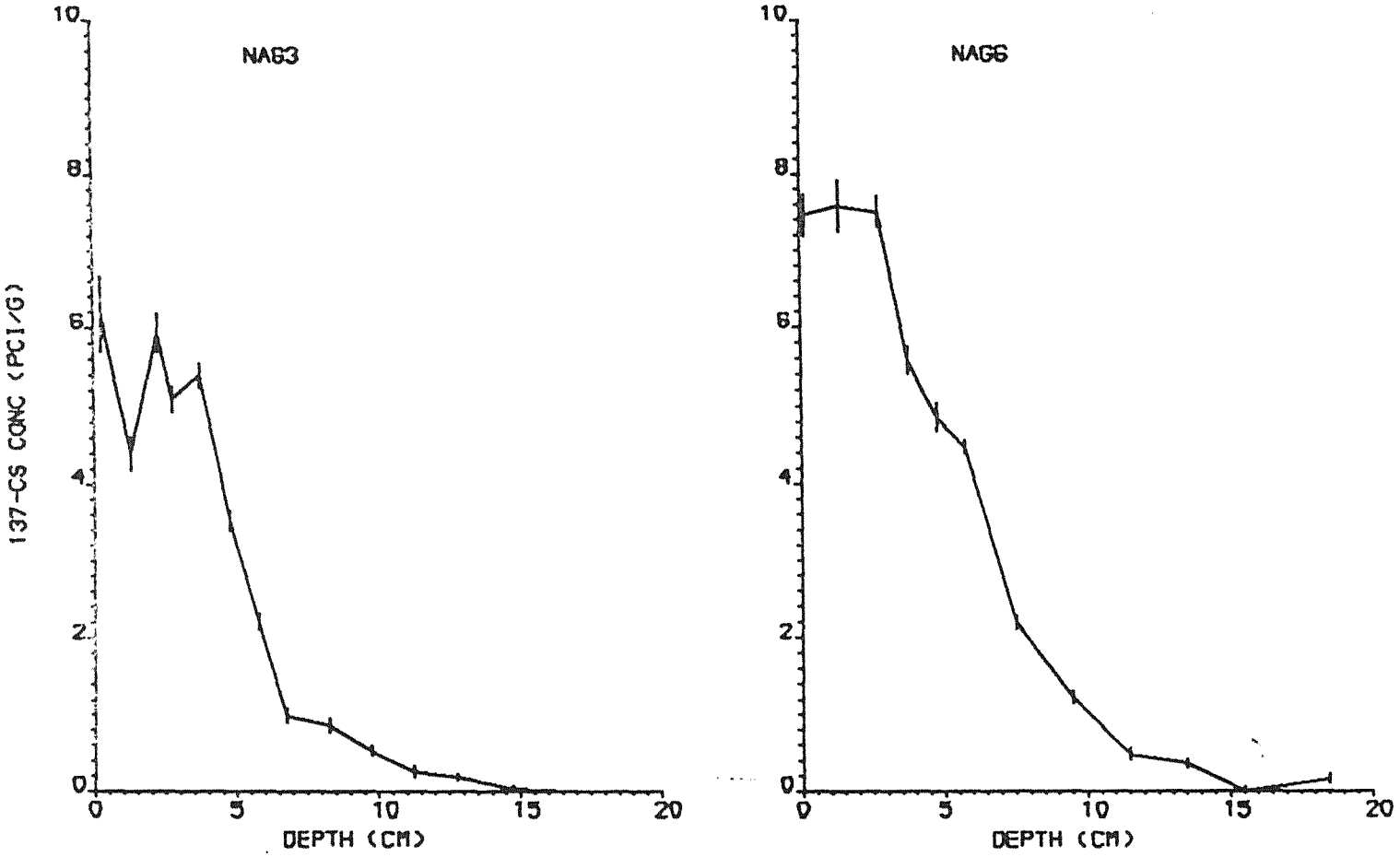

FIG. 3.6.5

LOCH NAGAR

AM-241 CONC V DEPTH

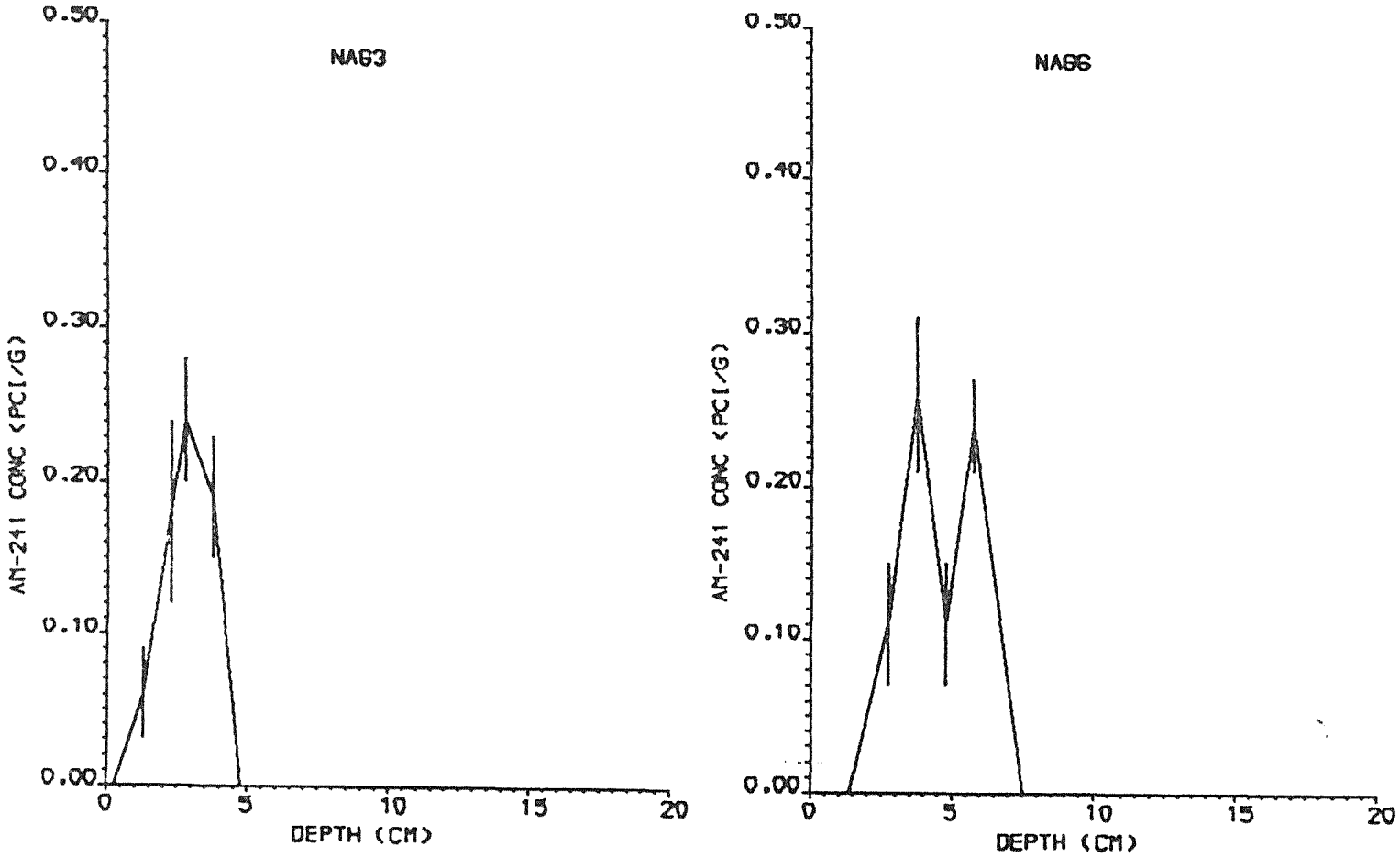

FIG. 3.6.6

LOCH NAGAR

DEPTH V AGE

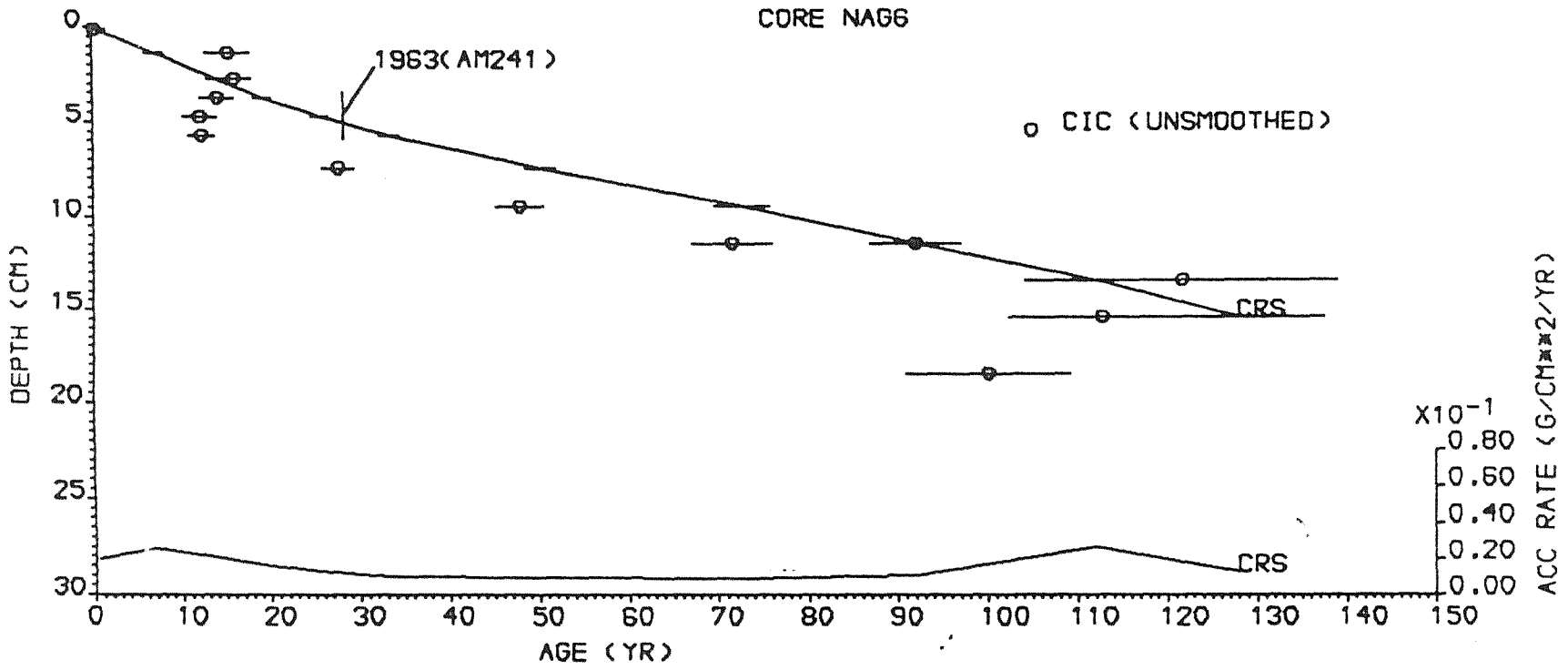

Lochnagar (NAG6) 1991

Carbonaceous Particle Concentration and Flux Profiles

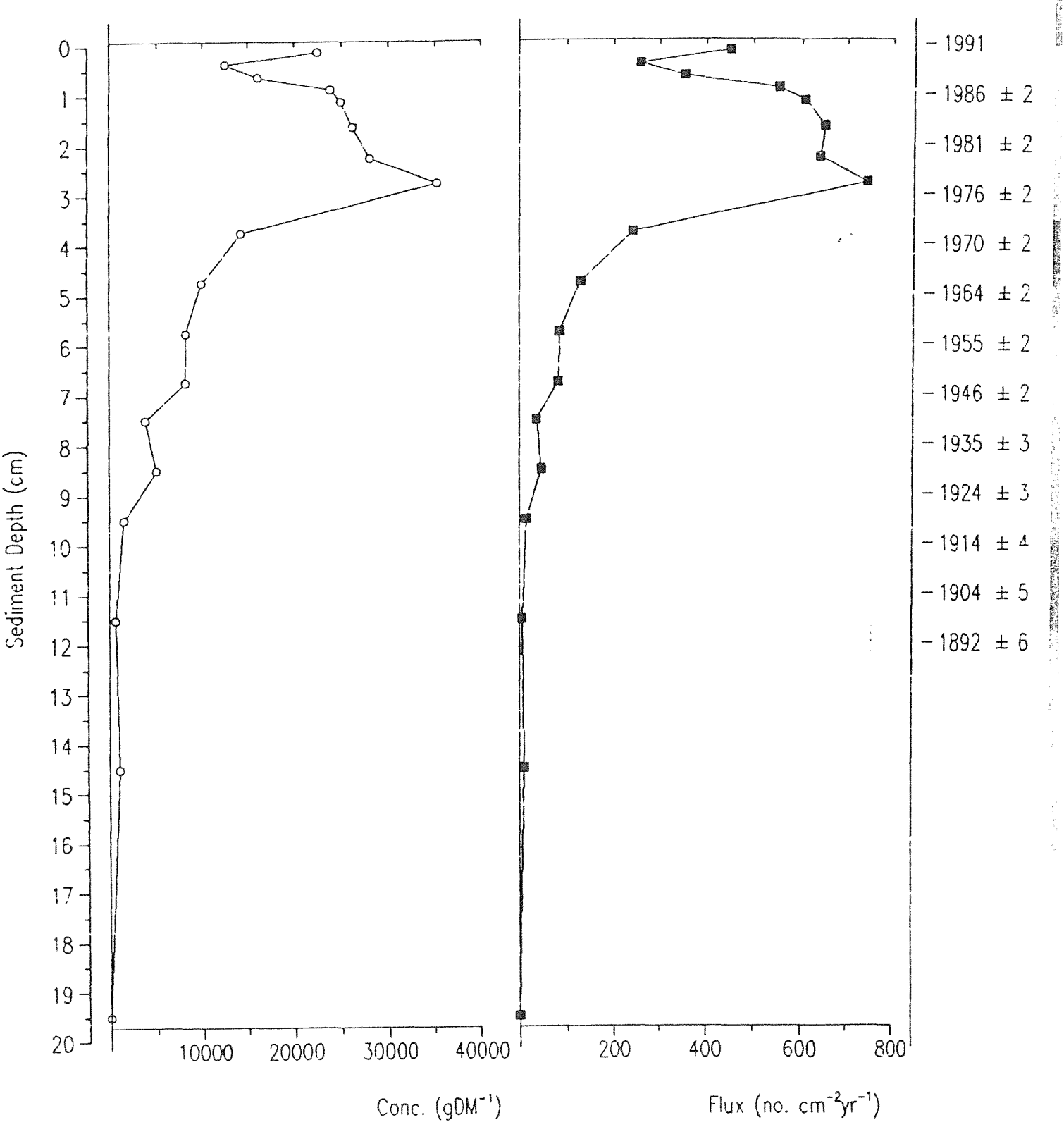

FIG. 3.6.8

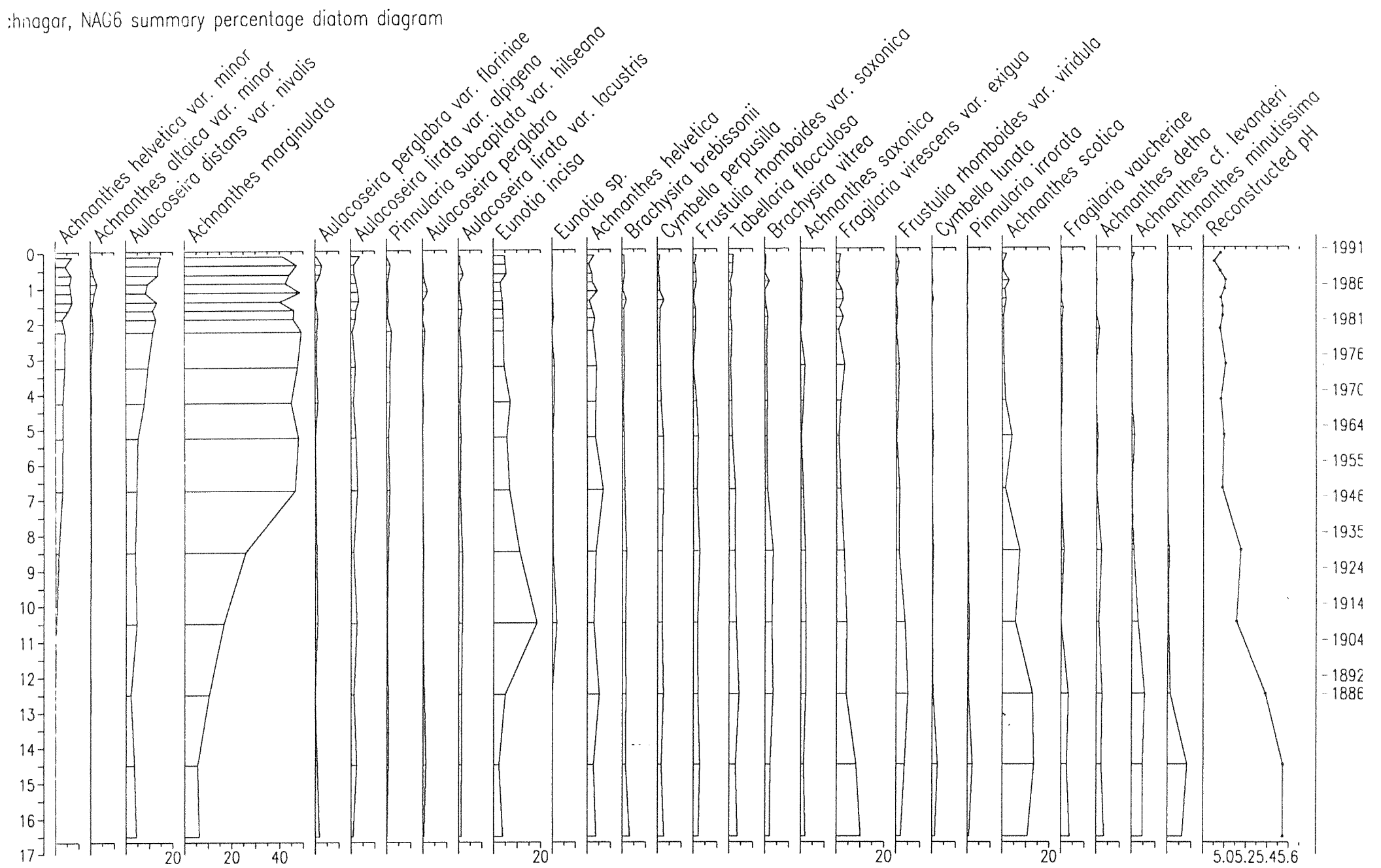
:hnagar, NAG6 summary percentage diatom diagram
Achnanthes helvetica var. minor
Achnanthes altaica var. minor
Aulacoseira distans var. nivalis
Achnanthes marginulata
Aulacoseira perglabra var. floriniae
Aulacoseira lirata var. alpigena
Pinnularia subcapitata var. hilseana
Aulacoseira perglabra
Aulacoseira lirata var. lacustris
Eunotia incisa
Eunotia sp.
Achnanthes helvetica
Brachysira brebissonii
Cymbella perpusilla
Frustulia rhomboides var. saxonica
Tabellaria flocculosa
Brachysira vitrea
Achnanthes saxonica
Fragilaria virescens var. exigua
Frustulia rhomboides var. viridula
Cymbella lunata
Pinnularia irrorata
Achnanthes scotica
Fragilaria vaucheriae
Achnanthes detha
Achnanthes cf. levanderi
Achnanthes minutissima
Reconstructed pH
0
1
2
3
4
5
6
7
8
9
10
11
12
13
14
15
16
17
20
20
40
20
20
20
5.05.25.45.6
1991
1986
1981
1976
1970
1964
1955
1946
1935
1924
1914
1904
1892
1886

Depth	Dry Mass	^{210}Pb Concentration				^{226}Ra Concentration	
		Total		Unsupp			
cm	gcm^{-2}	$pCig^{-1}$	±	$pCig^{-1}$	±	$pCig^{-1}$	±
0.125	0.0101	40.69	1.46	37.07	1.53	3.62	0.47
1.375	0.1509	27.94	1.49	23.23	1.56	4.71	0.47
2.75	0.3111	28.53	0.93	22.73	0.97	5.80	0.26
3.75	0.4111	30.22	0.96	24.11	1.00	6.11	0.28
4.75	0.5052	30.10	1.01	25.64	1.05	4.46	0.28
5.75	0.5959	29.26	0.52	25.47	0.54	3.79	0.14
7.50	0.7659	20.31	0.60	15.84	0.63	4.47	0.19
9.50	0.9747	14.68	0.57	8.40	0.61	6.28	0.23
11.50	1.1573	10.34	0.49	4.01	0.54	6.33	0.23
13.50	1.4172	9.07	0.40	0.84	0.45	8.23	0.21
15.50	1.7109	7.85	0.32	1.11	0.36	6.74	0.16
18.50	2.1499	9.62	0.42	1.65	0.47	7.97	0.21

TABLE 3.6.2 Loch Nagar: ^{137}Cs and ^{241}Am Data for Core Nag6

Depth	^{137}Cs Conc		^{241}Am Conc	
cm	$pCig^{-1}$	±	$pCig^{-1}$	±
0.125	7.45	0.28	0.00	0.00
1.375	7.57	0.34	0.00	0.00
2.75	7.49	0.20	0.11	0.04
3.75	5.57	0.18	0.26	0.05
4.75	4.84	0.19	0.11	0.04
5.75	4.46	0.09	0.24	0.03
7.50	2.18	0.09	0.00	0.00
9.50	1.22	0.09	0.00	0.00
11.50	0.48	0.09	0.00	0.00
13.50	0.36	0.06	0.00	0.00
15.50	0.00	0.05	0.00	0.00
18.50	0.15	0.07	0.00	0.00
Inventories:	5.17 ± 0.13 $pCicm^{-2}$		0.09 ± 0.01 $pCicm^{-2}$	

TABLE 3.6.3 Loch Nagar: ^{210}Pb chronology for Core Nag6

Depth	Dry Mass	Date	Age		Sedimentation Rate		
cm	gcm^{-2}	AD	yr	±	$gcm^{-2}yr^{-1}$	$cmyr^{-1}$	± (%)
0.00	0.0000	1991	0				
0.25	0.0236	1990	1	2	0.0201	0.183	4.7
0.50	0.0518	1989	2	2	0.0214	0.192	5.1
0.75	0.0799	1987	4	2	0.0226	0.201	5.5
1.00	0.1081	1986	5	2	0.0238	0.210	6.0
1.25	0.1363	1985	6	2	0.0250	0.218	6.4
1.50	0.1649	1984	7	2	0.0252	0.220	6.5
1.75	0.1942	1982	9	2	0.0244	0.215	6.2
2.00	0.2234	1981	10	2	0.0236	0.209	5.8
2.25	0.2526	1980	11	2	0.0228	0.204	5.5
2.50	0.2819	1979	12	2	0.0219	0.198	5.2
2.75	0.3111	1977	14	2	0.0211	0.192	4.9
3.00	0.3361	1976	15	2	0.0201	0.188	4.9
3.25	0.3611	1975	16	2	0.0190	0.183	5.0
3.50	0.3861	1973	18	2	0.0180	0.179	5.0
3.75	0.4111	1972	19	2	0.0169	0.174	5.0
4.00	0.4346	1970	21	2	0.0159	0.166	5.0
4.25	0.4582	1969	22	2	0.0150	0.158	5.1
4.50	0.4817	1967	24	2	0.0140	0.149	5.1
4.75	0.5052	1966	25	2	0.0130	0.141	5.2
5.00	0.5279	1964	27	2	0.0124	0.133	5.1
5.25	0.5506	1962	29	2	0.0117	0.125	5.0
5.50	0.5732	1960	31	2	0.0110	0.117	4.8
5.75	0.5959	1958	33	2	0.0103	0.109	4.7
6.00	0.6202	1955	36	2	0.0102	0.107	5.0
6.25	0.6445	1953	38	2	0.0101	0.105	5.3
6.50	0.6688	1951	40	2	0.0101	0.103	5.6
6.75	0.6930	1948	43	2	0.0100	0.102	5.9
7.00	0.7173	1946	45	2	0.0099	0.100	6.2
7.50	0.7659	1941	50	2	0.0097	0.096	6.7
8.00	0.8181	1935	56	3	0.0096	0.096	7.9
8.50	0.8703	1930	61	3	↑	↑	
9.00	0.9225	1924	67	3	↑	↑	
9.50	0.9747	1919	72	4	↑	↑	
10.00	1.0203	1914	77	4	↑	↑	
10.50	1.0660	1909	82	5	0.0095	0.098	~16%
11.00	1.1116	1904	87	5	↓	↓	
11.50	1.1573	1899	92	6	↓	↓	
12.00	1.2223	1892	99	6	↓	↓	
12.50	1.2872	1886	105	7	↓	↓	

FIGURE 4.1.1

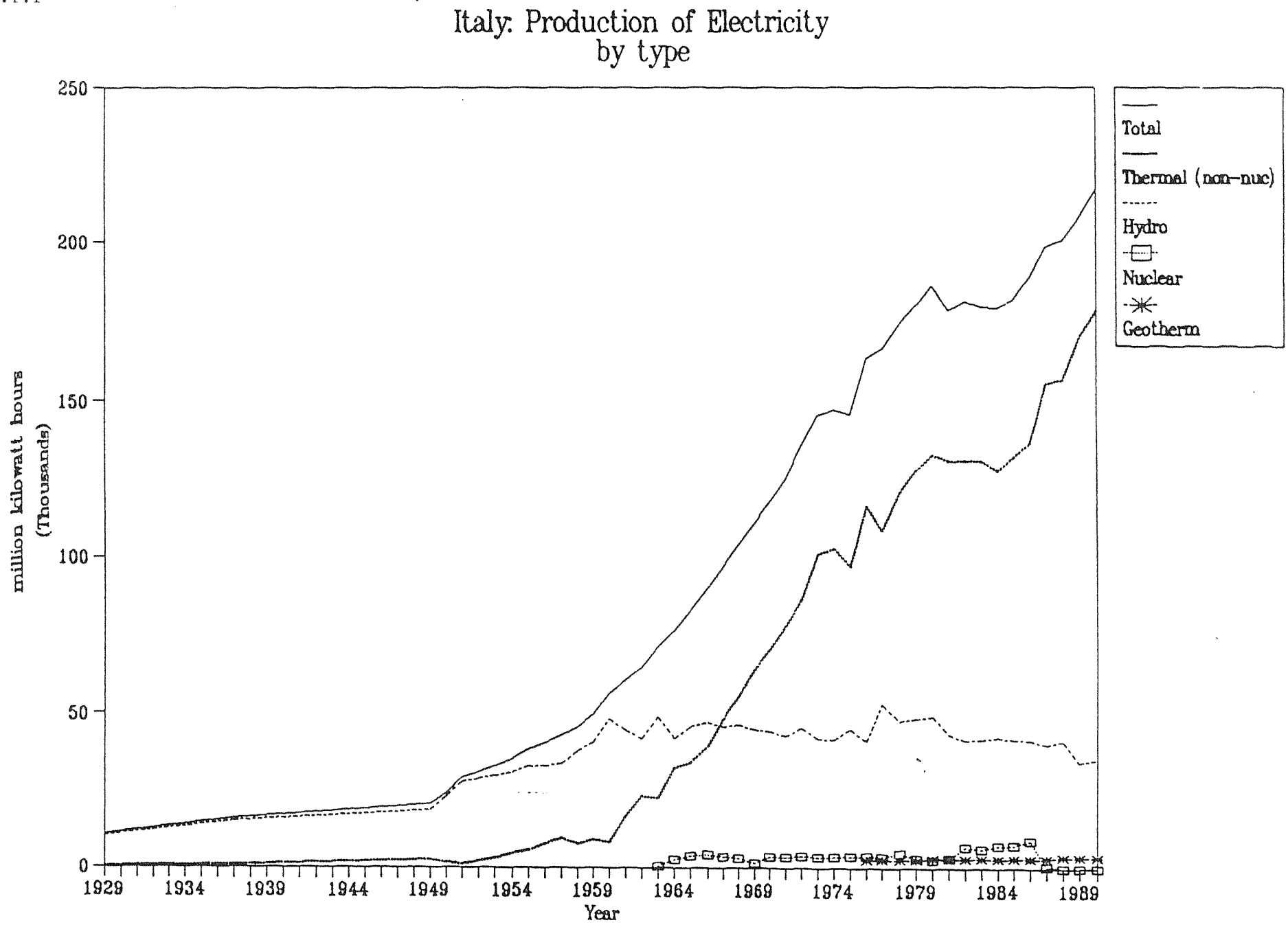
Italy: Production of Electricity
by type
250
200
150
100
50
0
million kilowatt hours
(Thousands)
1929
1934
1939
1944
1949
1954
1959
1964
1969
1974
1979
1984
1989
Year
Total
Thermal (non-nuc)
Hydro
Nuclear
Geotherm

FIG. 4.1.2

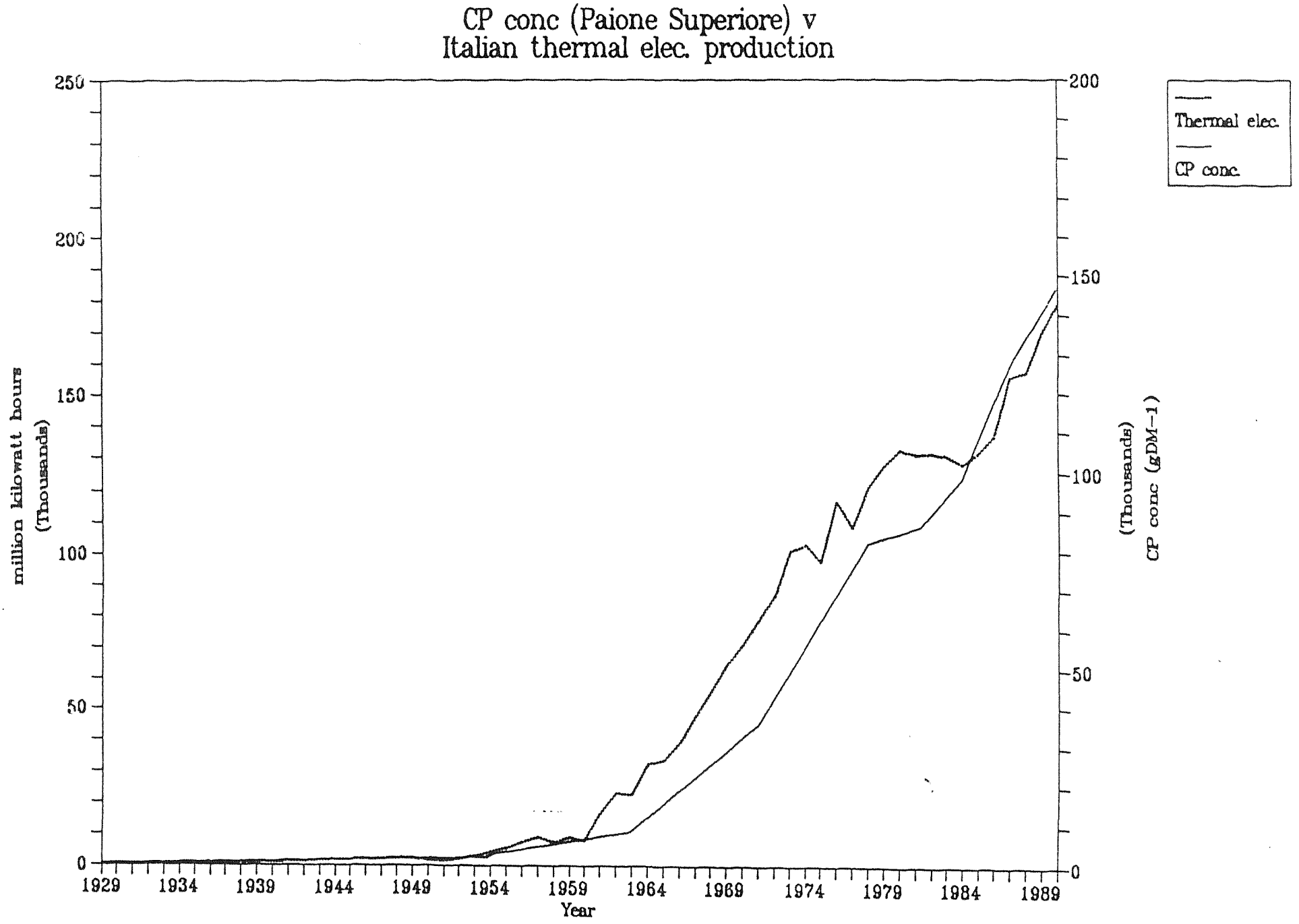
CP conc (Paione Superiore) v
Italian thermal elec. production
Thermal elec.
CP conc.
million kilowatt hours
(Thousands)
CP conc (gDM-1)
(Thousands)
Year
250
200
150
100
50
0
200
150
100
50
0
1929
1934
1939
1944
1949
1954
1959
1964
1969
1974
1979
1984
1989

FIG. 4.1.3

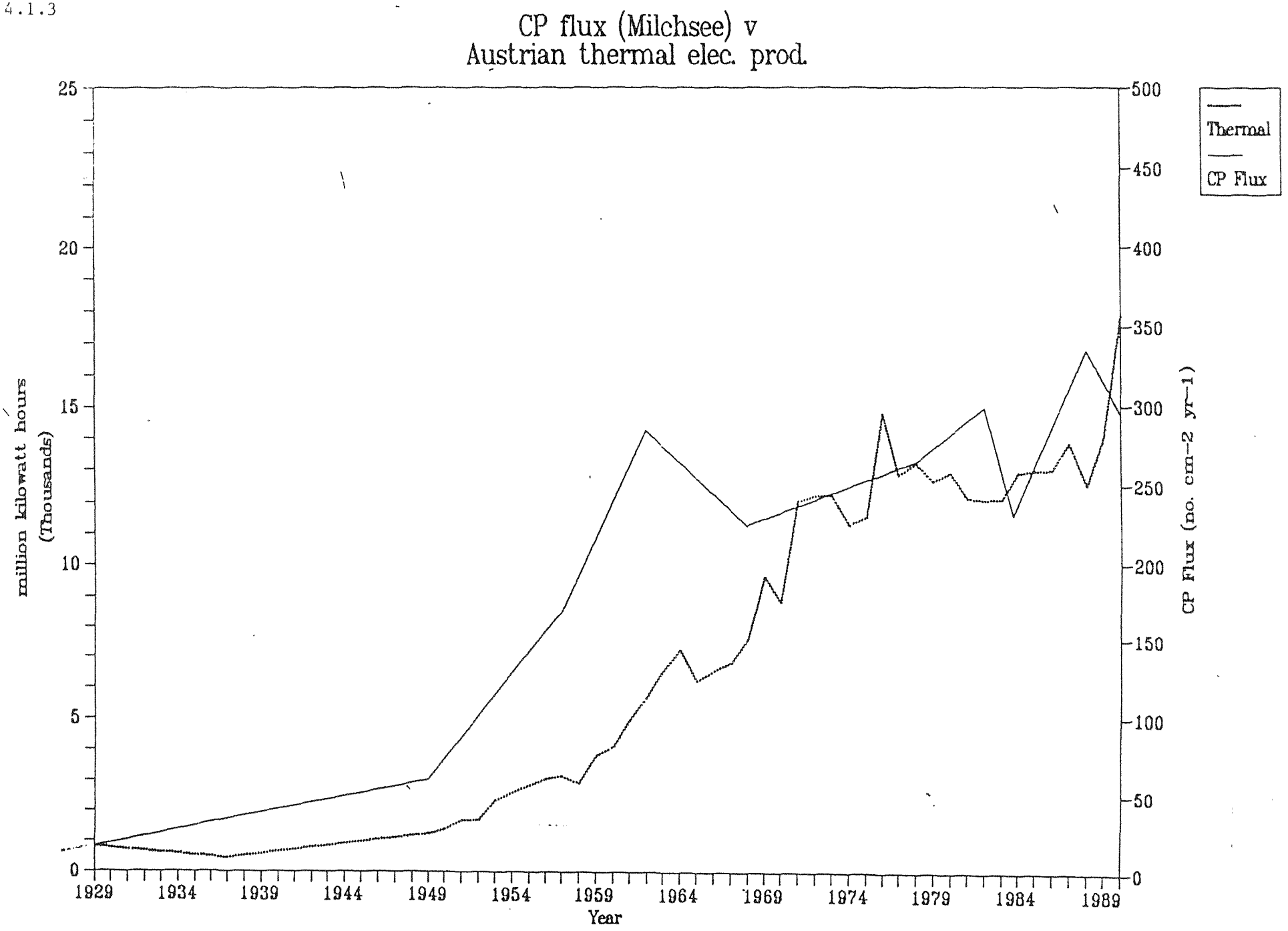
CP flux (Milchsee) v
Austrian thermal elec. prod.
million kilowatt hours
(Thousands)
CP Flux (no. cm-2 yr-1)
Year
Thermal
CP Flux
0
5
10
15
20
25
0
50
100
150
200
250
300
350
400
450
500
1929
1934
1939
1944
1949
1954
1959
1964
1969
1974
1979
1984
1989

FIG. 4.1.4

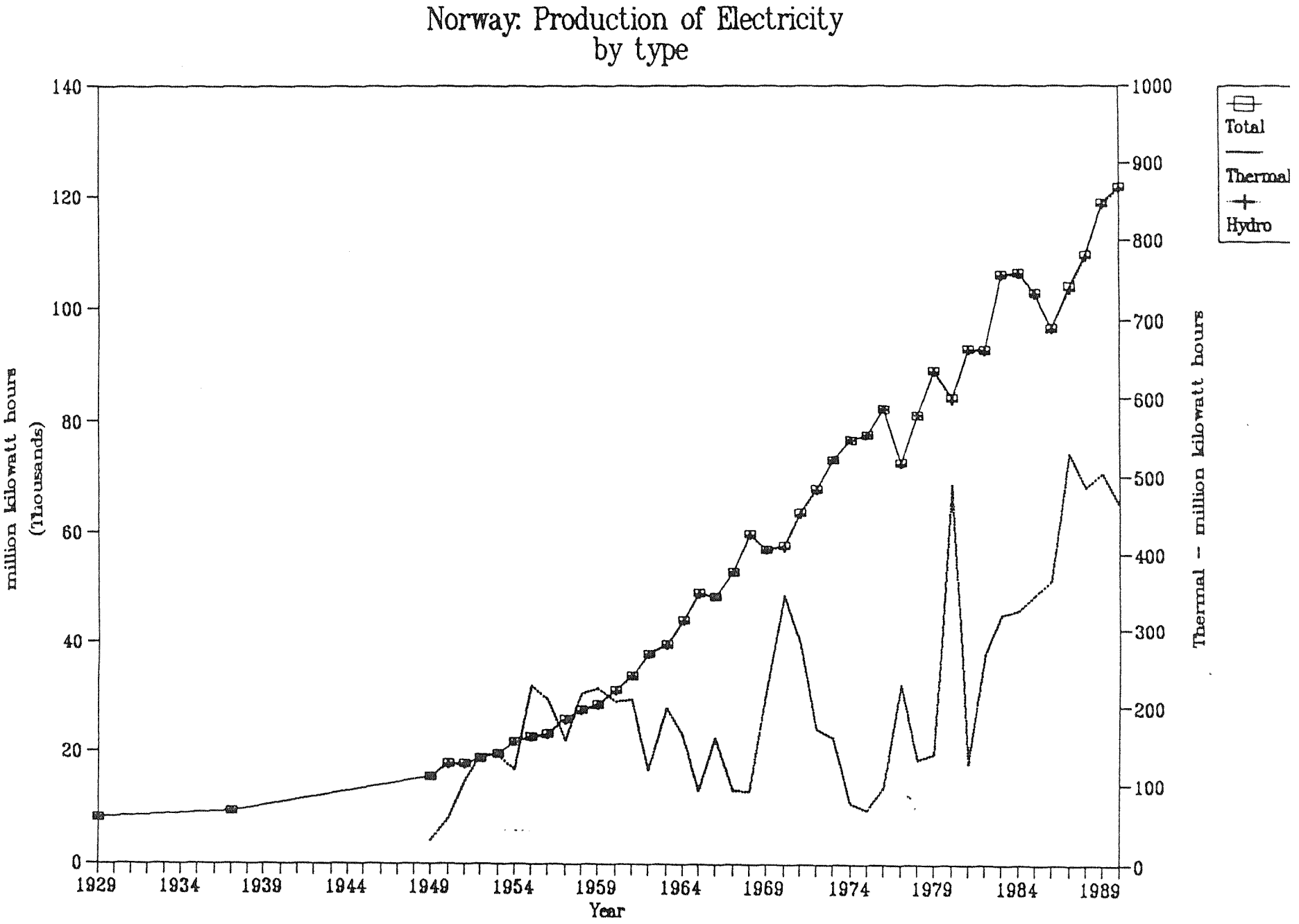
Norway: Production of Electricity
by type
million kilowatt hours
(Thousands)
Thermal - million kilowatt hours
Year
Total
Thermal
Hydro
0
20
40
60
80
100
120
140
0
100
200
300
400
500
600
700
800
900
1000
1929
1934
1939
1944
1949
1954
1959
1964
1969
1974
1979
1984
1989

FIG. 4.1.5

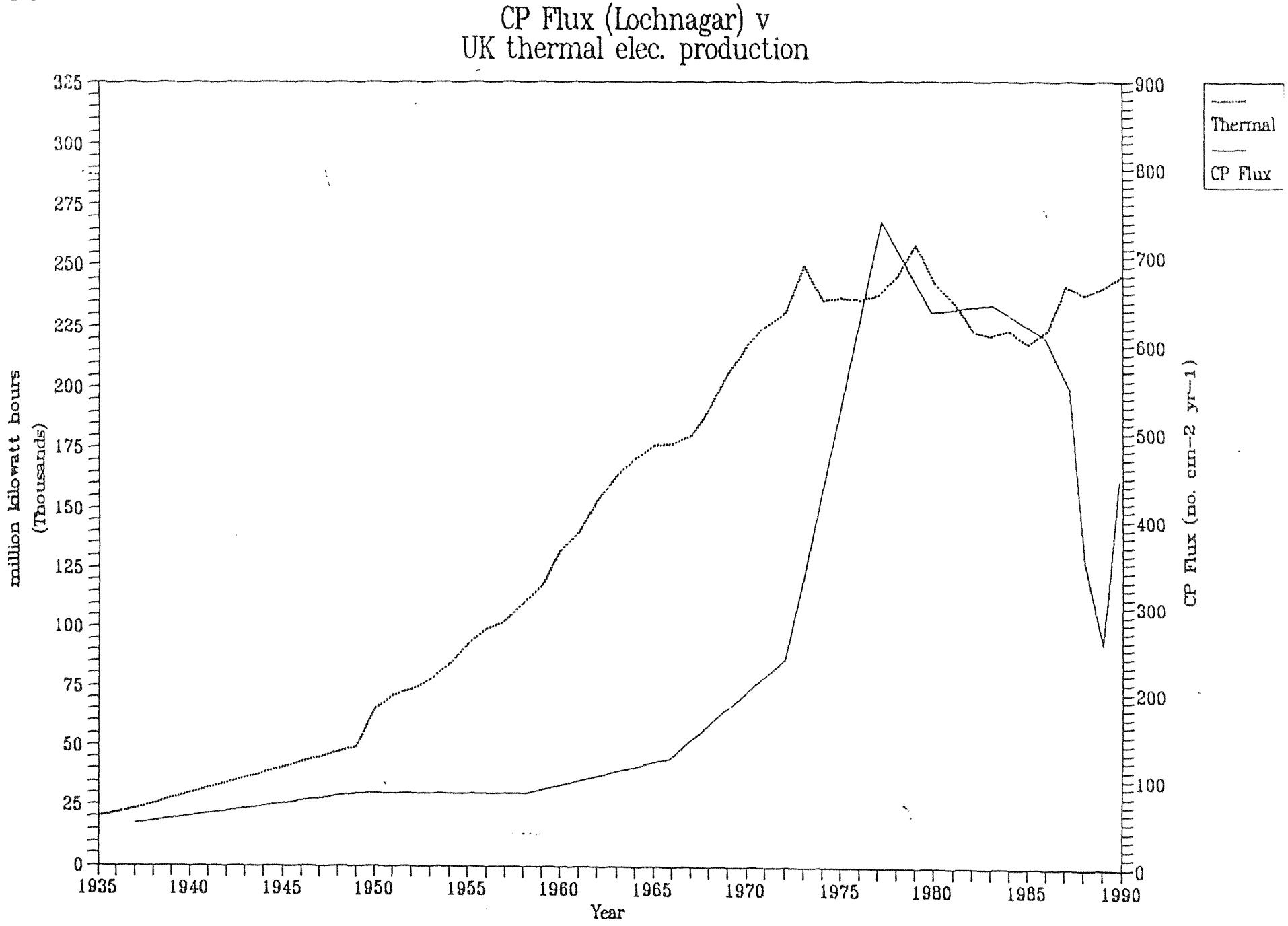
CP Flux (Lochnagar) v
UK thermal elec. production
million kilowatt hours
(Thousands)
CP Flux (no. cm-2 yr-1)
Year
Thermal
CP Flux
0
25
50
75
100
125
150
175
200
225
250
275
300
325
0
100
200
300
400
500
600
700
800
900
1935
1940
1945
1950
1955
1960
1965
1970
1975
1980
1985
1990

Table 4.1.1 Summary table of the dates for the main features of the carbonaceous particle profiles for AL:PE 1 lake sites.

Site	Location	Start of Record	Rapid Increase	Concentration Peak
Paione Superiore	Italian Alps	1892 - 1911	1959 - 1967	-
Milchsee	Italian Tyrol	1906 - 1929	1951 - 1960	1977 - 1986
Ovre Neådalsvatn	Mid-Norway	1928 - 1946	1974 - 1981	-
Stavsvatn	Southern Norway	1860 - 1911	1964 - 1968	1982 - 1988
Etang d'Aube	French Pyrenees	1934 - 1941	1978 - 1982	-
Lochnagar	Cairngorms, Scotland	1850's	1962 - 1969	1974 - 1981

Table 4.2.1 Principle pH-related changes in diatom assemblages from primary sediment cores (< & > indicate decreases and increases in species respectively)

Site	pH related change in diatoms	Change in reconstructed pH	Onset of change	Acidification status
Ovre Neadalsvatn	none	none	----	no acidification
Stavsvatn	< Cy.kuetz.	1 pH unit	1860+	acidified
Lochnagar	< Achn. minutis. > Achn. margin.	0.6 pH units	1850's	acidified
Etang d'Aube	slight < Achn.minutis.	0.1 pH units	1934-1941	slight acidification
Paione Superiore	> Eun. exigua > Au. dist.nival.	not sensitive	c. 1956	recent acidification
Milchsee	none	-----	----	not sensitive

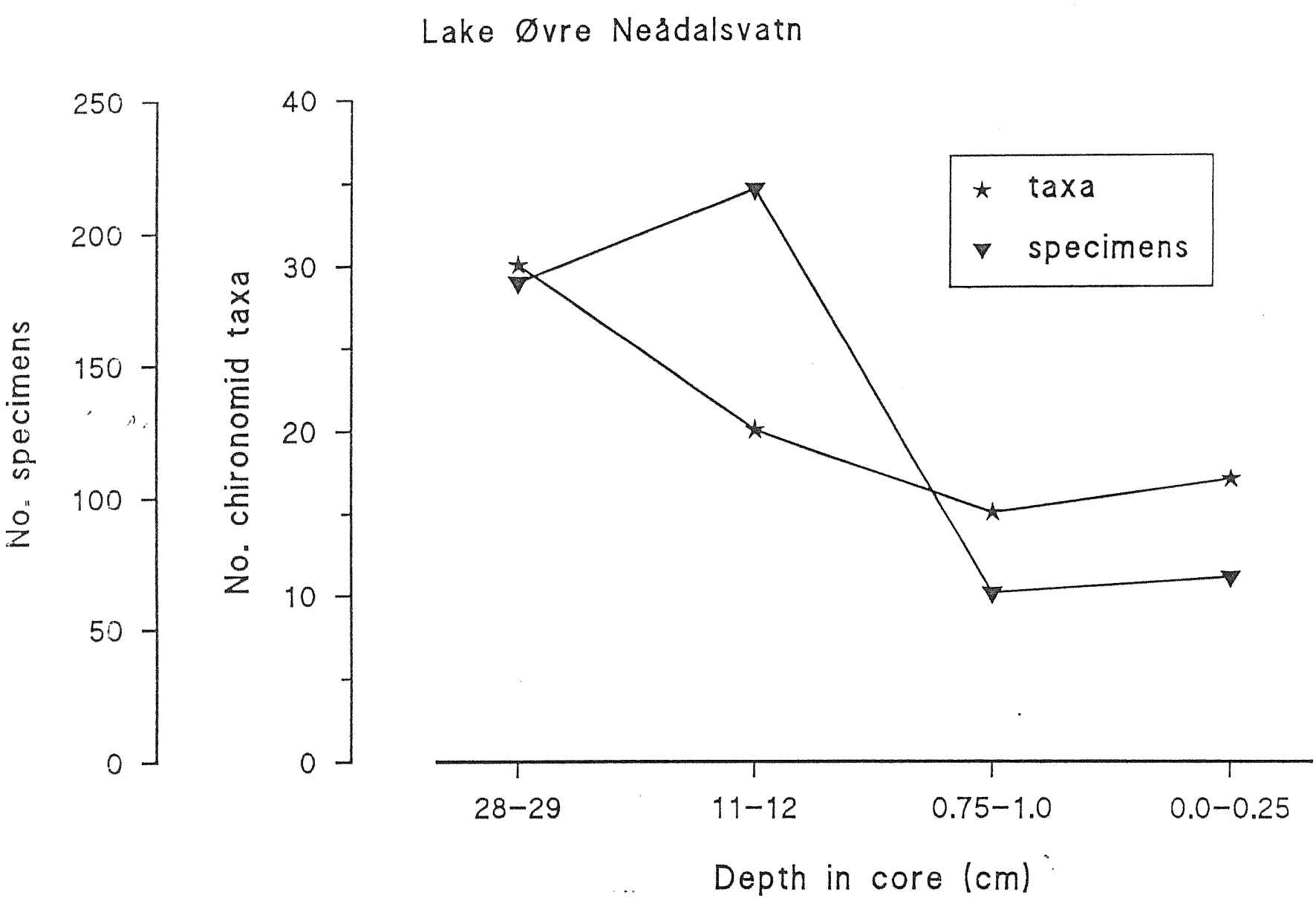

Chir. Fig. 1 OVNE2 No. of chironomid specimens & taxa / depth

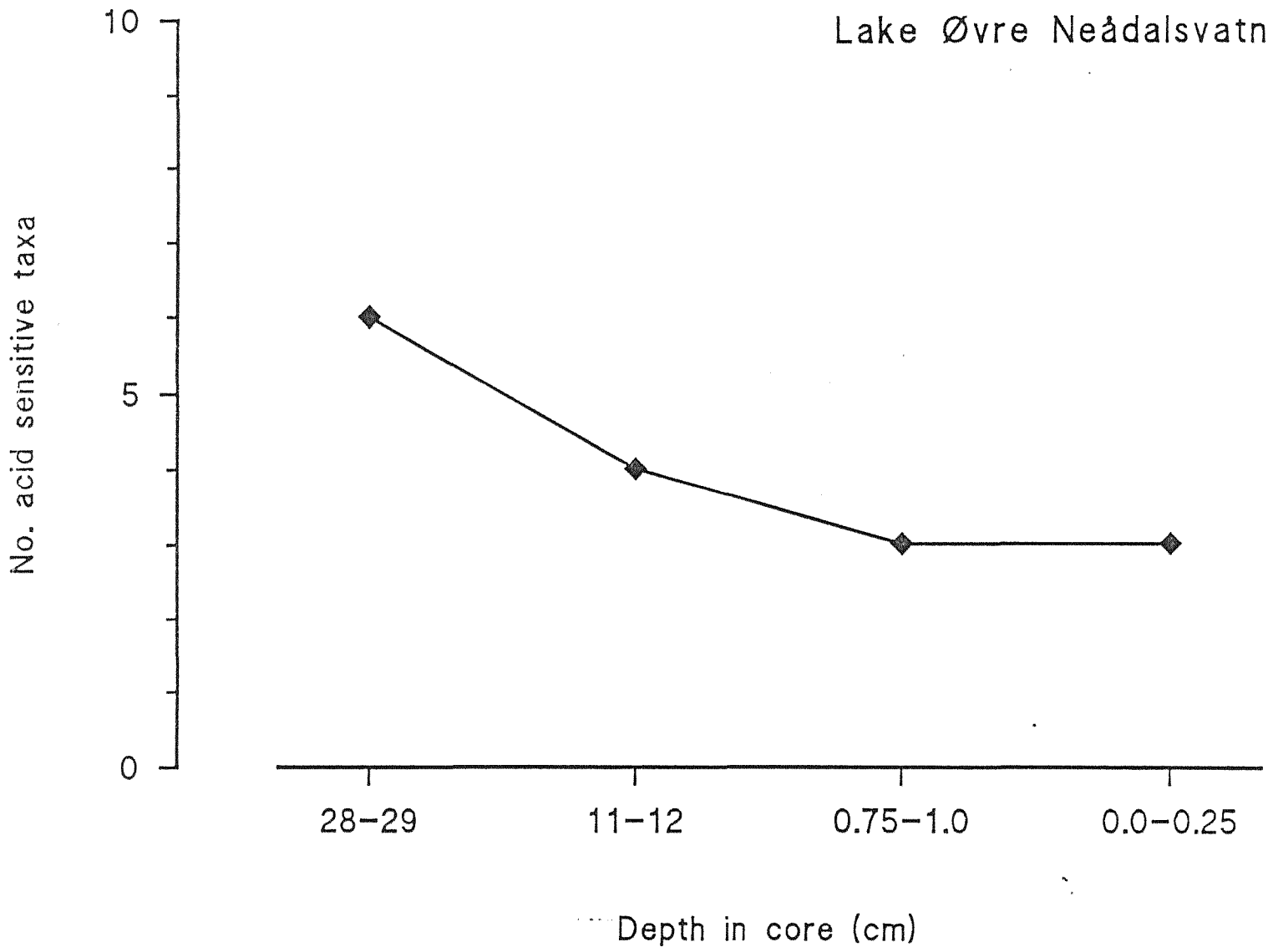

Chir. Fig. 2 OVNE2 No. of acid sensitive chironomid taxa / depth

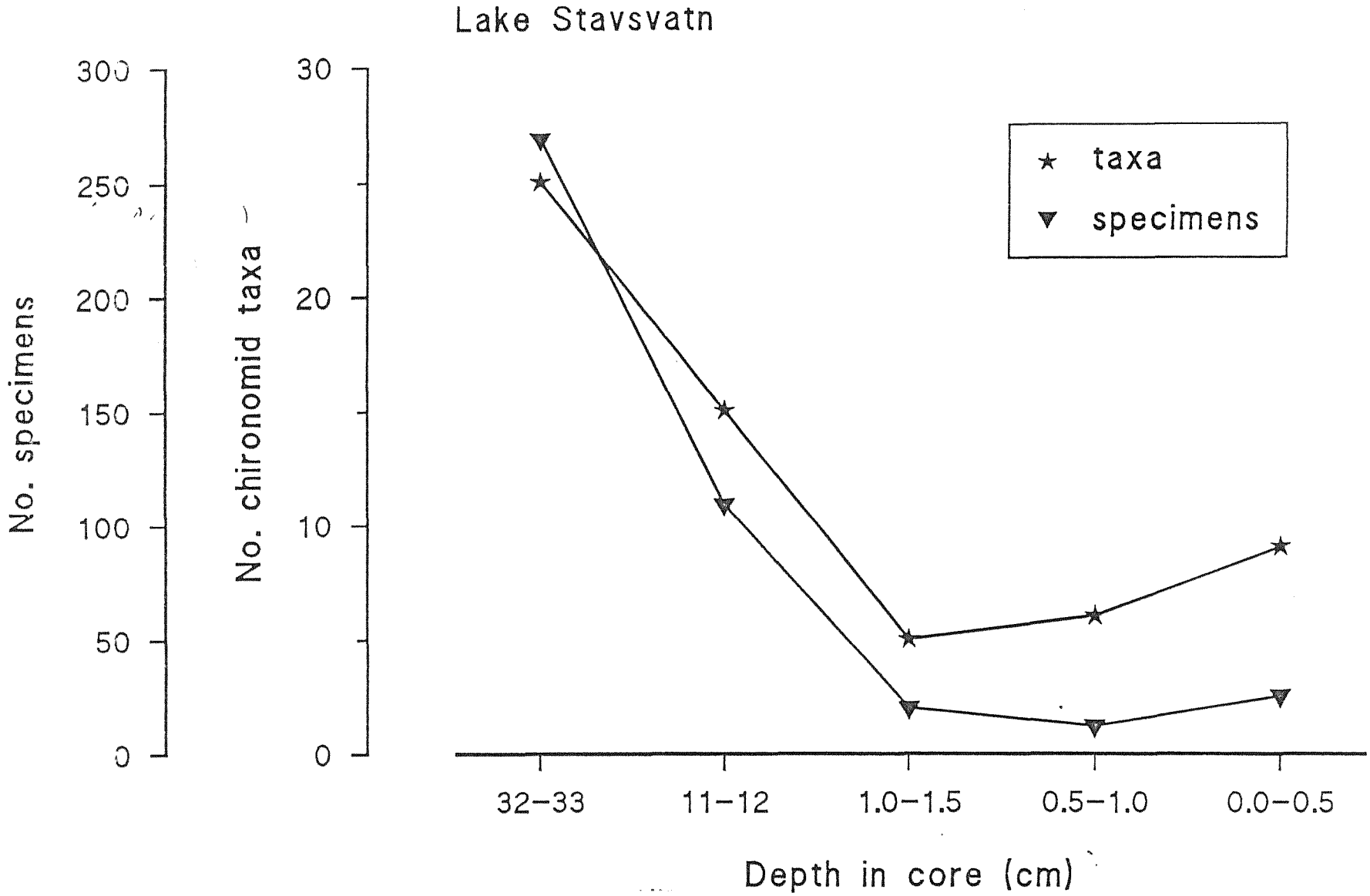

Chir. Fig. 3 STVN3 No. of chironomid specimens & taxa / depth

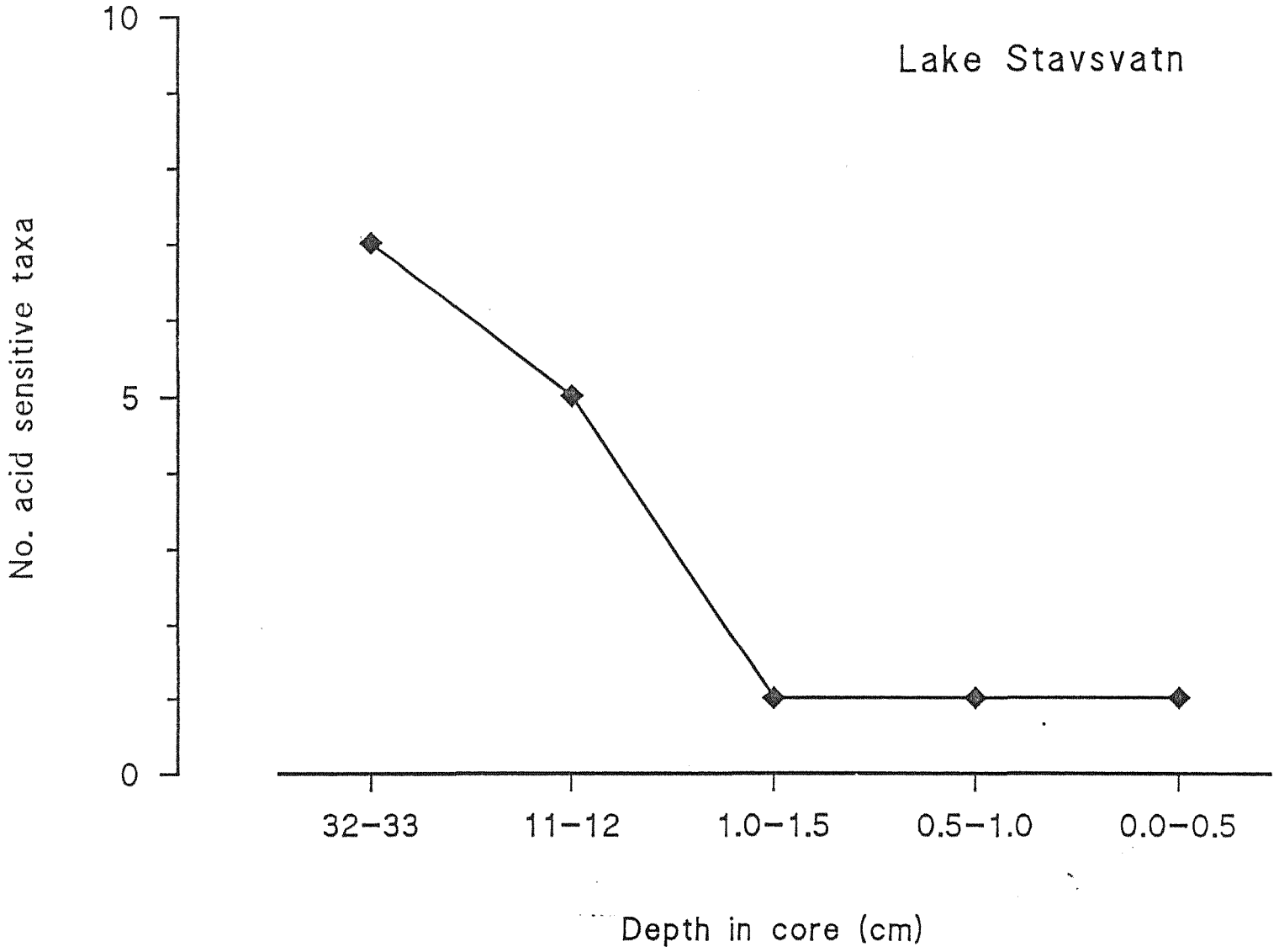

Chir. Fig. 4 SVTN3 No. of acid sensitive chironomid taxa / depth

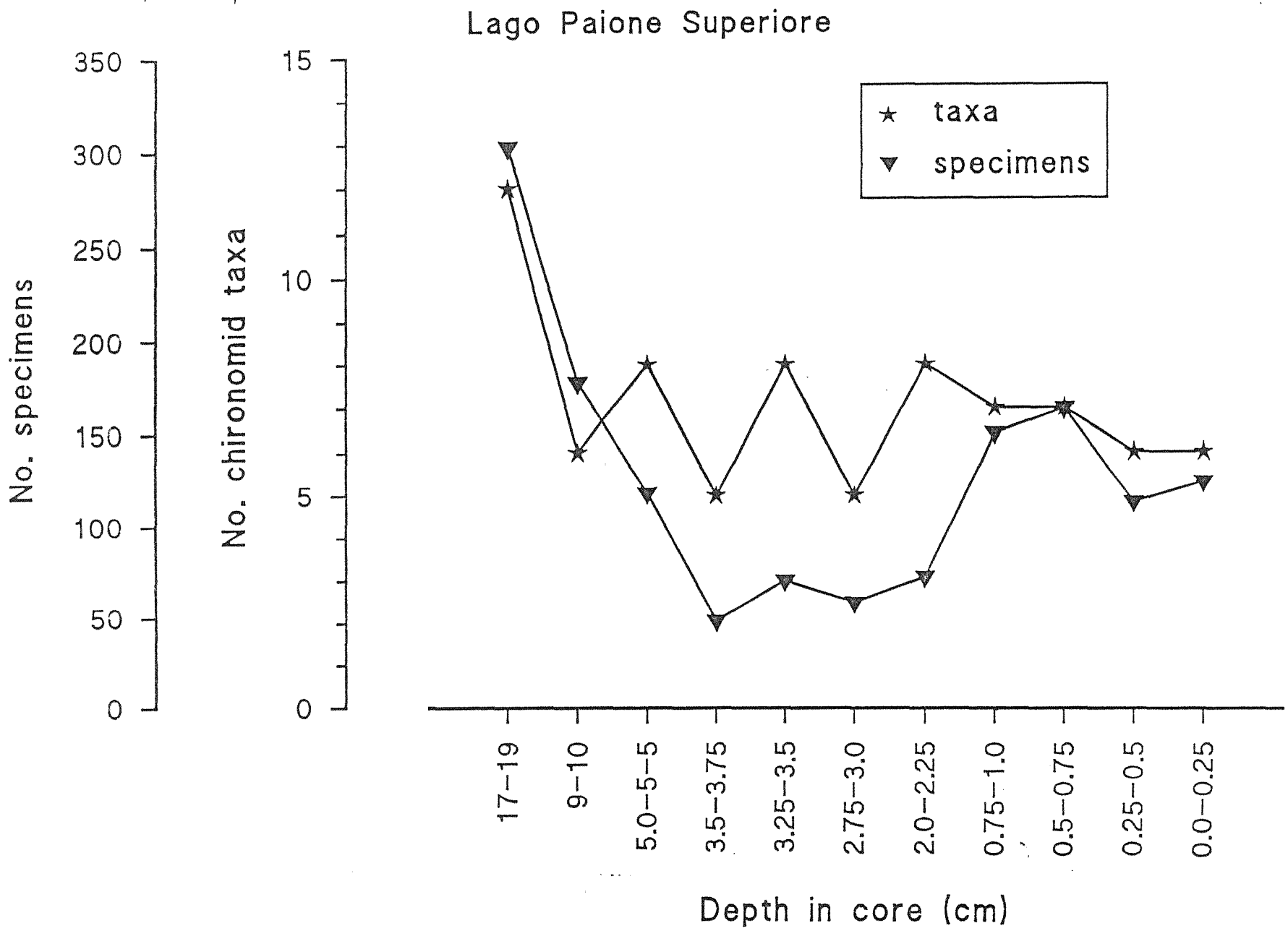

Chir. Fig. 5 PSUP2 No. of chironomid specimens & taxa / depth

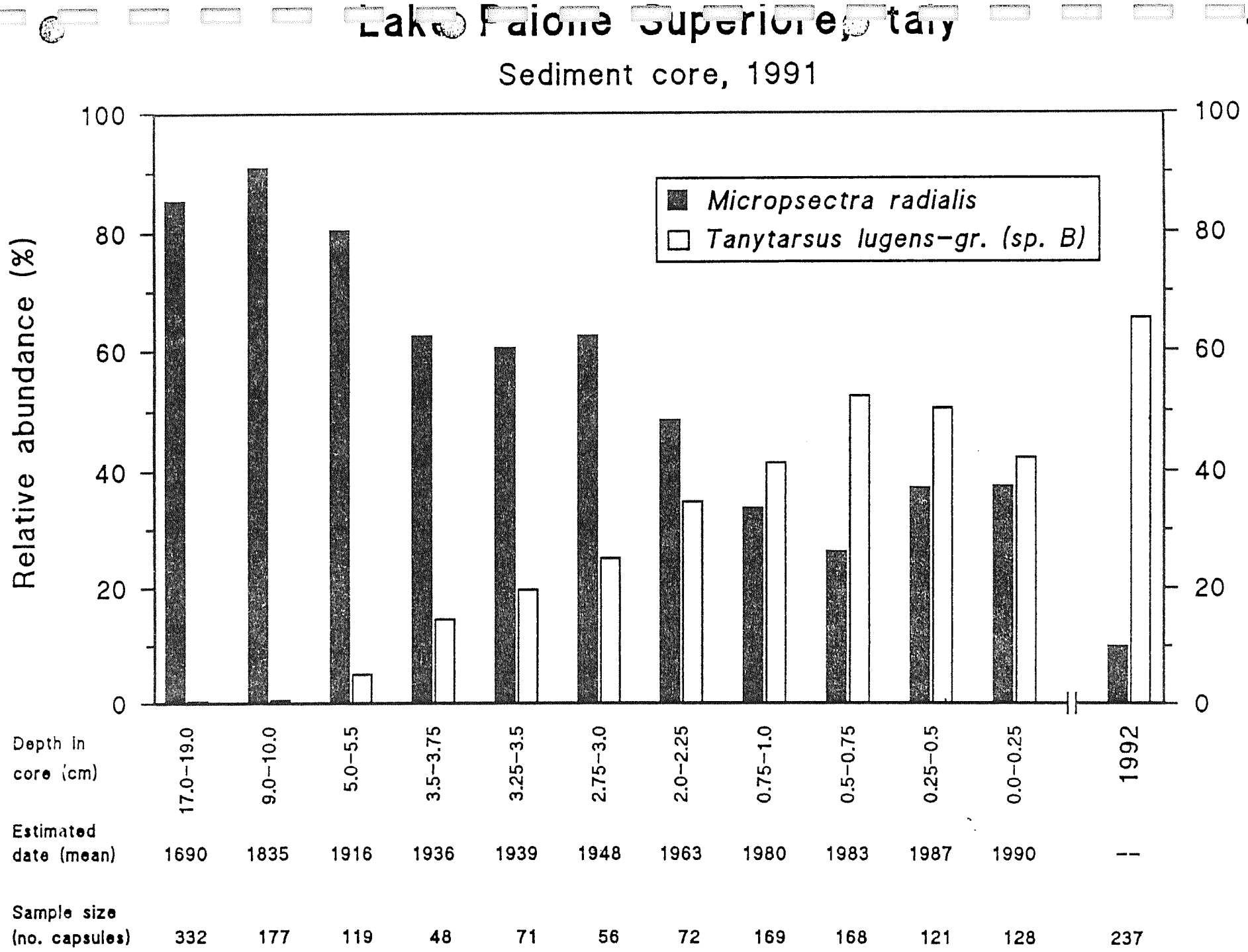

Chir. Fig. 6 PSUP2 Changes in relative abundances of, *M.radialis* a n d *T.lugens*-group (sp.B), 2 acid sensitive chironomid taxa

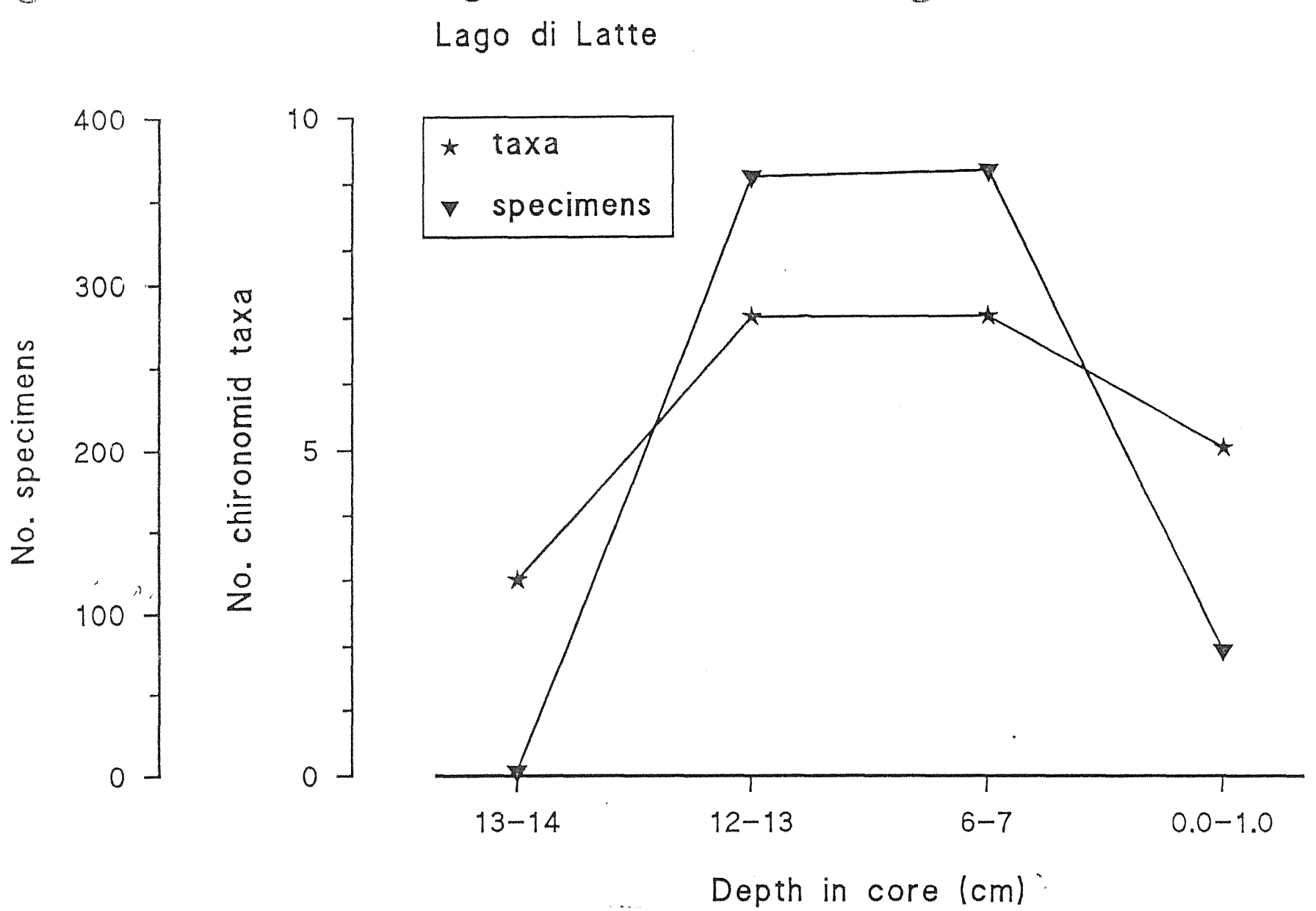

Chir. Fig. 7 MILC2 No. of chironomid specimens & taxa / depth

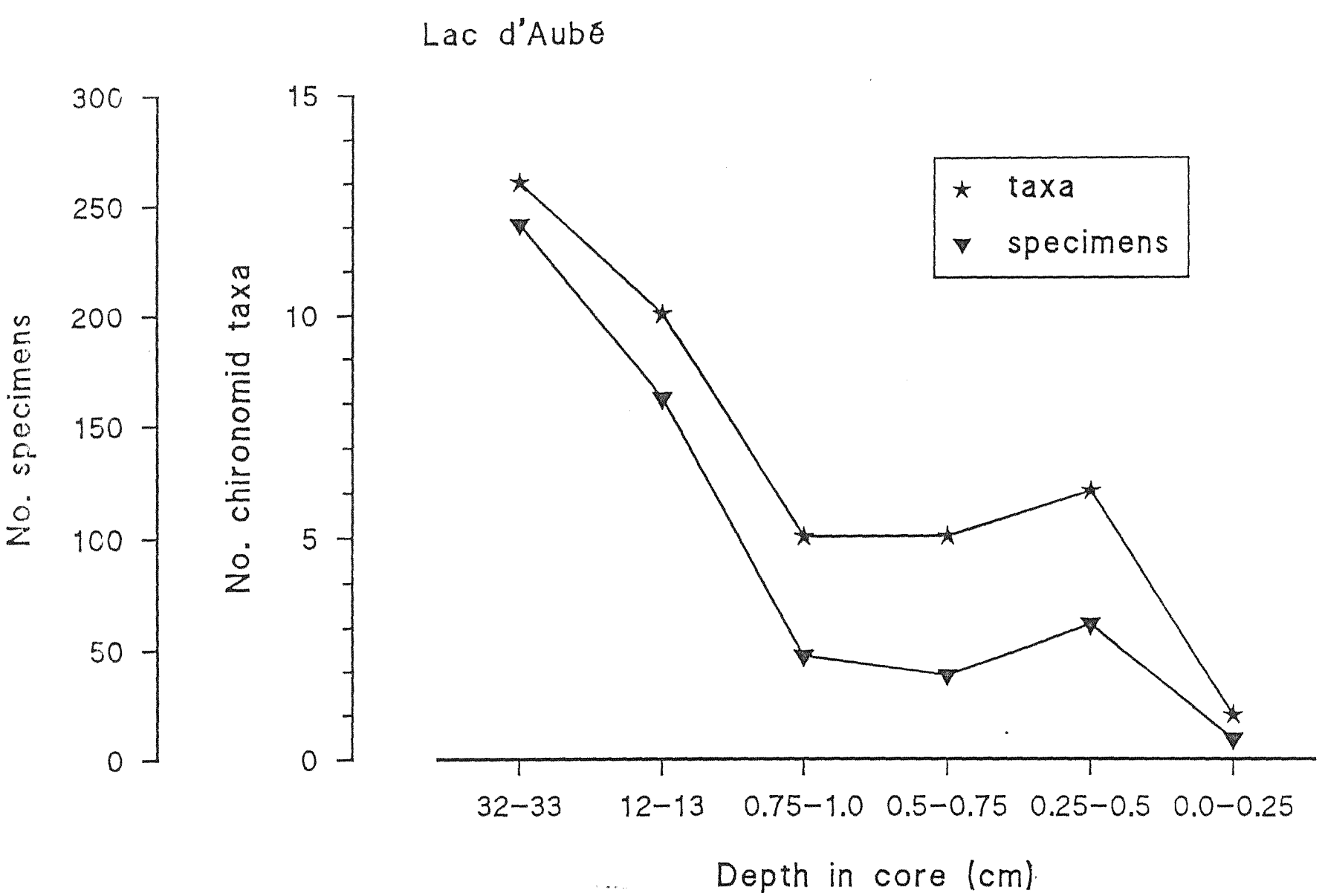

Chir. Fig. 8 AUBE2 No. of chironomid specimens & taxa / depth

Lake Øvre Neådalsvatn, Norway. Chir.X-1

Chironomid head capsules from sediment core.

Depth in core (cm)	28-29	11-12	0.75-1.0	0.0-0.25
No. specimens	181	216	63	69
No. taxa (minimum estimates)	30	20	15	17
TANYPODINAE				
Arctopelopia melanosoma	2	0	3	0
Procladius spp.	6	1	1	2
Zavrelimyia cf. *barbatipes*	2	0	0	0
Pentaneurini indet.	2	0	0	1
DIAMESINAE				
Diamesa spp.	8	9	0	1
Protanypus morio	2	8	1	2
Pseudodiamesa cf. *arctica*	3	0	0	0
ORTHOCLADIINAE				
Acamptocladius submontanus	0	0	0	1
Chaetocladius spp.	8	0	0	2
Corynoneura lobata	1	0	0	0
Corynoneura cf. *arctica*	2	0	0	0
Corynoneura spp. indet.	2	0	0	2
Cricotopus (*Cricotopus*) sp.	1	0	0	0
Cricotopus (*Isocladius*) sp.	0	1	0	0
Eukiefferiella cf. *minor*	15	7	2	3
Eukiefferiella spp.	8	0	0	0
Georthocladius luteicornis	2	0	0	0
Heterotanytarsus apicalis	3	11	2	3
Heterotrissocladius brundini	19	91	29	33
Heterotrissocladius grimshawi	3	0	0	0
Heterotrissocladius marcidus	6	8	1	1
Heterotrissocladius subpilosus	1	2	0	0
Limnophyes sp.	0	1	0	0
Orthocladius (*Orthocladius*) *frigidus*	1	1	0	1
Psectrocladius fennicus	0	3	0	1
Psectrocladius sp. *limbatellus*-group	1	2	1	1
Thienemanniella sp.	4	1	1	0
Zalutschia tornetraeskensis	5	0	2	0
Orthocladiinae indet.	8	2	3	1
CHIRONOMINAE				
Corynocera ambigua	2	0	0	0
Dicrotendipes modestus	0	1	0	0
Micropsectra radialis	1	27	4	4
Micropsectra groenlandica/insignilobus	18	19	2	8
Micropsectra indet.	15	0	2	0
Paracladopelma nigritula	0	0	1	0
Paratanytarsus penicillatus	4	0	1	0
Sergentia coracina	12	7	1	0
Stictochironomus rosenshoeldi	2	8	0	0
Tanytarsus lugens-group (sp. A)	10	4	0	1
Tanytarsini indet.	0	2	6	1
Chironomidae indet.	2	0	0	0

Lake Stavsvatn, Norway. Chir.X-2

Chironomid head capsules from sediment core.

Depth in core (cm)	32-33	11-12	1.0-1.5	0.5-1.0	0.0-0.5
No. specimens	269	109	20	12	25
No. taxa (minimum estimates)	25	15	5	6	9
TANYPODINAE					
Arctopelopia sp.	2	0	0	0	0
Procladius sp.	7	5	1	2	3
Pentaneurini indet.	1	1	0	0	1
DIAMESINAE					
Protanypus morio	9	10	0	0	2
ORTHOCLADIINAE					
Cricotopus (*Cricotopus*) sp. *festivellus*-group	1	0	0	0	0
Cricotopus (*Cricotopus*) sp. indet.	1	0	0	0	0
Heterotanytarsus apicalis	31	10	0	1	1
Heterotrissocladius brundini	52	35	7	3	6
Heterotrissocladius grimshawi	19	3	0	0	0
Heterotrissocladius marcidus	20	6	1	0	2
Limnophyes sp.	1	0	0	0	0
Mesocricotopus thienemanni	1	0	0	0	0
Parakiefferiella bathophila	1	0	0	0	0
Psectrocladius septentrionalis	7	3	0	0	0
Psectrocladius spp. *limbatellus*-group	18	8	0	1	3
Psectrocladius indet.	1	0	0	0	0
Orthocladiinae sp. cf. gen. nov.	1	0	0	0	0
Orthocladiinae indet.	9	1	1	0	0
CHIRONOMINAE					
Chironomus sp.	2	0	0	0	0
Dicrotendipes modestus	3	0	0	0	0
Micropsectra radialis	1	4	6	1	1
Micropsectra groenlandica/insignilobus	20	1	0	0	0
Micropsectra indet.	5	0	0	2	3
Microtendipes cf. *pedellus*	10	6	0	0	0
Paracladopelma nigritula	1	0	0	0	0
Paratanytarsus penicillatus	2	0	0	0	0
Sergentia coracina	16	7	4	2	2
Stictochironomus rosenshoeldi	0	2	0	0	0
Tanytarsus lugens-group (sp. A)	20	6	0	0	0
Tanytarsini indet.	7	1	0	0	1
(*Chaoborus* cf. *flavicans*)	1	0	0	0	0

Lago Paione Superiore, Italy.

Chir.X-3

Chironomid head capsules from sediment core.

Depth in core (cm)	17-19	9-10	5.0-5.5	3.5-3.75	3.25-3.5	2.75-3.0	2.0-2.25	0.75-1.0	0.5-0.75	0.25-0.5	0.0-0.25
No. specimens	302	177	118	48	70	58	72	150	163	113	124
No. taxa (minimum estimates)	12	6	8	5	8	5	8	7	7	6	6
TANYPODINAE											
Procladius spp.	13	9	5	4	7	5	2	2	9	2	4
Zavrelimyia cf. *barbatipes*	0	0	0	0	1	0	0	1	1	1	0
DIAMESINAE											
Diamesa sp.	2	0	0	0	0	0	0	0	0	0	0
Protanypus sp.	0	0	0	0	0	0	0	1	0	0	0
ORTHOCLADIINAE											
Bryophaenocladius sp.	1	1	2	0	0	0	1	0	0	0	0
Chaetocladius sp.	1	1	0	0	0	0	0	0	0	0	0
Heterotrissocladius marcidus	15	4	3	4	2	1	5	26	18	8	13
Heterotrissocladius indet.	0	0	0	0	1	0	0	0	0	0	0
Limnophyes sp.	1	0	2	0	0	0	0	0	1	0	0
Paratrichocladius sp.	1	0	1	0	0	0	1	0	0	0	0
Pseudosmittia sp.	2	0	4	2	2	1	1	1	1	0	0
Orthocladiinae indet.	1	0	0	0	1	0	0	0	0	0	1
CHIRONOMINAE											
Micropsectra radialis	261	161	95	31	42	37	36	48	44	40	48
Micropsectra sp. indet.	3	0	0	0	0	0	1	0	0	1	2
Tanytarsus lugens (sp. B)	1	1	6	7	14	14	25	71	89	61	56

Lago di Latte, Italy. Chir. X-4

Chironomid head capsules from sediment core.

Depth in core (cm)	13-14	12-13	6-7	0.0-1.0
No. specimens	3	364	367	77
No. taxa	3	7	7	5
DIAMESINAE				
Diamesa sp.	0	4	2	1
Protanypus sp.	0	9	7	1
Pseudodiamesa sp.	1	0	2	0
ORTHOCLADIINAE				
Corynoneura (cf.) *scutellata*	0	1	2	1
Heterotrissocladius marcidus	0	15	6	4
Heterotrissocladius sp. indet.	1	2	1	0
Orthocladiinae sp. indet.	0	1	0	0
CHIRONOMINAE				
Micropsectra radialis	1	332	347	70

Lac d'Aubé, France. Chir.X-5

Chironomid head capsules from sediment core.

Depth in core (cm)	32-33	12-13	0.75-1.0	0.5-0.75	0.25-0.5	0.0-0.25
No. specimens	241	162	47	38	61	9
No. taxa (minimum estimates)	13	10	5	5	6	1
TANYPODINAE:						
Macropelopia sp.	4	0	0	0	0	0
Procladius spp.	17	19	5	2	0	0
Zavrelimyia cf. *barbatipes*	39	8	2	2	0	0
Pentaneurini indet.	3	0	0	0	0	0
DIAMESINAE:						
Diamesa spp.	5	3	0	0	0	0
ORTHOCLADIINAE:						
Chaetocladius spp.	3	2	1	0	2	0
Corynoneura cf. *lacustris*	0	0	0	0	2	0
Heleniella sp.	1	1	0	0	0	0
Heterotrissocladius marcidus	32	17	4	3	2	0
Psectrocladius sp. *limbatellus*-group	3	1	0	0	0	0
Psectrocladius indet.	1	0	0	0	0	0
Synorthocladius semivirens	1	0	0	0	0	0
Orthocladiinae spp. indet.	7	0	0	0	0	0
CHIRONOMINAE:						
Polypedilum sp.	1	0	0	0	0	0
Micropsectra cf. *insignilobus*	16	1	0	1	1	0
Micropsectra radialis	73	87	31	26	44	9
Micropsectra spp. indet.	10	5	0	1	1	0
Tanytarsus lugens-group (sp. B)	0	9	0	0	3	0
Tanytarsus spp. indet.	0	0	0	0	3	0
Tanytarsini indet.	25	9	4	3	3	0

PRELIMINARY LIST OF SOME OLIGOTROPHIC LITTORAL AND PROFUNDAL CHIRONOMIDS GROUPED ACCORDING TO ACID SENSITIVITY

Sensitive species (Index between 0.5 and 1.0, i.e pH > 5.0)

Heterotrissocladius grimshawi
Monodiamesa bathyphila
Micropsectra groenlandica
Micropsectra insignilobus
Micropsectra radialis
Paracladopelma nigritula
Stictochironomus rosenshoeldi
Tanytarsus lugens
Zavrelimyia barbatipes

Indifferent species (Index between 0.0 and 0.5)

Arctopelopia barbitarsis
Conchapelopia melanops
Dicrotendipes modestus
Heterotanytarsus apicalis
Mesocricotopus thienemanni
Microtendipes cf. *pedellus*
Pagastiella orophila
Protanypus caudatus
Psectrocladius (Mesopsectrocladius) barbatipes
Psectrocladius (Psectrocladius) psilopterus
Stictochironomus pictulus

Tolerant species (Index = 0)

Chironomus anthracinus
Heterotrissocladius brundini
Heterotrissocladius marcidus
Macropelopia adaucta
Parakiefferiella bathophila
Paratanytarsus penicillatus
Protanypus morio
Psectrocladius septentrionalis
Psectrocladius (Psectrocladius) limbatellus
Sergentia coracina
Tanytarsus buchonius
Zalutschia zalutschicola